

Enantiomer separation
using
membrane systems

CENTRALE LANDBOUWCATALOGUS



0000 0924 7228

Promotoren:

Prof. dr. ir. K. van 't Riet

voormalig hoogleraar levensmiddelenproceskunde

Prof. dr. ir. J.T.F. Keurentjes

hoogleraar proces- en apparaatontwerp, Technische Universiteit Eindhoven

Prof. dr. ir. M.A. Cohen Stuart

hoogleraar fysische chemie m.b.a.v. de kolloïdchemie

Co-promotor:

dr. ir. A. van der Padt

voormalig universitair docent, verbonden aan het departement

levensmiddelentechnologie, leerstoelgroep levensmiddelenproceskunde

ISBN 90-5808-600-3

1. Enantioselectieve membranen kunnen verdeeld worden in 2 subgroepen; Sorptie-selectieve membranen en diffusie-selectieve membranen. Het erkennen van deze verdeling is van groot belang voor het fundamentele onderzoek naar deze membranen.

Hoofdstuk 2, dit proefschrift.

2. Anders dan men zou vermoeden zijn enkelfasige concentratiegedreven processen energetisch ongunstig, waarmee dit soort processen van ondergeschikt belang zijn voor industriële toepassingen.
3. Een economisch model waarin ethische aspecten verweven zijn is per definitie waardeloos en zou derhalve niet gebruikt moeten worden voor besluitvorming.
4. Ondanks het feit dat niet reproduceerbare data tot nieuwe ideeën kunnen leiden, zou het voor de beeldvorming van de wetenschap beter zijn wanneer slechts reproduceerbare data gepubliceerd zouden worden.

T. Masawaki, T. Hamada, and S. Tone, The effect of charge density on the permeation flux of amino acid through positively charged membranes under pressure gradient, J. Chem. Eng. Jpn. 27 (1994) 182.

S. Tone, T. Masawaki, and K. Eguchi, The optical resolution of amino acids by plasma polymerized terpene membranes, J. Membrane Sci. 118 (1996) 31.

5. Het feit dat een luchtaanjager in een auto 250 Watt verbruikt en dat met dat zelfde vermogen in een gestroomlijnde ligfiets 40 km/uur kan worden gereden, zou op zijn minst de automobieliindustrie tot nadenken moeten zetten.

<http://www.m5-ligfietsen.com/snelheid.htm>

6. Het begrip ochtendmens/avondmens bestaat niet, dit schijnbegrip is slechts gerelateerd aan het tijdstip van naar bed gaan.

*Het geloof nu is de zekerheid van wat men hoopt,
de overtuiging van wat men niet ziet.*

*Want in dit geloof hebben de ouden getuigenis
verkregen.*

*Door het geloof begrijpen wij dat de werelden
door Gods woord bereid zijn, zodat wat men ziet,
niet ontstaan is uit wat zichtbaar is.*

Hebreeën 11:1-3

Dankwoord

Het is een vreemd gevoel om het dankwoord van mijn proefschrift hier vanuit Amerika te schrijven. In essentie geeft het aan dat het moment is gekomen om een geweldige periode bij proceskunde af te sluiten en daarnaast een nieuwe periode te starten. Deze nieuwe periode zie ik met veel vertrouwen tegemoet, omdat ik kan steunen op een solide basis van kennis en ervaring welke gevormd is bij proceskunde. Maar voordat die basis er was zijn er vijf jaren met hoogtepunten en natuurlijk ook dieptepunten voorbij gegaan. Echter, altijd met veel plezier heb ik mijn werk mogen doen. En dat plezier is mij voornamelijk gegeven door de mensen waarmee ik mocht samenwerken. Allereerst, als voornaamste persoon hierin, wil ik Albert noemen. Twee maanden nadat ik in juni 1996 was begonnen bleek dat Klaas niet meer fulltime aan de vakgroep verbonden zou zijn. Dit heeft er voor gezorgd dat de samenwerking tussen Albert en mij zeer intensief is geweest en ik durf zelfs te beweren dat dit proefschrift er niet had gelegen zonder zijn motivering, inspiratie en gedrevenheid. Hiervoor wil ik hem bedanken. Dat neemt niet weg dat meerdere mensen een onmisbare bijdrage hebben geleverd. Daar horen als eerste de personen bij die onze gedachtekrachten hebben beoordeeld op hun haalbaarheid: Martien, Klaas en Jos. Martien wil ik bedanken voor zijn inzet als fysisch- en kolloïdkundige in een procestechnologisch onderwerp. Ook in dit onderzoek hebben we kunnen en moeten ervaren dat deze twee vakgebieden niet zonder elkaar kunnen. Ook wil ik de andere mensen van de vakgroep Fysische en kolloïdchemie die een steentje hebben bijgedragen aan de totstandkoming van dit proefschrift bedanken. In het bijzonder wil ik Arie de Keizer noemen. Voor de tweede maal heb ik onze samenwerking als zeer positief ervaren en je kritisch wetenschappelijke opstelling als motiverend. Klaas, ook jou wil ik bedanken. Ondanks dat je na twee maanden niet meer volledig bij de vakgroep betrokken was, is jou invloed in dit onderzoek naar mijn mening niet minder geweest. Ik stond er iedere keer weer versteld van hoe je op de kritieke momenten aanwezig was, het geheel overzag en telkens weer voor de goede oplossingen kon zorgen. Jos, van jou heb ik toch wel het meeste geleerd. In proceskundig opzicht, maar zeker ook in persoonlijk en wetenschappelijk opzicht. Ook moet ik je bedanken omdat je mij de laatste zet hebt gegeven die nodig was om te willen promoveren op dit onderwerp.

Naast de vakinhoudelijke mensen ben ik ook veel dank verschuldigd aan de mensen die aan het sociale aspect van mijn werk inhoud hebben gegeven. Dat is begonnen met mijn oud kamergenoten Pieter en Floor. Ik heb er altijd van genoten dat, ondanks dat we alle drie zo verschillend van karakter waren, we

een gezellige en motiverende tijd hebben gehad. Na deze tijd begon er een nieuwe periode met Anneke, René en Mark. Ook deze drie mensen wil ik bedanken. We zijn met z'n vieren letterlijk en figuurlijk tot grote hoogten geklommen, maar ook met de zekerheid dat er altijd iemand was die je op kon vangen. René, ik denk dat ik de rommel om jou heen in positieve zin zal gaan missen. Mark, we hebben samen een hoop lol beleefd en veel van elkaar mogen leren. Anneke, ik zal het uitzicht zeker gaan missen, maar ook de gesprekken over van alles en nog wat die we hadden als we van dat uitzicht zaten te genieten.

De uitvoerende werkzaamheden voor dit onderzoek heb ik niet alleen gedaan, daar hebben een aantal studenten mij bij geholpen. Daniël (Goede methode uitgevonden om bijna alles tot poeder te vermalen.....), Joost (Al weer een beetje bijgekomen van de geëxplodeerde Scottfles? Toen ik laatst aan het opruimen was kwam ik de glassplinters nog tegen), Tom (De enige echte bikkelaar van het tweede bordes en omgeving), Pim (In jou heb ik altijd veel van mezelf herkend, lekker fanatiek bezig zijn) en Bart (Op de valreep nog een mooi stukje werk kunnen toevoegen aan het geheel). Ik wil ze allemaal bedanken voor hun inzet en hun kritische vraagstelling, welke mij steeds weer scherp hielden.

Dan zijn daar nog de mensen die mij hebben bijgestaan in de tijd die ik overhield als ik niet aan het werk was. Allereerst wil ik mijn ouders bedanken. Zij hebben mij mentaal gesteund door steeds te proberen begrijpen waar ik mee bezig was. Ook wil ik ze bedanken voor de vele zaterdagen waarin "er altijd wel wat te doen was". Daarnaast wil ik ook mijn schoonfamilie bedanken waarmee ik veel samen heb mogen delen, maar Beursplein 5 bleef toch altijd wel de "klapper" waar we in op konden gaan. Ook jullie bedankt voor alle goede zorgen.

Dan als laatste, maar zeker toch ook als belangrijkste persoon in mijn leven wil ik Marie-Anne noemen. We hebben samen veel meegemaakt in de afgelopen tijd van mijn promotiewerk, rijkelijk zijn we gezegend met drie gezonde kinderen en ik hoop dat we ook in de nieuwe periode die voor ons ligt elkaar altijd mogen blijven steunen in liefde en dankbaarheid zoals we dat de afgelopen jaren hebben mogen doen.

Contents

1	Membrane technology for the separation of enantiomers	1
2	Design criteria for dense permeation-selective membranes for enantiomer separations	11
3	Electrodialysis system for large-scale enantiomer separation	37
4	Enantioselective binding of tryptophan to α -cyclodextrin: A thermodynamic study	57
5	Multistage electrodialysis for large-scale separation of racemic mixtures	73
6	Concluding remarks	95
	Summary	107
	Samenvatting	111
	Curriculum vitae	115

*Voor Marie-Anne, Nils, Luuc, Marion
Voor mijn ouders*

1 Membrane technology for the separation of enantiomers

1.1 Chirality

Chirality is an important character of biological systems, since it represents an intrinsic property of the building blocks of life, such as amino acids and sugars. Peptides, proteins and polysaccharides contain many chiral centers and as a consequence, metabolic and regulatory processes in biological systems are sensitive to stereochemistry. Comparing the activities of two enantiomers, different responses can often be observed, e.g. one of the two enantiomers has the required biological activity, whereas the other enantiomer is responsible for severe side effects or is at least a 50% impurity. Therefore, these effects have to be taken into account for the application of chiral molecules in e.g. drugs, agrochemicals, food additives, flavours or fragrances [1].

Chirality: concerning chiral molecules.

Chiral molecule: a molecule that is not superimposable on its mirror image.

The word 'chiral' comes from the ancient Greek 'cheir', which means hand. The two mirror images are comparable to the left and right hand.

Enantiomers: the two mirror images of a chiral molecule.

Enantiomeric excess: A measure for the purity of an enantiomer mixture.

This is defined as the difference of both enantiomer concentrations divided by the sum of both enantiomer concentrations.

Racemic mixture: A mixture of the two enantiomers in equal proportions.

The interest in chirality and its consequences is not a new phenomenon. However, during the last decade the research efforts have increased drastically, for which the pharmaceutical industry is the main contributor and driving force. The increasing need for single enantiomers as key intermediates in the chemical and pharmaceutical industry has stimulated a significant demand for efficient processes to resolve racemic mixtures [1]. Approaches which may be applied to obtain optically pure compounds are the utilization of chiral pool materials, asymmetric synthesis and separation of a racemic mixture [2]. Crystallization and enzymatic resolution have been the two classical methods for the separation of a racemic mixture [4]. However, crystallization usually requires many process steps, thus making the process complicated and inducing considerable losses of product. For enzymatic resolution an appropriate route has to be developed for each individual compound, leading to considerable costs and increased development time [3]. On the other hand, the focus on alternative technologies performing enantioseparation in a continuous fashion has drastically increased during the last decade. Apart from the promising

concept of SMB chromatography with chiral stationary phases [5], considerable efforts have been concentrated on the development of enantioseparation procedures based on membrane processes [4].

1.2 Membrane technology in chiral separations

Technically, membrane separation processes are particularly suited for large-scale applications as they combine a number of attractive features. They allow for a continuous mode of operation, easy adaptation to different production-relevant process configurations, convenient scaling up and, in most cases, ambient-temperature processing [6]. There are two categories of membrane processes for enantiomer separation: direct separation using an "intrinsically" enantioselective membrane (applying enantioselective polymers) and separation in which a non-selective membrane assists an enantioselective process.

Intrinsically selective membranes

The group of intrinsically selective membranes can be divided into two groups: liquid membranes [7-11] and dense polymer membranes [12-20]. A liquid membrane for chiral separation contains an enantiospecific carrier, which selectively forms a complex with one of the enantiomers at the feed side and transports it across the membrane, where it is released into the receptor phase [21] (Figure 1). One of the critical parameters for this process is that the carrier should not dissolve in the feed liquid or receptor phase to avoid leakage from

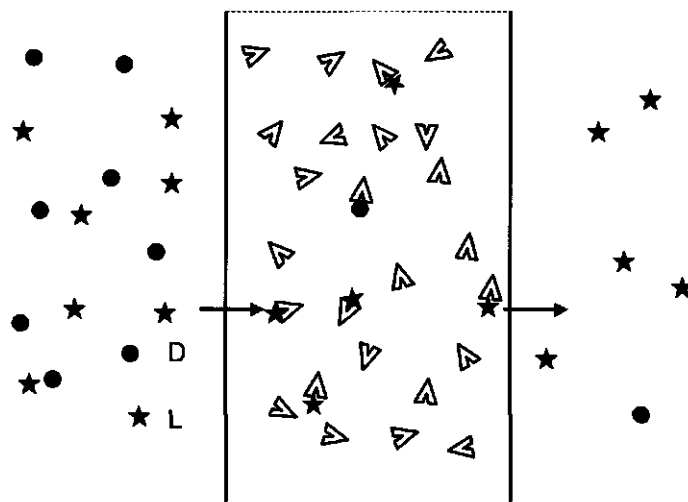


Figure 1: Schematic representation of a liquid membrane for enantiomer separation.

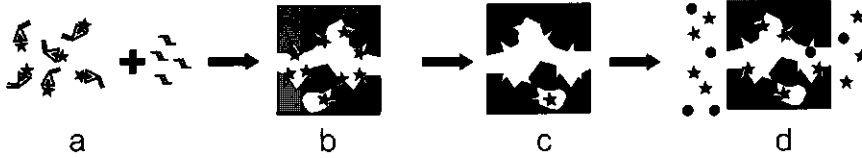


Figure 2: The preparation procedure and use of molecular imprinted polymers. Polymerization of a template-monomer complex with cross-linking agent (a) yields a geometry in which the self-assembled template monomer is captured in a polymer matrix (b). After removal of the templates, the cavities of the molecular imprinted polymer possess a shape and arrangement corresponding to the functional groups of the template (c). This polymer matrix can be used in chiral separation techniques (d).

the liquid membrane. For optimal selectivity of these membranes, a-selective diffusion through the liquid phase in these membranes has to be minimal. Also, the carrier liquid has to provide a stable boundary over a longer period of time between the feed phase and the acceptor phase. However, in practice this is often not observed. Therefore, alternative approaches are used, i.e. the application of dense polymer membranes.

Enantioselective polymer membranes consist of a nonselective porous support coated with a thin layer of an enantioselective polymer. The separation mechanism involves enantiospecific interaction (solution and diffusion) between the isomers to be separated and the top layer polymer matrix. Both the permeability (normalized flux) and the enantioselectivity (ratio of the permeability coefficients of the two enantiomers) determine the performance of an enantioselective membrane. Another approach for dense enantioselective membranes is the molecular imprinting technique [22], which involves the introduction of molecular recognition sites into polymeric materials (Figure 2).

Membrane assisted enantiomer separations

The membrane assisted separation processes described in literature can be divided into two groups: 1) liquid-liquid extraction, based on hollow fiber

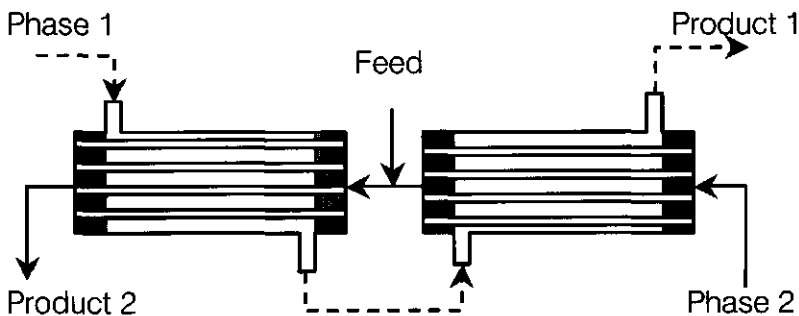


Figure 3: Fractional extraction, using liquid-liquid membrane extraction

fractionation (Figure 3) [3,23-28] and II) micellar-enhanced ultrafiltration [29-32]. For liquid-liquid extraction, the same chiral selectors can be used as are applied in liquid membranes. Frequently, the selector is solubilized in one of the two extraction phases, requiring the selector design to be optimized for selectivity as well as solubility, which can be a disadvantage. To prevent flooding of the extraction phases and to allow choosing the flow ratio freely, membranes are used to immobilize the liquid-liquid interface in the pores of the membrane. Additionally, these membrane modules have a high surface area per unit of volume, thus providing compact process equipment.

Micellar-enhanced ultrafiltration (MEUF) is a technique that uses nonionic micelles containing chiral selector molecules in combination with the membrane process ultrafiltration. During ultrafiltration, the micelles are retained, including the preferentially bound enantiomer, while the unbound enantiomers will pass the membrane. Since a single separation step often is not capable of producing single enantiomers at high purity, multi-staging is necessary (Figure 4). The enantioselective micellar phase flows in opposite direction to the water phase. Depending on the flow velocities through the system and the system dimensions, this counter-current micellar enhanced ultrafiltration process can accomplish any desired degree of separation.

1.3 Outline of this thesis

As stated above, enantiomer separation using membrane systems can be divided into two groups, intrinsically enantioselective membranes and a-selective membranes assisting an enantioselective process. Both separation mechanisms have been the subject of the research described in this thesis. In Chapter 2 the development of an intrinsically enantioselective membrane is described, resulting in the design criteria for this type of membrane. In Chapters 3-6 a separation process is described in which a non-selective membrane

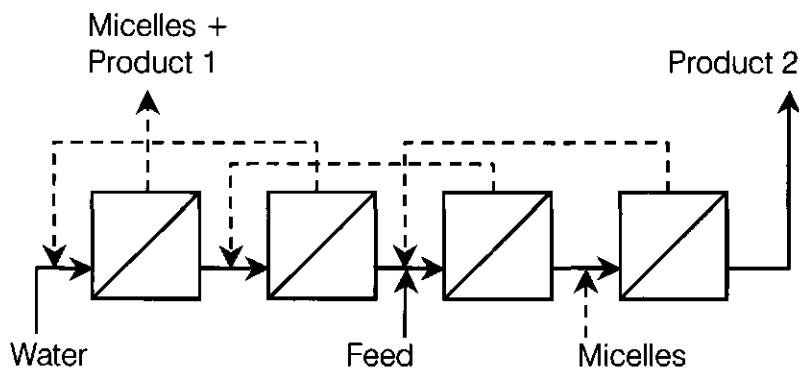


Figure 4: Counter-current cascade micellar enhanced ultrafiltration system

assists an enantioselective process. The separation concept is shown in Figure 5. A chiral selector, solubilized in an aqueous solution, preferentially forms a complex with one of the two enantiomers, resulting in an enrichment of the free enantiomers. Since the free enantiomer and the complex differ in size, a separation can be obtained by using size-selective synthetic membranes. However, since the complexation often is only partially selective, a complete separation cannot be obtained using one single separation step. Therefore, several subsequent separation steps are required for a complete separation. To perform these steps in a single apparatus, we developed a multi-stage counter-current electro dialysis process.

Electrodialysis is a widely applied technique and has the advantage of incorporating hundreds of stages in one single module. The electrical potential is used to transport the free enantiomer phase counter-currently compared to the complexant phase. In principle, this process configuration is a scaled up version of the analytical capillary electrophoresis method. The possibility to use available chiral stationary phases (CSP) from analytical methods will reduce the development time and costs substantially.

In Chapter 3 an experimental set-up is suggested to evaluate the separation principle as is shown in Figure 5. As a model system D,L-tryptophan has been used as the enantiomer and α -cyclodextrin as the chiral selector. For the batch system described in Chapter 3 the mathematical model equations for the enantiomer concentrations as a function of time have been derived as well as the resulting enantiomeric excess profiles. Using this system, the influence of the pH and various process parameters on the operational selectivity and the

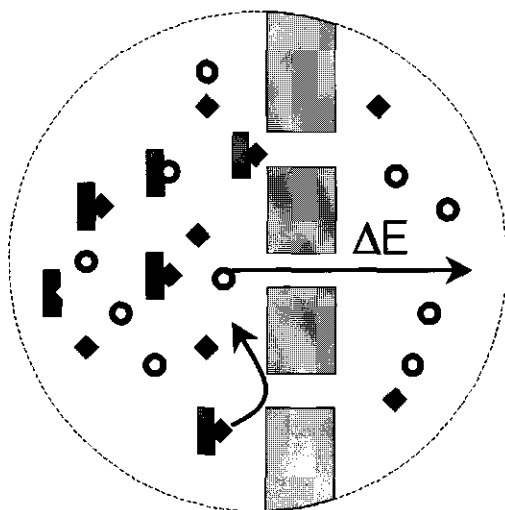


Figure 5: Separation concept of an membrane assisted enantioselective process.

transport efficiency have been examined. It has been found that the operational selectivity is a function of pH. In order to compare this pH dependency with the pH dependency of the intrinsic selectivity, measurements have been performed using isothermal titration calorimetry (Chapter 4). Using ITC the thermodynamic complexation parameters (affinity, enthalpy and entropy) for both enantiomers are determined as a function of pH.

In Chapter 5 a model is developed for the continuous multi-stage electro dialysis process. This model is validated using experiments with a 20-compartment electro dialysis system. Using extensive model calculations, the viability of the process for large-scale enantiomer separations is discussed. Additionally, in Chapter 6 the two separation processes described in this thesis are critically analyzed. The limits in operating conditions as well as potential improvements are discussed, resulting in an overview of the application potential of the two processes.

References

1. N. M. Maier, P. Franco, and W. Lindner, Separation of enantiomers: needs, challenges, perspectives, *J. Chromatogr. A*, 906 (2001) 3.
2. A. N. Collins, G. N. Sheldrake and J. Crosby, *Chirality in industry; The commercial manufacture and applications of optically active compounds*, John Wiley & Sons, Chichester, 1992.
3. J. T. F. Keurentjes, L. J. W. M. Nabuurs, and E. A. Vegter, Liquid membrane technology for the separation of racemic mixtures, *J. Membrane Sci.*, 113 (1996) 351.
4. A. N. Collins, G. N. Sheldrake and J. Crosby, *Chirality in industry II; Developments in the commercial manufacture and applications of optically active compounds*, John Wiley & Sons, Chichester, 1997.
5. M. Schulte and J. Strube, Preparative enantioseparation by simulated moving bed chromatography, *J. Chromatogr. A*, 906 (2001) 399.
6. J. D. Henry, Novel separation processes, in Perry, R. H., Green, D. W., and Maloney, J. O. (Ed.), *Perry's chemical engineering's handbook*, McGraw-Hill book company, New York, 1984,
7. D. W. Armstrong and H. L. Jin, Enrichment of enantiomers and other isomers with aqueous liquid membranes containing cyclodextrin carriers, *Anal. Chem.*, 59 (1987) 2237.
8. M. Bryjak, J. Kozłowski, P. Wierzchorek, and P. Kafarski, Enantioselective transport of amino acid through supported chiral liquid membranes, *J. Membrane Sci.*, 85 (1993) 221.
9. P. Dzygiel, P. Wierzchorek, J. A. Jonsson, M. Milewska, and P. Kafarski, Separation of amino acid enantiomers using supported liquid membrane extraction with chiral phosphates, *Tetrahedron*, 55 (1999) 9923.
10. P. J. Pickering and J. B. Chaudhuri, Emulsion liquid membranes for chiral separations: selective extraction of rac-Phenylalanine enantiomers, *Chirality*, 9 (1997) 261.

11. P. Wieczorek, J. A. Jonsson, and L. Mathiasson, Extraction of dansylated amino acids using the supported liquid membrane technique, *Anal. Chim. Acta*, 337 (1997) 183.
12. T. Aoki, A. Maruyama, K. Shinohara, and E. Oikawa, Optical resolution by use of surface modified poly(methyl methacrylate) membrane containing (-)-oligo{methyl(10-pinanyl)siloxane}, *Polym. J.*, 27 (1995) 547.
13. E. Yashima, J. Noguchi, and Y. Okamoto, Enantiomer enrichment of oxprenolol through cellulose tris(3,5-dimethylphenylcarbamate) membrane, *J. Appl. Polym. Sci.*, 54 (1994) 1087.
14. N. Ogata, Supramolecular polymers having chiral interactions, *Macromol. Symp.*, 98 (1995) 543.
15. T. Masawaki, M. Sasai, and S. Tone, Optical resolution of an amino acid by an enantioselective ultrafiltration membrane, *J. Chem. Eng. Jpn.*, 25 (1992) 33.
16. T. Aoki, S. Tomizawa, and E. Oikawa, Enantioselective permeation through poly{g-[3-(pentamethyldisiloxanyl)propyl]-L-glutamate} membranes., *J. Membrane Sci.*, 99 (1995) 117.
17. T. Aoki, K. I. Shinohara, and E. Oikawa, Optical resolution through the solid membrane from (+)-poly{1-[dimethyl(10-pinanyl)silyl]-1-propyne}, *Makromol. Chem-Rapid.*, 13 (1992) 565.
18. A. Maruyama, N. Adachi, T. Takatsuki, M. Torii, K. Sanui, and N. Ogata, Enantioselective permeation of α -amino acid isomers through poly(amino acid)-derived membranes, *Macromolecules*, 23 (1990) 2748.
19. T. Aoki, K. Shinohara, T. Kaneko, and E. Oikawa, Enantioselective permeation of various racemates through an optically active poly{1-[dimethyl(10-pinanyl)silyl]-1-propyne} membrane, *Macromolecules*, 29 (1996) 4192.
20. T. Aoki, M. Ohshima, K. Shinohara, T. Kaneko, and E. Oikawa, Enantioselective permeation of racemates through a solid (+)-poly{2-[dimethyl(10-pinanyl)silyl]norbornadiene} membrane, *Polymer*, 38 (1997) 235.

21. M. F. Kemmere and J. T. F. Keurentjes, Membranes in chiral separations, in Subramanian, G. (Ed.), *Chiral separation techniques, a practical approach*, Wiley-VCH, New York, 2001, pp. 127-150.
22. S. A. Piletsky, T. L. Panasyuk, E. V. Piletskaya, J. A. Nicholls, and M. Ulbricht, Receptor and transport properties of imprinted polymer membranes- a review, *J. Membrane Sci.*, 157 (1999) 263.
23. H. B. Ding and E. L. Cussler, Fractional extraction with hollow fibers with hydrogel-filled walls, *AIChE J.*, 37 (1991) 855.
24. H. B. Ding, M. C. Yang, D. K. Schisla, and E. L. Cussler, Hollow fiber liquid chromatography, *AIChE J.*, 35 (1989) 814.
25. H. B. Ding, P. W. Carr, and E. L. Cussler, Racemic leucine separation by hollow-fiber extraction, *AIChE J.*, 38 (1992) 1493.
26. T. Takeuchi, R. Horikawa, and T. Tanimura, Complete resolution of DL-isoleucine by droplet counter-current chromatography, *J. Chromatogr.*, 284 (1984) 285.
27. T. Takeuchi, R. Horikawa, and T. Tanimura, Enantioselective solvent extraction of neutral DL-amino acids in two-phase systems containing N-n-alkyl-L-proline derivatives and copper (II) ion, *Anal. Chem.*, 56 (1984) 1152.
28. T. Takeuchi, R. Horikawa, T. Tanimura, and Y. Kabasawa, Resolution of DL-Valine by counter-current solvent extraction with continuous sample feeding, *Sep. Sci. Technol.*, 25 (1990) 941.
29. A. L. Creagh, B. B. E. Hasenack, A. v. d. Padt, E. J. R. Sudhölter, and K. v. 't Riet, Separation of amino acid enantiomers using micellar enhanced ultrafiltration, *Biotechnol. Bioeng.*, 44 (1994) 690.
30. Overdevest, P. E. M., Enantiomer separation by ultrafiltration of enantioselective micelles in multistage systems, Thesis (2000) Wageningen University and Research centre.
31. P. E. M. Overdevest, A. v. d. Padt, J. T. F. Keurentjes, and K. v. 't Riet, Langmuir isotherms for enantioselective complexation of (D)-L-phenylalanine by cholesteryl-L-glutamate in nonionic micelles, *Colloids Surfaces A*, 163 (2000) 209.

Chapter 1

32. P. E. M. Overdeest and A. v. d. Padt, Optically pure compounds from ultrafiltration, *Chemtech*, 29 (1999) 17.

2 Design criteria for dense permeation-selective membranes for enantiomer separations

Abstract

Dense enantioselective membranes can distinguish between two enantiomers by different mechanisms. At this moment it is not clear which mechanism provides the best membranes for large-scale enantiomer separations. Therefore, we studied the design criteria for permeation-selective membranes combining literature data, experiments and model calculations. Literature data on dense permeation-selective membranes for enantiomer separation show that these membranes could be divided into two different classes: diffusion selective and sorption selective. Reviewing the literature on diffusion-selective membranes shows that these membranes have one main disadvantage: the inverse proportionality relation between the permeability and selectivity. This disadvantage is absent for sorption-selective membranes. As a model system, the diffusion of phenylalanine through a packed bed of polypropylene beads coated with N-dodecyl-L-hydroxyproline:Cu(II) was studied. The experiments showed that the material could selectively adsorb phenylalanine (Phe) with a selectivity (D/L) of 1.25. However, no permeation selectivity could be detected. With a dual sorption model these results could be interpreted. These model calculations showed that the permeation selectivity only approaches the intrinsic selectivity of the selector if the selectively adsorbed population is mobile and the non-selective permeation is minimized. Therefore, in our opinion more emphasis should be put on the development of sorption selective membranes.

This chapter has been published as: E.M. van der Ent, K. van 't Riet, J.T.F. Keurentjes, A. van der Padt, "Design criteria for dense permeation-selective membranes for enantiomer separations", *Journal of Membrane Science*, 185 (2001) 207-221.

2.1 Introduction

Many compounds applied in the agrochemical, food and pharmaceutical industry contain one or more chiral centers. The enantiomers of one pair often have different effects on their targets. Therefore, they have to be applied in their optically pure form to prevent unwanted side effects or environmental burden [1]. There are several ways to arrive at optically pure enantiomers such as chemical synthesis using a chiral substrate or using a chiral (bio)catalyst. Another routine is chemical synthesis of a racemate in combination with a resolution step [2]. Unfortunately, separation of enantiomers is difficult because of their equal physical properties. The only way to tackle this problem is to apply the separation of enantiomers in a chiral environment.

In the past decades many research groups have focussed their research on enantiomer separations in a chiral environment [3-8]. Most of this work has been performed for the separation of enantiomers on an analytical scale. As a result, for almost every enantiomer pair an analytical method exists for the complete separation via e.g. gas chromatography, liquid chromatography or capillary electrophoresis. However, for large-scale production of optically pure products no generally applicable method exists in spite of the effort that has been made to arrive at large-scale enantiomer separation processes [9-11].

One of the potential areas for large-scale separations of enantiomers is the application of chiral membranes, because of the advantages of membrane systems in general. Of course, research challenges still exist for membrane system design e.g. their low number of transfer units per apparatus in comparison with chromatographic systems. Membrane systems tend to be inherently low-energy consuming and operate by a different mechanism than do other separation methods, thus providing a unique profile of strengths [12].

Three classes of membrane systems can be distinguished for the separation of enantiomers. One system makes use of enantiospecific catalysis, which has large-scale potential [13]. The other two systems are based on diastereomeric interactions, which are still in their research phase, i.e. liquid membranes and dense chiral membranes. In the case of liquid membranes, an enantioselective carrier dissolved in a liquid transports the enantiomer via selective binding from the donating phase to the receptor phase [14]. A common problem of liquid membranes is their lack of long-term stability. Dense membranes do not have this stability problem. These membranes consist of a dense matrix of a chiral polymer that can invoke enantiospecific interactions during sorption and/or diffusion. This so-called solution/diffusion mechanism causes a selective permeation through the membrane. For the development of these membranes,

several design criteria must be taken into account to arrive at membranes that show selective permeation.

In this paper we present a study on the properties required by dense permeation-selective membranes for enantiomer separation.

2.2 Theory

For a given productivity, the two most important membrane properties that determine the dimensions of the process are the permeability and the permeation selectivity [15].

The permeability of a membrane is defined as the normalized flux with respect to the concentration difference and the thickness of the membrane. This parameter is therefore an intrinsic membrane property. The permeation through a homogeneous film is determined by the solubility and the diffusivity of the molecules in the polymer matrix. This so-called solution-diffusion mechanism can be described analogous to the gas separation theory [16] for enantiomers:

$$P_e = S_e \cdot D_e \quad (1)$$

where P is the permeability, S is the sorption coefficient and D is the diffusion coefficient. The subscript e indicates the D or L enantiomer.

The sorption coefficient (S) is a thermodynamically determined parameter; it is defined as the ratio of the equilibrium membrane concentration (c_{membrane}) and the concentration in the bulk liquid (c_{bulk}):

$$S = \frac{c_{\text{membrane}}}{c_{\text{bulk}}} \quad (2)$$

In the ideal case, the relation between these two concentrations is a linear relation i.e. S is constant. When the number of binding sites is limited, the solubility cannot be described by a linear partitioning relation but can e.g. be described by a Langmuir relation. Contrary to the sorption coefficient, the diffusion coefficient is a kinetically determined parameter. To what extent the diffusion interactions are dissimilar for the two enantiomers depends on the properties of the polymer matrix, e.g. the mutual attractive forces between the polymer segments and secondary structures like helices, crystalline structures and pores. As a result, enlargement of the space between the polymer segments could cause an increase of the permeability, however, this will also strongly effect the chiral discrimination during diffusion, i.e. it will lower the membrane selectivity.

Permeation selectivity

The permeation selectivity of a membrane is defined as the permeability ratio of the penetrants, in our case the two enantiomers. Analogous to Equation (1),

the permeation selectivity ($\alpha_{D,L}^P$) is the product of the "sorption selectivity" ($\alpha_{D,L}^S$) and the "diffusion selectivity" ($\alpha_{D,L}^D$):

$$\alpha_{D,L}^P = \frac{P_D}{P_L} = \frac{S_D}{S_L} \cdot \frac{D_D}{D_L} = \alpha_{D,L}^S \cdot \alpha_{D,L}^D \quad (3)$$

Although many enantioselective membranes have been described in literature, the distinction between these two selectivities is only made implicitly. In the following paragraphs we will denote the differences between these two selection mechanisms.

Diffusion-selective membranes

In this thesis, the definition of a diffusion-selective membrane is a membrane consisting of a chiral polymer, which do not have any specific chiral selector sites. These chiral polymers can either be coated on a non-chiral support layer or can be self supporting [17-25]. Diffusion selectivity is caused by chiral discrimination during diffusion, i.e. the summation of chiral interactions causing one enantiomer to diffuse more readily than the other. Examples of polymers that can yield such a difference in diffusion velocity are cellulose, chitosan, poly(hydroxyethyl methacrylate), poly(amino acids). Most of the diffusion-selective membranes also exhibit some sorption selectivity, however, these membranes still are denoted diffusion-selective because their sorption selectivity is not caused by a one-to-one molecular interaction.

Literature data show that the main disadvantage of diffusion selective

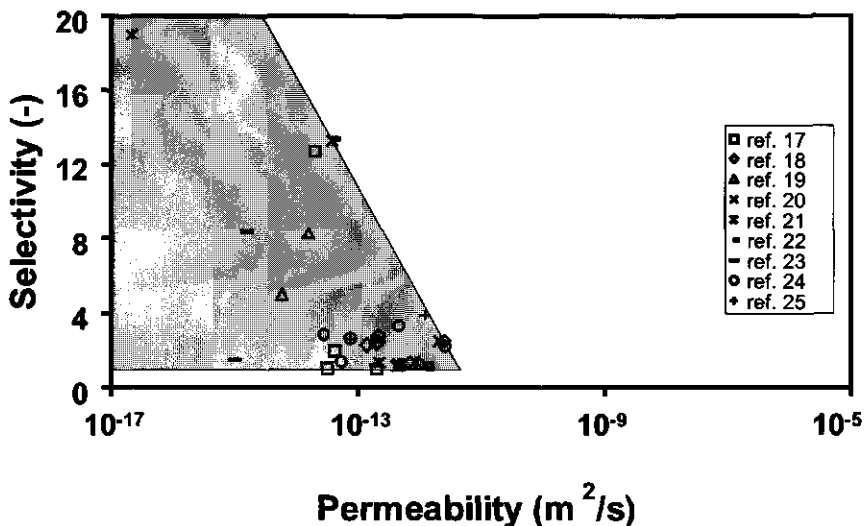


Figure 1: The relation between the permeability and the selectivity of diffusion-selective membranes. Presented data are derived from literature data [17-25].

membranes is the relation between the permeability and the selectivity. When the selectivity of these membranes is high the permeability usually is very low and vice versa. This is shown in Figure 1 in which the permeability versus the selectivity is plotted for a number of diffusion-selective membranes described in literature [17-25].

Figure 1 shows a well-defined area in which all points are located. The best membranes would have a high permeability and high selectivity; this is the right upper part of the figure. However, the membranes cited in literature are in the lower left part of the figure. In order to evaluate these membranes for large-scale separation processes, we calculated the required membrane area for the production of 1 kg of 99% pure enantiomer per day.

The calculations are carried out with the relations for a counter-current cascade of single dialyzers (Figure 2) as described by Noda and Gryte [26]. This system appears most appropriate due to its ability to separate binary mixtures in high purity products by means of a dialysis process. Additionally, the dilution of the end products is minimal due to concentrating steps in the cascade. High product concentrations are desirable for a feasible process. The mathematical relations describing this system are analogous to the design relations for a distillation column. For an optimization of the system, the minimal number of stages is calculated with the Fenske relation, and the minimal reflux ratio can be calculated with the Underwood relations as given in [27]. With the

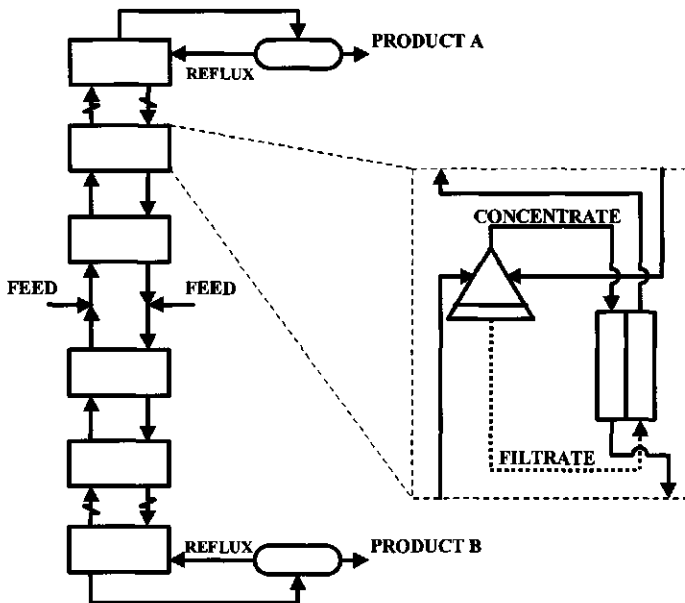


Figure 2: Counter-current cascade. Each stage corresponds with a concentrator-dialyzer pair. From Noda and Gryte [26].

minimal number of stages and the minimal reflux ratio, the actual reflux ratio can be calculated with the Molokanov equation [27]. The number of stages is set to 2 times the minimal number of stages. The number 2 is a rule of thumb as is described in [27]. The reflux ratio and the number of stages can then be used for the overall input-output response equations [26] to calculate the dialysis coefficient (θ). This dialysis coefficient is a function of the membrane surface area (A) as described by Noda and Gryte [26]:

$$\theta = \frac{K_{ov} \cdot A}{Q} \quad (4)$$

where K_{ov} is the overall mass transfer coefficient and Q is the volumetric flow rate.

Rewriting Equation (4) yields the total membrane surface area. By neglecting the mass transfer resistance in the liquid –which is in most cases optimistic– the overall mass transfer coefficient is approximated by the membrane permeability divided by the membrane thickness ($=10 \mu\text{m}$; arbitrarily chosen). The permeability is calculated as a function of the selectivity using the right borderline of the shaded area in Figure 1. This borderline describes the best membrane parameters currently available. The results of the calculations for the production of 1 kg enantiomer per day, with a 99% purity and a feed concentration of 1 wt-% are shown in Figure 3.

This figure shows that at least a total membrane area of about 4000 m² and 15 equilibrium stages are needed. The internal reflux ratio for this case equals

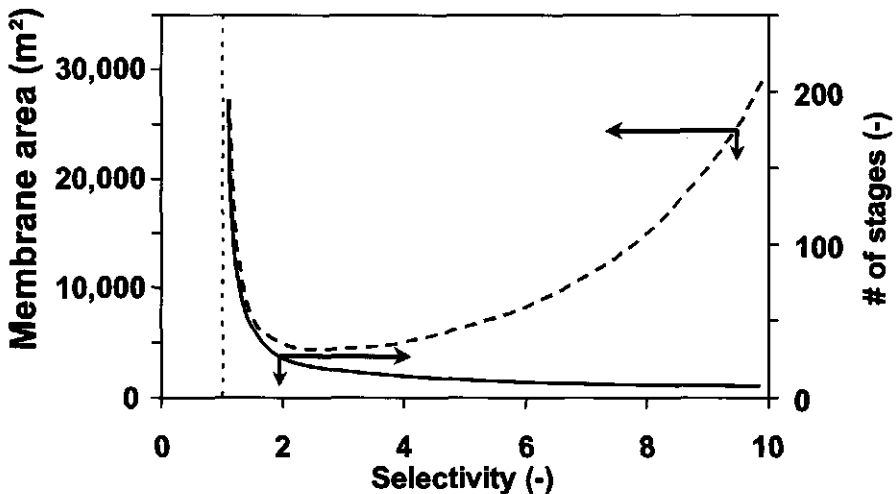


Figure 3: Total membrane surface area and total number of stages versus membrane selectivity for a counter-current cascade of single dialyzers as described by Noda and Gryte [26]. The permeability used for the calculations is a function of the selectivity, i.e. the right border of the shaded area in Figure 1. Production = 1 kg/day, feed concentration = 1 wt-% and purity = 99%,

0.5. Whether these parameters are suitable for a feasible separation process will depend on the enantiomer and its economical profits. Of course, also the demanded purity of the end product determines the total membrane area. It has to be noted, however, that these calculations assume that the fluid stream has the same average concentration throughout the stages. Hence, for each membrane separation stage also one reverse osmosis or evaporator unit has to be installed. According to Noda and Gryte [26] this will be the cost determining aspect.

Figure 3 also shows that the number of stages decreases with increasing selectivity. If the permeability is taken to be constant, the total membrane area will be proportional to the number of stages. In that case, a selectivity in excess of 3 hardly decreases the total membrane surface area. This is also shown for pressure driven membrane processes by Keurentjes *et al.* [15]. However, the permeation decreases upon increasing selectivity, resulting in an increase of the total membrane area. Therefore, it might be obvious to look for membranes using a different separation principle.

Sorption-selective membranes

Sorption-selective membranes mainly make use of a chiral selector embedded in a polymer matrix. In most cases, these selectors are known from analytical separation methods and form a one-to-one complex with the enantiomer by means of a specific molecular interaction. Examples are amino acid copper complexes [28,29], cyclodextrins [30], crown ether derivatives [31] and Pirkle type selectors [32]. Also molecular imprinted polymers can be regarded as sorption-selective membranes, because during the imprinting procedure cavities are formed that can form one-to-one molecular complexes.

For sorption-selective membranes the inverse proportionality between the permeability and the permeation selectivity is not expected. By loosening the polymer matrix the diffusivity increases, but the chiral recognition remains the same. Of course this still gives an optimization problem since an increasing diffusivity is generally not an increase of selective diffusion only. To find the optimization criteria, we have set up a model for permeation through sorption-selective membranes.

2.3 Modeling

For the modeling of sorption-selective membranes, we assumed two populations of each enantiomer in a homogeneous membrane: one population is selectively adsorbed by the chiral selectors while the other population is non-selectively absorbed in the polymer matrix (see also Figure 4). In total, two populations of both enantiomers are present and, therefore, four mass balances

are required. The selectively adsorbed population and non-selectively adsorbed population are assumed to be in equilibrium, i.e. no reaction limitation but only diffusion limitation is assumed.

Fick's second law can describe the diffusion through a plane sheet. During the diffusion process adsorption and desorption take place with the chiral selectors. This adsorption/diffusion process can be described with the following dimensionless mass balance equations (Appendix A):

$$\frac{dC_{D,L}}{dF_0} = \frac{d^2 C_{D,L}}{dX^2} - Da \cdot (-Q_{D,L} + K_{D,L} \cdot C_{D,L} \cdot (Z \cdot S - Q_D - Q_L)) \quad (5)$$

$$\frac{dQ_{D,L}}{dF_0} = F \cdot \frac{d^2 Q_{D,L}}{dX^2} + Da \cdot (-Q_{D,L} + K_{D,L} \cdot C_{D,L} \cdot (Z \cdot S - Q_D - Q_L)) \quad (6)$$

with the boundary conditions:

at $X = 0$:

$$C_{e0}^* = C_{e0} \cdot S; \quad Q_{e0}^* = \frac{K_e \cdot C_{e0} \cdot Z \cdot S}{1 + \sum_{i=D,L} K_i \cdot C_{i0}}; \quad C_{e0} = 1 \quad (7)$$

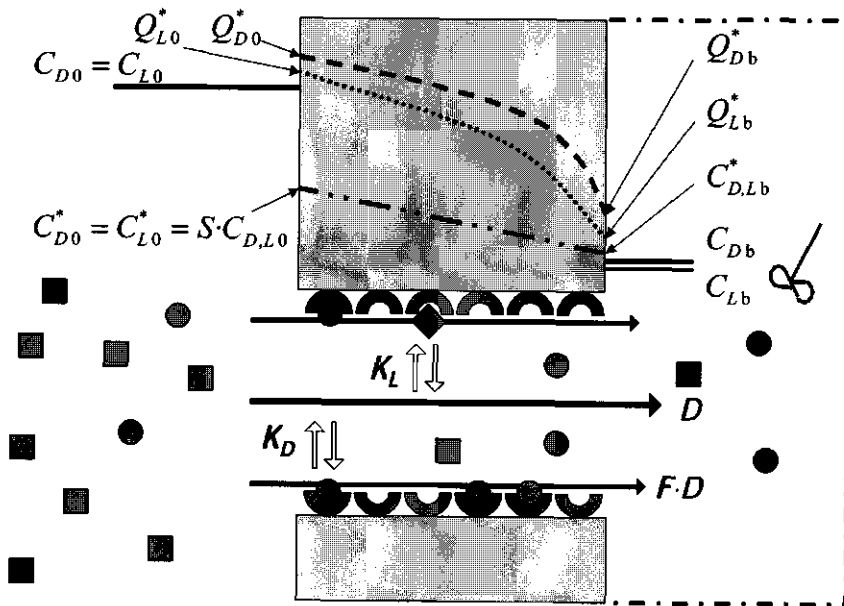


Figure 4: Schematic representation of transport through a sorption-selective membrane, including an indication of the concentration profiles and accompanying symbols

at $X=1$:

$$C_e^* = Cb_e \cdot S; Q_{e0}^* = \frac{K_e \cdot Cb_e \cdot Z \cdot S}{1 + \sum_{i=D,L} K_i \cdot Cb_i}; \quad (8)$$

$$\frac{dCb_e}{dFo} = \left(\frac{dC_e}{dX} + F \cdot \frac{dQ_e}{dX} \right) \cdot \lambda$$

where C_e ($=c_d/c_0$) is the dimensionless free concentration of D or L enantiomer, c_0 is the retentate concentration which is a constant, Fo ($=D \cdot t/l^2$) is the Fourier number, t is time, l the membrane thickness and D the diffusion coefficient of the non-selectively absorbed population, X ($=x/l$) is the dimensionless distance, Da ($=k_f \cdot l^2/D$) is the Damköhler number, in which k_f is the adsorption rate constant, Q_e ($=q_d/c_0$) is the dimensionless complexed concentration of the D or L enantiomer, K_e ($=k_e \cdot c_0$) is the dimensionless affinity constant for the D or L enantiomer of the chiral selector, Z ($=Q_s/S$) is the ratio of the dimensionless capacity of the chiral selector in membrane ($Q_s = q_s/c_0$) and the non-selective sorption coefficient (S), Cb_e ($=c_d/c_0$) is the dimensionless permeate concentration, and λ ($=l \cdot A/V$) is the ratio of membrane thickness (l) and vessel 'thickness' (V/A = volume-area ratio). The index * stands for the membrane surface concentration, 0 for the retentate concentration at $t = 0$, e for the D or L-enantiomer and s for the saturation concentration (maximum capacity).

This model is analogous to the dual sorption theory for gas separation modeling. The differences are in the boundary conditions and the split of the calculation into two populations: the selectively adsorbed population (Q) and the non-selectively absorbed population (C). This is in contrast to what is usually done in gas separation modeling: usually only one single mass balance for the total concentration is used ($=Q + C$). Consequently, an additional boundary condition must be defined: the selectively adsorbed population at the membrane surface is in equilibrium with the bulk concentration and not via the non-selectively adsorbed population. This split up of the concentrations has the benefit that if no non-selective adsorption takes place still a permeation flux can be present.

Most of the dimensionless model parameters are rather straightforward. The Damköhler (Da) number is the ratio of the diffusion rate and reaction rate for complexation. For diffusion limitation $Da \gg 1$ and for reaction limitation Da approaches 0. In this study only diffusion limitation was modeled. The ratio of the membrane volume and the vessel volume (λ) is an important parameter in the determination of the overall permeability. This determines whether the concentration in the permeate vessel remains more or less at the starting condition, i.e. a constant concentration difference between the retentate and permeate side while the membrane concentration profile is at pseudo steady

state. At pseudo steady state the intrinsic permeability is found while at changing concentration gradients the apparent permeability is found as a function of the concentration gradient. The parameter F is the ratio of the mobilities of the selectively adsorbed population and the non-selectively adsorbed population. This parameter is important for sorption-selective membranes since it determines whether or not the membrane is permeation selective. This will be shown with the calculation results.

The sorption coefficient for the non-selective population can be interpreted in two different ways. The first one is to interpret the polymer matrix as a dense homogeneous matrix in which the molecules can dissolve with a certain concentration. The second interpretation is that the membrane is considered as a porous matrix; in the polymer part, the molecules cannot dissolve (solubility equals 0) and in the pores the solubility equals 1. In the latter model the non-selective sorption coefficient is proportional to the membrane porosity.

2.4 Experimental

To study the effects of adsorption and permeation in sorption-selective membranes, diffusion through a packed bed was studied. This packed bed consisted of material coated with a chiral selector. We chose for a packed bed instead of a coated membrane to mimic a porous membrane with a large pore length (3 cm) to increase the adsorption capacity, thus allowing for a larger distinction between selective adsorption and selective permeation.

Chemicals

Amino acids D,L-phenylalanine and 4-hydroxy-L-proline were purchased from Sigma and were used without any further purification. Dodecylhydroxyproline was synthesized according to the method described by Takeuchi et al [33]. The yield was about 30% and the $[\alpha]_D^{20}$ was -44.6° . All other chemicals were of analytical grade or better and were used as received.

Packed bed

The packed bed consisted of macro porous polypropylene (PP) beads (Accurel EP100; $d_{\text{particle}} = 250\text{--}600 \mu\text{m}$; $d_{\text{pore}} = 0.1\text{--}1 \mu\text{m}$; $A_{\text{specific}} = 50 \text{ m}^2/\text{g}$; void volume = 75 % v/v) coated with dodecylhydroxyproline (DHP) and Cu(II). For the coating, ten grams of the PP-beads were first wetted with 50 mL 100% methanol solution. After ten minutes of sonification 200 mL of coating solution was added under continuous stirring. The coating solution consisted of $2 \cdot 10^{-2}$ M NaOH (pH was about 11.8), 1 M NaCl and 0.02 M DHP. The suspension was stirred overnight. The beads were filtered and washed with 0.1 M acetate buffer

solution (pH =6) and were subsequently washed with double distilled water. The material was packed in a column (height x diameter = 3 x 3 cm). The column was rinsed with 200 mL CuCl_2 (5 mM) solution and was subsequently rinsed with 250 mL double distilled water. The column was placed in a batch set-up (Figure 5) and the retentate side, column void and permeate side were filled with 200 mL double distilled water. The experiment started by addition of 20 mL D,L-phenylalanine (50 mM) to the retentate side resulting in a starting concentration (c_0) of about 2.3 mM for both enantiomers. Samples of 1 mL were taken twice a day from both retentate and permeate.

Analysis

For the analysis of enantiomer ratios the samples were analyzed by HPLC. The system consisted of a Spectra Physics SP8810 pump, a Thermo Separation® Products AS1000 autosampler and a Separations UV detector. The column used for the separation was a 150 mm x 4 mm i.d. Daicel Crownpak CR(+) (5 μm). Mobile phase elution (0.8 mL/min) was performed isocratically using a filtered (0.45 μm) and degassed aqueous solution of perchloric acid (pH =2.0). The column temperature during analysis was maintained at 5°C. The injected sample volume was 20 μL and the samples were injected without any pre-treatment. The wavelength setting of the UV detection was fixed at 254 nm. The calibration curves showed a linear relation up to a total (D-Phe plus L-Phe) concentration of 5 mM.

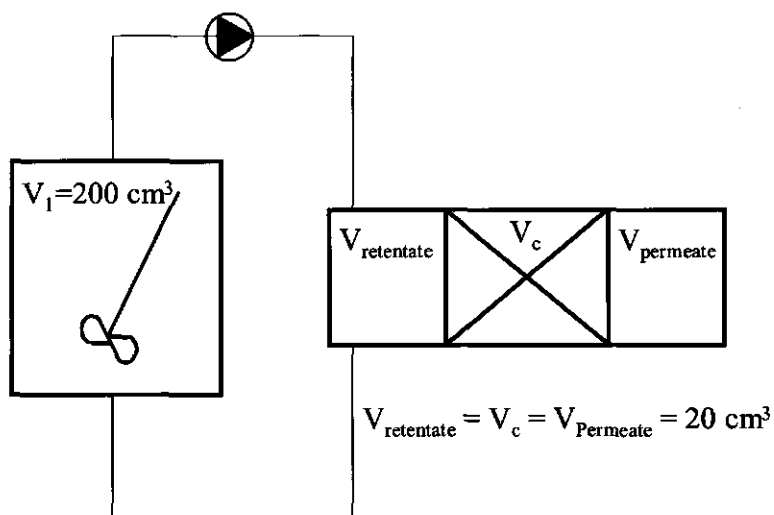


Figure 5: Schematic drawing of the experimental set-up. $V_{\text{permeate}} = 20 \cdot 10^{-6} \text{ m}^3$; bed length = $3 \cdot 10^{-2} \text{ m}$; bed diameter = $3 \cdot 10^{-2} \text{ m}$; $V_{\text{retentate}} = 220 \cdot 10^{-6} \text{ m}^3$.

Transport-model simulations

With Equations (5) and (6) and the boundary conditions (7) and (8), the concentration as a function of time was calculated. The equations were approximated by a finite difference method (appendix A) and were implemented in the software package Matlab 5.3 of Mathworks Inc. The number of spatial steps for the finite difference method was 20 and the number of time steps was variable, determined by the Matlab differential equation solver. The permeability for the D and L enantiomer was calculated from this concentration versus time curve in the usual way [34]. With these permeabilities the selectivity could be calculated according to Equation (3). The parameters K_D , Z and F were varied over the ranges indicated in Table 1, which have been divided in 25 logarithmically scaled points.

Table 1: Simulation parameters

Parameter	Value
Dimensionless affinity constant (K_D)	10^{-2} - 10^2
Sorption coefficient (S)	10^{-2} - 10^2
Dimensionless mobility of adsorbed population (F)	10^{-10} - 10^2
Number of place steps	20
Capacity of chiral selectors (Q_s)	1
Intrinsic selectivity	10
Damköhler number (Da)	10^6
Volume ratio of membrane and retentate phase (λ)	10^{-6}

2.5 Results and discussion

Diffusion through a packed bed

The results of phenylalanine (Phe) diffusion through a packed bed are shown in Figure 6. This figure shows that the breakthrough curve of D-Phe differs from the breakthrough curve of L-Phe. This is caused by selective adsorption of D-Phe onto the column material. The affinity of the selector for D-Phe is higher than for L-Phe, which is in agreement with the results of Davankov and co-workers [35] and Takeuchi and co-workers [11]. The selectivity that could be calculated from this experiment was 1.25 by assuming a diffusion coefficient for phenylalanine of $1 \cdot 10^{-10}$ m²/s and by assuming that 25% of the dodecylhydroxyproline in the coating solution was adsorbed on the polypropylene beads. This value of 1.25 is lower than described by Davankov and co-workers. They found for hexadecylhydroxyproline coated on a LiChrosorb RP-18 column a value for the selectivity for phenylalanine of around

2. This is probably due to the difference in coating technique. The dodecylhydroxyproline (DHP) is coated at $\text{pH} = 12$ because it is insoluble at $\text{pH} = 6$. To prevent desorption from the polypropylene beads, the pH is lowered during the coating procedure from 12 to 6, thus precipitation of DHP will occur. This will probably result in an unfavorable configuration. On the other hand the material can still selectively adsorb phenylalanine. Unfortunately, from these results we could not calculate a reasonable value for the affinity parameters. This is probably due to the high affinity of these types of complexes [36]. When the affinity is high, the equilibrium concentration is in the plateau region of the Langmuir isotherm and therefore the affinity cannot be calculated. Below, it will be shown that we are able to calculate the appropriate affinity constants by using the permeation model we developed.

Figure 6 also shows that although the adsorption onto the material is selective, the permeation of phenylalanine through the packed bed is not selective. The slopes for D-Phe and L-Phe are the same in the linear part of the curve. If the slopes are equal, the fluxes and consequently the permeabilities will be the same. According to Equation (3) the permeation selectivity then equals unity. The only effect observed is a start up effect: first the column material is 'loaded', and once the adsorbed concentration is in equilibrium with the free concentration only non-selective permeation takes place.

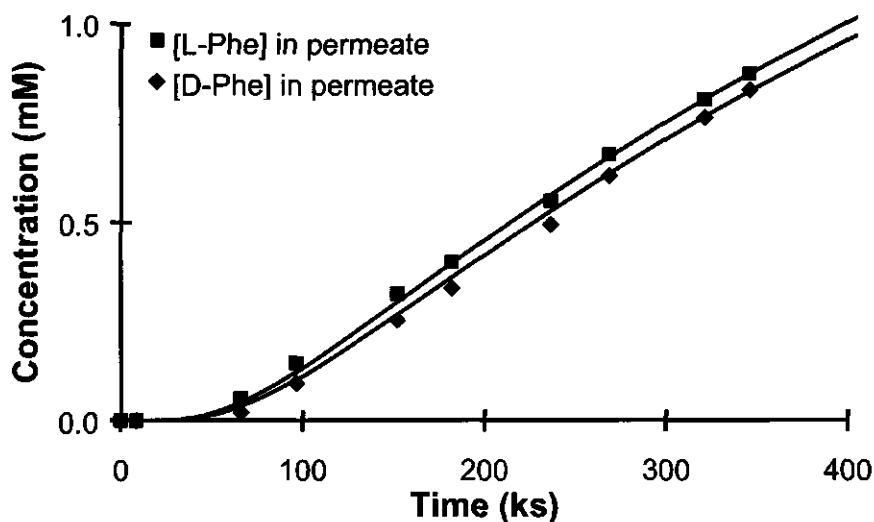


Figure 6: The permeate concentration of D-Phe and L-Phe versus time for the diffusion through a packed bed of polypropylene coated with N-dodecyl-L-hydroxyproline:Cu(II).; $V_{\text{permeate}} = 20 \text{ cm}^3$; $V_{\text{retentate}} = 220 \text{ cm}^3$; $C_{\text{retentate}, D}^0 = 2.3 \text{ mol/m}^3$; $C_{\text{retentate}, L}^0 = 2.3 \text{ mol/m}^3$. The solid lines are the best fit of the model described in paragraph 2.2; $k_D = 23.9 \text{ mM}^{-1}$; $k_D/k_L = 1.25$.

Near the end of the curve it seems as if the two curves come together. This is due to the driving force over the column for the two enantiomers. The retentate contains approximately the same concentration D-Phe as L-Phe because of the large volume of the retentate phase compared to the permeate phase. Therefore, after an infinitely long period of time the retentate concentration should equal the permeate concentration.

This type of experiments has also been done with dodecylhydroxyproline adsorbed on a polypropylene microfiltration membrane. There we found that even the start up effect could not be detected, probably because of the low capacity of the membrane.

The main conclusion from the above-mentioned results is that, although sorption selectivity can be observed with this type of selectors (amino acid:Cu(II)), the operational selectivity will equal unity. The explanation for this will be shown by the model calculation results.

Model calculations

The permeation selectivity is calculated as function of three parameters: the dimensionless mobility of the selectively adsorbed population (F), the ratio of the chiral selector maximum capacity and the non-selective solubility (Z) for various dimensionless affinity constants (K_D). Figure 7 shows the operational permeation selectivity as a function of Z and F , for $K_D = 10^{-2}$ (left graph) and $K_D = 10^2$ (right graph), respectively.

Figure 7 shows a large area where the permeation selectivity equals unity. This is the case where both F is low (low diffusion coefficient of the selective population) and Z is low (high non-selective sorption). The boundary between the selective area and the non-selective area ($\alpha > 1.1$) appears to be a linear relation between $\log(F)$ and $\log(Z)$:

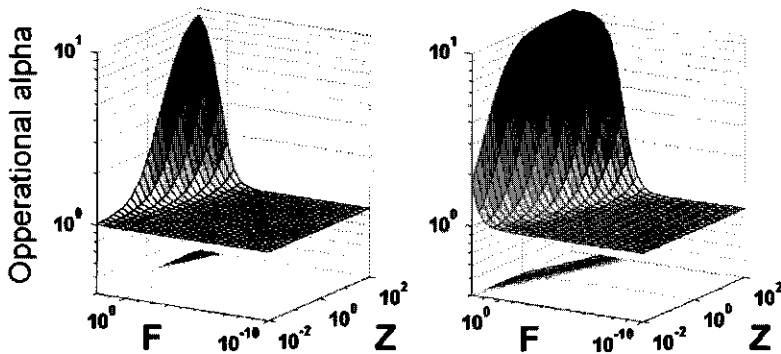


Figure 7: Operational selectivities as function of the ratio of the chiral selector capacity and the non-selective solubility (Z) and the dimensionless mobility of the selective adsorbed population (F).

$$\log(F)|_{\alpha=1.1} = -a \cdot \log(Z) + b \quad (9)$$

Here a is the slope and b is the intercept with $\log(Z)=0$ ($Z=1$).

Hence, in case of selective membranes the following equation must hold:

$$\log(F)|_{\alpha>1.1} + a \cdot \log(Z) > b \quad (10)$$

The slope (a) is for all cases of K_D equal to one. In contrast, the intercept (b) depends on K_D . The relation between K_D and b is shown in Figure 8, where the line is a one parameter fit using the equation:

$$b = \frac{1}{c \cdot (1 - e^{-K_D})} \quad (11)$$

Here c is the fit parameter; for Figure 8, c equals 10.

The left part of the curve (range 1) shows a linear relation between the $\log(K_D)$ and $\log(b)$ and the right part of the curve (range 3) shows a plateau value. The linear part of the curve (range 1) is explained by the fact that for this range of dimensionless affinities the selectively adsorbed membrane concentration is linearly dependent on the bulk concentration, i.e. the linear part of the Langmuir isotherm. The plateau value is explained by the fact that for a high affinity –or high feed concentration– the membrane concentration will be constant, i.e. equal to the maximum adsorption capacity (Q_s). The range between the ranges

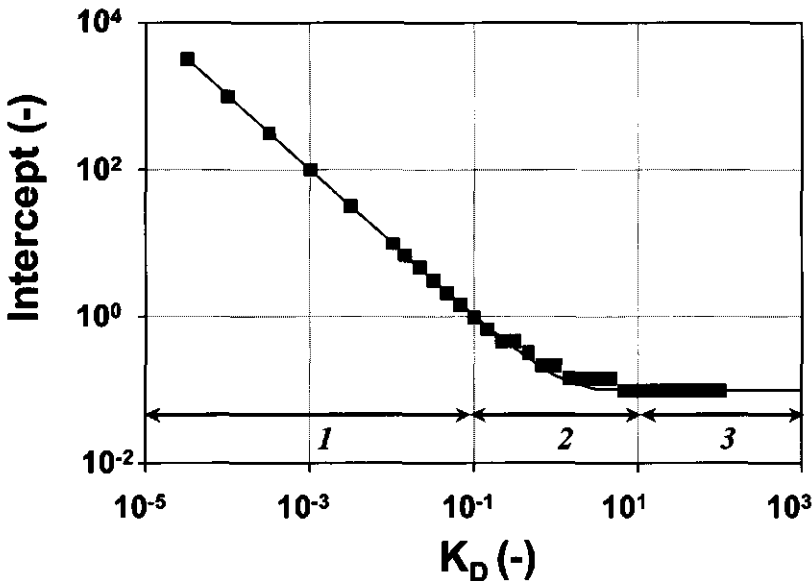


Figure 8: Relation between intercept b and the dimensionless affinity constant K_D . The points are the intercepts of the fitted borders from the calculations with 25 different K_D values. The line is a one parameter fit (Equation (11)). The discrete values of K_D at the bend of the curve ($10^{-1} < K_D < 10^1$) show that the number of grid points of F and Z is rather low.

1 and 3 (range 2) is the transition range between the two regimes. The discretization procedure followed leads to a relatively low number of data points in this range. However, the curve draws the points in this range ($10^{-1} < K_D < 10^1$) still rather well.

To obtain an efficient membrane, b should be as low as possible. Therefore, K_D should be larger than 0.1. This implies that for an efficient process the affinity must not be too low in comparison with the feed concentration. Combination of Equations (10) and (11) yields a relation between F , Z and K_D for the boundary conditions for permeation-selective membranes with a sorption-selective mechanism:

$$\log(F \cdot Z) \Big|_{\alpha > 1.1} > \frac{1}{10 \cdot (1 - e^{-K_D})} \quad (12)$$

This Equation shows that both mobility (F) and sorption (Z) are important for the design of chiral membranes. When the adsorbed population is not mobile, the membrane will not show any permeation selectivity although the adsorption is selective. Most sorption-selective membranes do not have a mobile selectively adsorbed population [31,37]. Also our experiments showed that the adsorbed population was not mobile (see above). In order to enforce a mobile selectively adsorbed population, additional forces on the population should be applied. Yoshikawa *et al.* have shown that this concept can work for molecular imprinted membranes [38]. They have shown that by using electrical forces the mobility increased, thus leading to a selectivity deviating from unity.

Besides the significance of the mobility, also the ratio of selector capacity and non-selective sorption coefficient (Z) is of importance. For the selective part of the curve, i.e. where Equation (12) is valid, the operational selectivity (α) decreases with increasing non-selective sorption (Z is low). Therefore, non-selective sorption should be minimized (Z is high) in order to have the highest benefit of the intrinsic selectivity.

With this model we are able to describe the data of the diffusion through the packed bed when the velocity of the selectively adsorbed population is set to zero (solid lines in Figure 6). Therefore, the affinity parameters, k_D and k_L , and the diffusion coefficient are used as fit parameters. From this fit we found that k_D equals 23.9 mM^{-1} . This result is in good agreement with results, which has been found by Overvest and co-workers [36]. They have found for the cholesterol-L-glutamate selector with Cu(II) as complexant a k_D value of 28 mM^{-1} for phenylalanine. From the fitted k_L , a selectivity of 1.25 was found. This value is also in good agreement with the before mentioned value (1.25), which was calculated from the experimental data. So also from these results can be concluded that these types of chiral selectors, coated on a hydrophobic

substrate, are not very suitable for sorption-selective membranes, in spite of their ability to selectively complex with one of the enantiomers.

2.6 Conclusions

Dense enantioselective membranes can be divided into two classes: diffusion-selective membranes and sorption-selective membranes. A literature review shows that diffusion-selective membranes have an inverse proportionality between permeability and selectivity, which is the main disadvantage of these membranes. A system evaluation for diffusion selective membranes illustrated that today's working area of permeability and selectivity is likely not good enough to be applied for large-scale enantiomer separations. Therefore, it is concluded that the focus should be on a different separation principle, i.e. sorption-selectivity.

Sorption-selective membranes have their own characteristics: no selective permeation can be observed despite the fact that they show selective sorption. Model calculations showed that in order to reach permeation selectivity with this type of membranes, the selectively adsorbed population has to be mobile and non-selective permeation has to be minimal.

In our opinion, these model calculations and the literature data review show that the development of enantioselective membranes should focus more on the development of sorption-selective membranes with a mobile selectively adsorbed population to arrive at feasible large-scale enantiomer separation processes.

Appendix

Ficks' second law describes the diffusion of compound A through a plane sheet, e.g. a membrane:

$$\frac{dc_A}{dt} = D \cdot \frac{d^2c_A}{dx^2} \quad (\text{A.1})$$

where c_A is the concentration of component A, t is the time, D is the diffusion coefficient of component A through the membrane and x is the distance from the membrane surface.

If during diffusion also complexation takes place, an adsorption term must be added:

$$\frac{dc_A}{dt} = D \cdot \frac{d^2c_A}{dx^2} - \frac{dq_A}{dt}$$

where q_A is the adsorbed concentration in the membrane.

The complexation process between compound A and complexant B can be described by:



where k_1 and k_{-1} are the complexation and decomplexation rate constants.

The complex formation rate (r_{AB}) will be equal to:

$$r_{A+B \rightarrow AB} = k_1 \cdot c_A \cdot c_B \quad (\text{A.3})$$

For decomplexation:

$$r_{AB \rightarrow A+B} = -k_{-1} \cdot c_{AB} \quad (\text{A.4})$$

At equilibrium, the rates of complexation and decomplexation are equal.

Combining Equations (A.1), (A.3) and (A.4) yields:

$$\frac{dc_A}{dt} = D \cdot \frac{d^2c_A}{dx^2} - (k_1 \cdot c_A \cdot c_B - k_{-1} \cdot c_{AB}) \quad (\text{A.5})$$

For the complexant B the following mass balance holds:

$$c_B = c_B^0 - c_{AB} \quad (\text{A.6})$$

where c_B^0 is the membrane capacity. For clarity we further denote all complexed species with a 'q', so c_{AB} becomes q_A and the membrane capacity c_B^0 becomes q_s . Hence, combining Equations (A.5) and (A.6) yields:

$$\frac{dc_A}{dt} = D \cdot \frac{d^2c_A}{dx^2} - (k_1 \cdot c_A \cdot (q_s - q_A) - k_{-1} \cdot q_A) \quad (\text{A.7})$$

Introducing the affinity constant ($k_A = \frac{k_{-1}}{k_1}$) yields:

$$\frac{dc_A}{dt} = D \cdot \frac{d^2c_A}{dx^2} - k_1 \cdot (c_A \cdot (q_s - q_A) - k_A \cdot q_A) \quad (\text{A.8})$$

Dimensionless numbers

To facilitate modeling the following dimensionless variables are introduced:

$$X = x/l, \quad Fo = \frac{D \cdot t}{l^2}, \quad Da = \frac{k_1 \cdot \bar{f}}{D}, \quad (A.9)$$

and for the concentrations and the affinity:

$$C_A = \frac{c_A}{c_A^0}, \quad Q_s = \frac{q_s}{c_A^0}, \quad Q_A = \frac{q_A}{c_A^0}, \quad K_A = k_A \cdot c_A^0 \quad (A.10)$$

where c_A^0 is the feed bulk concentration.

For the derivatives this yields:

$$\frac{dc}{dx} = \frac{dc}{dX} \cdot \frac{dX}{dx} = \frac{dc}{dX} \cdot \frac{1}{l}, \quad \frac{d^2c}{dx^2} = \frac{d^2c}{dX^2} \cdot \frac{1}{l^2}, \quad (A.11)$$

and

$$\frac{dc}{dt} = \frac{dc}{dFo} \cdot \frac{dFo}{dt} = \frac{dc}{dFo} \cdot \frac{D}{l^2}, \quad (A.12)$$

Combining Equations (A.8)-(A.12) yields:

$$\frac{dC_A}{dFo} = \frac{d^2C_A}{dX^2} - Da \cdot (-Q_A + K_A \cdot C_A \cdot (Q_s - Q_A)) \quad (A.13)$$

This equation is analogous to Equation (4) with the exception that Equation (A.13) is valid for one component while Equation (4) is valid for two components. The only difference is in the mass balance of c_B . The mass balance for a two-component (e.g. A and C) system is defined as:

$$C_B = Q_s - C_A - C_C \quad (A.14)$$

Analogous to Equation (A.13), an equation can be derived for the adsorbed population:

$$\frac{dQ_A}{dFo} = F \cdot \frac{d^2Q_A}{dX^2} + Da \cdot (-Q_A + K_A \cdot C_A \cdot (Q_s - Q_A)) \quad (A.15)$$

where F is the dimensionless diffusion coefficient:

$$F = \frac{D_q}{D_c} \quad (A.16)$$

where D_q is the diffusion coefficient of the complexed population and D_c is the diffusion coefficient of the free concentration:

Numerical solution

The partial differential equation is approximated with the central difference method [34]:

$$\frac{d^2 C_{A_i}}{dX^2} = \frac{C_{A_{i+1}} - 2 \cdot C_{A_i} + C_{A_{i-1}}}{\Delta X^2} \quad (\text{A.17})$$

Combining this equation with Equation (A.13) yields:

$$\frac{dC_{A_i}}{dFo} = \frac{C_{A_{i+1}} - 2 \cdot C_{A_i} + C_{A_{i-1}}}{\Delta X^2} - Da \cdot (-Q_{A_i} + K_A \cdot C_{A_i} \cdot (Q_s - Q_{A_i})) \quad (\text{A.18})$$

where i is the coordinate number for the places and ΔX is the step in the x -direction. The same holds for the adsorbed population:

$$\frac{dQ_{A_i}}{dFo} = F \cdot \frac{Q_{A_{i+1}} - 2 \cdot Q_{A_i} + Q_{A_{i-1}}}{\Delta X^2} + Da \cdot (-Q_{A_i} + K_A \cdot C_{A_i} \cdot (Q_s - Q_{A_i})) \quad (\text{A.19})$$

Boundary conditions

At the feed side no mass transfer limitation is assumed and the feed bulk concentration is assumed to be constant. Hence, at the membrane surface ($i=0$) the membrane surface concentration (C_{A_0}) and the adsorbed membrane surface concentration (Q_{A_0}) are:

$$C_{A_0} = S, \quad Q_{A_0} = \frac{K_A \cdot Q_s}{1 + \sum_i K_i} \quad (\text{A.20})$$

where i stand for the number of compounds.

For the permeate side also no mass transfer limitation is assumed but the compounds diffuse into a volume V which is ideally mixed. The mass balance over this volume is (in dimensionless numbers):

$$\frac{dCb_A}{dFo} = \left(\frac{dC_{i_A}}{dX} + F \cdot \frac{dQ_{i_A}}{dX} \right) \cdot \lambda \quad (\text{A.21})$$

where λ is the ratio of the membrane volume and the vessel volume.

The bulk concentration is used for the calculation of the boundary concentrations in the membrane:

$$C_{A_1} = Cb_A \cdot S, \quad Q_{A_1} = \frac{K_A \cdot Cb_A \cdot Q_s}{1 + \sum_k K_k \cdot Cb_k} \quad (\text{A.22})$$

The above equations are derived for one component, but the same equations hold in the case of more components. The only changing equation is the mass balance for the calculation of the free complexing agent (Equation (A.6)) where more terms, i.e. equal to the number of compounds, are added.

Nomenclature

a	= Slope of the selectivity boundary for the relation between F and S	
b	= Intercept of the selectivity boundary for the relation between F and S	
c	= Fit parameter for the function between b and K_D	
c_0	= Retentate concentration (= constant)	[mol/m ³]
Cb_e	= Dimensionless permeate concentration (= c_e/c_0)	[-]
C_e	= Dimensionless free concentration of D or L enantiomer (= c_e/c_0)	[-]
C_{e0}	= Dimensionless retentate concentration (= $c_0/c_0 = 1$)	[-]
Da	= Damköhler number (= $k_1 \cdot l/D$)	[-]
F	= Ratio of diffusion coefficients of the selective and non-selective population	[-]
Fo	= Dimensionless time (= $D \cdot t/l^2$);	[-]
k_1	= Reaction rate constant for complexation	[s ⁻¹]
K_e	= Dimensionless affinity of D or L for the chiral selector (= k_1/c_0)	[-]
l	= Membrane thickness	[m]
P	= Permeability	[mol · m · m ³ /m ² · s · mol]
Q_e	= Dimensionless complexed concentration of D or L enantiomer (= q_e/c_0)	[-]
Q_s	= Dimensionless total capacity of the chiral selector in membrane (= q_s/c_0)	[-]
S	= Solubility	[(mol/m ³)/(mol/m ³)]
t	= Time	[s]
X	= Dimensionless distance (= x/l)	[-]
Z	= Ratio of the dimensionless capacity of the chiral selector in membrane and the non-selective solubility (= Q_s/S)	[-]
D	= Diffusivity	[m ² /s]
α	= Permeation selectivity	[-]
λ	= Ratio of membrane volume and vessel volume (volume-area ratio)	[-]

Indices:

*	= Membrane surface concentration
0	= Retentate concentration at $t = 0$
s	= Saturated concentration (maximum capacity)
e	= D or L enantiomer

References

- [1] F. Jamali, R. Mehvar, and F. M. Pasutto, Enantioselective aspects of drug action and disposition therapeutic pitfalls, *J. Pharm. Sci.*, 78 (1989) 695.
- [2] R.A. Sheldon, *Chirotechnology; Industrial synthesis of optically active compounds*, Marcel Dekker Inc., New York, 1993.
- [3] W. H. Pirkle and T. C. Pochapsky, Consideration of chiral recognition relevant to the liquid chromatographic separation of enantiomers, *Chem. Rev.*, 89 (1989) 347.
- [4] C. H. Lochmuller and R. W. Souter, Chromatographic resolution of enantiomers selective review, *J. Chromatogr.*, 113 (1975) 283.
- [5] S. Fanali, Identification of chiral drug isomers by capillary electrophoresis, *J. Chromatogr. A*, 735 (1996) 77.
- [6] B. Gottfried, Chromatographic resolution of racemates, *Angew. chem. int. ed. eng.*, 19 (1980) 13.
- [7] O. Ramstrom and R. J. Ansell, Molecular imprinting technology: Challenges and prospects for the future, *Chirality*, 10 (1998) 195.
- [8] S. Li and W. C. Purdy, Cyclodextrins and their applications in analytical chemistry, *Chem. Rev.*, 92 (1992) 1457.
- [9] H. B. Ding, P. W. Carr, and E. L. Cussler, Racemic leucine separation by hollow-fiber extraction, *AIChE J.*, 38 (1992) 1493.
- [10] J. T. F. Keurentjes, L. J. W. M. Nabuurs, and E. A. Vegter, Liquid membrane technology for the separation of racemic mixtures, *J. Membrane Sci.*, 113 (1996) 351.
- [11] T. Takeuchi, R. Horikawa, T. Tanimura, and Y. Kabasawa, Resolution of DL-Valine by countercurrent solvent extraction with continuous sample feeding, *Separ. Sci. Technol.*, 25 (1990) 941.
- [12] J. D. Henry, Alternative separation processes, in Perry, R. H., Green, D. W., and Maloney, J. O. (Ed.), *Perry's chemical engineering's handbook*, McGraw-Hill book company, New York, 1984, pp. 22-37.

- [13] J. L. Lopez and S. L. Matson, A multiphase/extractive enzyme membrane reactor for production of diltiazem chiral intermediate, *J. Membrane Sci.*, 125 (1997) 189.
- [14] J. T. F. Keurentjes and F. J. M. Voermans, Membrane separations in the production of optically pure products, in Collins, A. N., Sheldrake, G. N., and Crosby, J. (Ed.), *Chirality in industry II*, John Wiley & sons Ltd., New York, 1997, pp. 157-180.
- [15] J. T. F. Keurentjes, L. J. M. Linders, W. A. Beverloo, and K. van 't Riet, Membrane cascades for the separation of binary mixtures, *Chem. Eng. Sci.*, 47 (1992) 1561.
- [16] D. R. Paul and W. J. Koros, Effect of partially immobilizing sorption on permeability and the diffusion time lag, *J. Polym. Sci. Pol. Phys.*, 14 (2000) 675.
- [17] T. Aoki, A. Maruyama, K. Shinohara, and E. Oikawa, Optical resolution by use of surface modified poly(methyl methacrylate) membrane containing (-)-oligo{methyl(10-pinanyl)siloxane}, *Polym. J.*, 27 (1995) 547.
- [18] E. Yashima, J. Noguchi, and Y. Okamoto, Enantiomer enrichment of oxprenolol through cellulose tris(3,5-dimethylphenylcarbamate) membrane, *J. Appl. Polym. Sci.*, 54 (1994) 1087.
- [19] N. Ogata, Supramolecular polymers having chiral interactions, *Macromol. Symp.*, 98 (1995) 543.
- [20] T. Masawaki, M. Sasai, and S. Tone, Optical resolution of an amino acid by an enantioselective ultrafiltration membrane, *J. Chem. Eng. Jpn.*, 25 (1992) 33.
- [21] T. Aoki, S. Tomizawa, and E. Oikawa, Enantioselective permeation through poly{g-[3-(pentamethyldisiloxanyl)propyl]-L-glutamate} membranes., *J. Membrane Sci.*, 99 (1995) 117.
- [22] T. Aoki, K. I. Shinohara, and E. Oikawa, Optical resolution through the solid membrane from (+)-poly{1-[dimethyl(10-pinanyl)silyl]-1-propyne}, *Makromol. Chem-Rapid.*, 13 (1992) 565.
- [23] A. Maruyama, N. Adachi, T. Takatsuki, M. Torii, K. Sanui, and N. Ogata, Enantioselective permeation of α -amino acid isomers through

- poly(amino acid)-derived membranes, *Macromolecules*, 23 (1990) 2748.
- [24] T. Aoki, K. Shinohara, T. Kaneko, and E. Oikawa, Enantioselective permeation of various racemates through an optically active poly{1-[dimethyl(10-pinanyl)silyl]-1-propyne} membrane, *Macromolecules*, 29 (1996) 4192.
- [25] T. Aoki, M. Ohshima, K. Shinohara, T. Kaneko, and E. Oikawa, Enantioselective permeation of racemates through a solid (+)-poly{2-[dimethyl(10-pinanyl)silyl]norbornadiene} membrane, *Polymer*, 38 (1997) 235.
- [26] I. Noda and C. C. Gryte, Multistage membrane separation processes for the continuous fractionation of solutes having similar permeabilities, *AIChE J.*, 27 (1981) 904.
- [27] J. D. Seader and Z. M. Kurtyka, Distillation, in Perry, R. H., Green, D. W., and Maloney, J. O. (Ed.), *Perry's chemical engineering's handbook*, McGraw-Hill book company, New York, 1984, pp. 13-1-13-97.
- [28] J. Ma, L. Chen, and B. He, Synthesis of crosslinked poly(vinyl alcohol) with L-proline pendant as the chiral stationary phase for resolution of amino acid enantiomers, *J. Appl. Polym. Sci.*, 61 (1996) 2029.
- [29] V. A. Davankov, Ligand-exchange chromatography of chiral compounds, in Cagniant, D. (Ed.), *Complexation chromatography*, Marcel Dekker, New York, 1992, pp. 197-245.
- [30] K. Ishihara, N. Suzuki, and K. Matsui, Optical resolution of amino acids by a polymer membrane having cyclodextrin moieties, *J. Chem. Soc. Jpn.*, 3 (1987) 446.
- [31] T. Kakuchi, T. Takaoka, and K. Yokota, Polymeric chiral crown ethers VI. Optical resolution of α -amino acid by polymers incorporating 1,3;4,6-di-O-benzylidene-D-mannitol residues., *Polym. J.*, 22 (1990) 199.
- [32] W. H. Pirkle and W. E. Bowen, Preparative separation of enantiomers using hollow-fibre membrane technology, *Tetrahedron-Asymmetr.*, 5 (1994) 773.

- [33] T. Takeuchi, R. Horikawa, and T. Tanimura, Enantioselective solvent extraction of neutral DL-amino acids in two-phase systems containing N-n-alkyl-L-proline derivatives and copper (II) ion, *Anal. Chem.*, 56 (1984) 1152.
- [34] J. Crank, *The mathematics of diffusion*, Clarendon press, Oxford, 1975.
- [35] V. A. Davankov, A. S. Bochkov, A. A. Kurganov, P. Roumeliotis, and K. K. Unger, Separation of unmodified α -amino acid enantiomers by reverse phase HPLC, *Chromatographia*, 13 (1980) 677.
- [36] P. E. M. Overdevest, A van der Padt, J. T. F. Keurentjes, and K. van 't Riet, Langmuir isotherms for enantioselective complexation of (D-L)-phenylalanine by cholesteryl-L-glutamate in nonionic micelles, *Colloids Surfaces A*, 163 (2000) 209.
- [37] N. Ogata, Supramolecular membranes for optical resolutions and molecular recognitions, *Macromol. Symp.*, 77 (1994) 167.
- [38] M. Yoshikawa, J. I. Izumi, and T. Kitao, Enantioselective electro dialysis of amino acids with charged polar side chains through molecularly imprinted polymeric membranes containing DIDE derivatives, *Polym. J.*, 29 (1997) 205

3 Electrodialysis system for large-scale enantiomer separation

Abstract

In contrast to analytical methods, the range of technologies currently applied for large-scale enantiomer separations is not extensive. Therefore, a new system has been developed for large-scale enantiomer separations that can be regarded as the scale-up of a capillary electrophoresis system. In this stacked membrane system chiral selectors are used, which are retained by size-selective membranes. When an electrical potential is applied, selective transport of the free enantiomer will occur, thus providing separation. In principle, this system can handle the same extensive range of enantiomers that can be separated in a capillary electrophoresis system on an analytical scale. In a system containing four separation compartments, α -cyclodextrin has been used as a chiral selector to separate D,L-Trp. Based on a transport model, a factorial design is used to investigate the effects of various process parameters. The results show that the addition of methanol is of minor influence, whereas the pH has a major effect, both on the operational selectivity and on the transport number. Experiments with AgNO_3 as the background electrolyte show that the operational selectivity has a plateau value of 1.08 at a pH ranging from 3 to 6. Due to the ease of scale-up of electro dialysis processes, this operational selectivity will allow for the separation of enantiomers on a large scale.

This chapter has been published as: Ed M. van der Ent, Tom P.H. Thielen, Martien A. Cohen Stuart, Albert van der Pacht, Jos T.F. Keurentjes, Electrodialysis system for large-scale enantiomer separation, *Ind. Eng. Chem. Res.* 40, (2001), 6021-6027.

3.1 Introduction

Resolution of enantiomers has become an important research area since it is known that individual enantiomers can have different effects on biological systems. Nowadays, crystallization [1] and enzymatic resolution [2,3] are the most widely applied large-scale processes (multi-tons/year) for enantiomeric resolution. However, the shortcomings of these processes are substantial. Crystallization processes often require a large number of process steps accompanied with the handling of high volumes of mother liquor and consequently high losses of valuable product. In the case of enzymatic resolution, the appropriate enzyme has to be found for each separation problem. Therefore, alternative large-scale enantiomer separation processes are of great relevance.

On an analytical scale, for almost every racemic mixture a separation method exists [4]: HPLC, GC and capillary electrophoresis (CE) are the major techniques. The enantioselectivities of the selectors used in these techniques are often low, typically between 1.1-2 [5-7]. Consequently, a large number of equilibrium stages is needed, which is not a problem for analytical methods. However, this represents the major challenge for large-scale processes.

Scale-up of the HPLC system has resulted in the development of the Simulating Moving Bed (SMB) technique [8]. It has been shown that SMB systems are easy to scale up, even for rather large quantities (1 kg/day).

Despite the broad range of racemic mixtures that can be separated using CE, currently no large-scale separation processes have been developed based on this concept. Although some work has been done on a preparative scale [9,10], this has not yet led to production rates higher than a few mg per day. This paper presents a multi-stage electro dialysis system for large-scale enantiomer separations, which can be considered as the scale-up of a CE method. The operational selectivities and transport efficiencies have been established experimentally for the separation of D,L-Tryptophan (D,L-Trp), for which the key optimization parameters for this system will be discussed.

3.2 Process description

When a chiral selector is added to a racemic mixture, it will selectively bind one of the two enantiomers by enantiospecific host-guest interactions [11-13]. This leads to an enriched free concentration of the other enantiomer. The complexed and free enantiomers are different in size and hence a separation can be established based on size discrimination, e.g. using synthetic membranes [14]. This is shown schematically in Figure 1. To achieve transport of the unbound enantiomers through the membrane, different driving forces can

be applied, which can be a pressure difference across the membrane or an electrical potential gradient, resulting in an ultrafiltration-based process [15] or electro dialysis, respectively. Depending on pH, many chiral compounds have charges thus allowing the use of an electrical potential gradient.

For the enantioselective complexation of amino acids, several selector molecules can be envisaged, including proteins [16,17], copper complexes [18,19] and cyclodextrins [20,21]. As cyclodextrins are non-charged, they probably represent the most effective group of chiral selectors for the electro dialysis system studied here. In practice, the different compartments of the system are loaded with an α -cyclodextrin solution. The racemic mixture is added to the system at one side, and travels through the consecutive compartments as a result of the electrical current. The enantiomer preferentially bound to the cyclodextrin is most strongly retarded, thus providing a separation between the two enantiomers. As the degree of separation in one single stage will be limited, a significant number of stages will be required. Since electro dialysis stacks typically consist of several hundreds of compartments between one single pair of electrodes [14], we expect scale-up of such system to be relatively straightforward.

The selectivity of the chiral selector is fully exploited when membranes with a perfect discrimination between the free enantiomer and the complexed one are used. This implies that only the free enantiomer will pass the membrane due to size exclusion of the complex. However, even for imperfect discrimination the transport can still be selective due to a velocity difference between the free enantiomer and the complexed form, as it is in CE. Using electro dialysis membranes, we assume that the membranes are perfectly size selective. Also, electro dialysis membranes have the advantage of higher transport efficiencies due to the prevention of counter-ion transport. Alternatively, nanofiltration or even ultrafiltration membranes can be used. These membranes are available with different characteristics such as pore sizes and charge densities [22].

3.3 Theory

For the system described above (Figure 1) we have derived the analytical solution for the concentration of the two enantiomers in the consecutive compartments as a function of time. These concentration profiles are modeled by n mass balances, describing the total enantiomer concentrations (D or L) in n compartments:

$$V \cdot \frac{d}{dt} \begin{pmatrix} c_{e,1}(t) \\ c_{e,2}(t) \\ c_{e,3}(t) \\ \vdots \\ c_{e,n}(t) \end{pmatrix} = A \cdot \begin{pmatrix} -J_{e,1} & 0 & 0 & \dots & 0 \\ J_{e,1} & -J_{e,2} & 0 & \dots & 0 \\ 0 & J_{e,2} & -J_{e,3} & \ddots & \vdots \\ \vdots & \ddots & \ddots & \ddots & 0 \\ 0 & \dots & 0 & J_{e,n-1} & -J_{e,n} \end{pmatrix} \cdot \begin{pmatrix} 1 \\ 1 \\ 1 \\ \vdots \\ 1 \end{pmatrix} \quad [\text{mol} \cdot \text{s}^{-1}] \quad (1)$$

where V is the compartment volume [m^3], A the membrane area between two compartments [m^2] and $c_{e,n}$ is the total enantiomer concentration (free and complexed) [$\text{mol} \cdot \text{m}^{-3}$] in compartment n , the index e stands for the D or L enantiomer, t is time [s] and $J_{e,n}$ is the enantiomer flux through the membrane [$\text{mol} \cdot \text{m}^{-2} \cdot \text{s}^{-1}$].

The enantiomer flux through the membrane is a function of the current density and the charged free enantiomer concentration. The fraction of the current used for the transport of charged free enantiomers (Tn_e) can be described by [23]:

$$Tn_e = \frac{z_e^2 \cdot \mu_e \cdot c_e}{\sum_j z_j^2 \cdot \mu_j \cdot c_j} \quad [-] \quad (2)$$

Here the index j indicates all ionic species including the enantiomer, z_e is the valence of Trp ($= +1$), μ is the electrophoretic mobility of the ionic species [$\text{m}^2 \cdot \text{s}^{-1} \cdot \text{V}^{-1}$] and c_e the charged enantiomer concentration [$\text{mol} \cdot \text{m}^{-3}$], which is determined by the pK_a , the pH of the system and the free enantiomer concentration ($c_{e,n}^{\text{free}}$). At high selector concentrations (q_s [$\text{mol} \cdot \text{m}^{-3}$]) the free

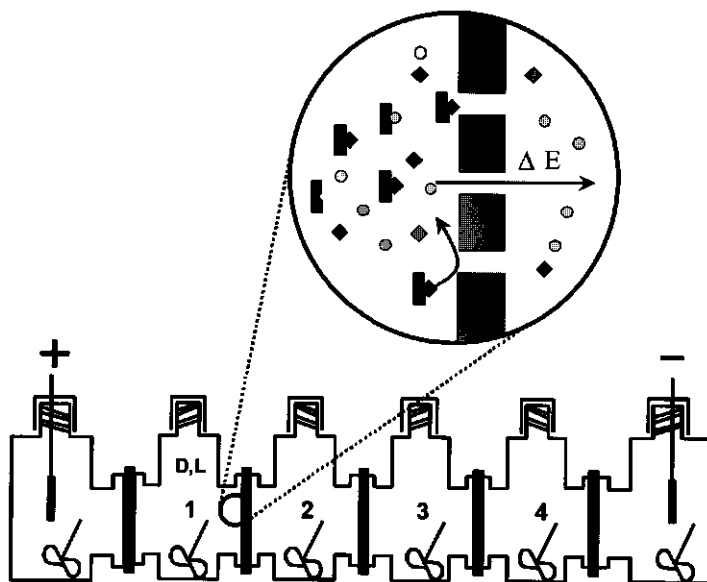


Figure 1: Schematic representation of the separation principle (enlargement). Also the experimental set-up used in this study is shown.

concentration is proportional to the total enantiomer concentration ($c_{e,n}$) (Henry's law):

$$c_{e,n}^{free} = K_e \cdot q_s \cdot c_{e,n} \quad [\text{mol} \cdot \text{m}^{-3}] \quad (3)$$

where K_e is the affinity constant [$\text{m}^3 \cdot \text{mol}^{-1}$].

Assuming that only H^+ and Trp^+ are transported, the normalized transport number ($Tn_e^* = Tn_e/c_{e,n}$) in our membrane system is given by:

$$Tn_e^* = \frac{1}{c_{e,n} + \frac{\mu_{e^+}}{\mu_{H^+}} \cdot (10^{(-pK_a)} + 10^{(-pH)}) \cdot (1 + K_e)} \quad [\text{m}^3 \cdot \text{mol}^{-1}] \quad (4)$$

Since $c_{e,n} \ll \frac{\mu_{e^+}}{\mu_{H^+}} \cdot (10^{(-pK_a)} + 10^{(-pH)}) \cdot (1 + K_e)$, Tn_e^* can be considered as a constant:

$$Tn_e^* = \frac{1}{\frac{\mu_{e^+}}{\mu_{H^+}} \cdot (10^{(-pK_a)} + 10^{(-pH)}) \cdot (1 + K_e)} \quad [\text{m}^3 \cdot \text{mol}^{-1}] \quad (5)$$

Using the standard equation describing the ion flux in electro dialysis¹³, we can describe the flux of the enantiomers through the membrane (J_e) as:

$$J_{e,n} = \frac{i}{z_e \cdot F} \cdot Tn_e^* \cdot c_{e,n} \quad [\text{mol} \cdot \text{m}^{-2} \cdot \text{s}^{-1}] \quad (6)$$

where i is the current density [$\text{A} \cdot \text{m}^{-2}$] and F the faraday constant [98486 $\text{C} \cdot \text{mol}^{-1}$]

Combining Equations (1) and (6) yields:

$$\frac{d}{dt} \begin{pmatrix} c_{e,1}(t) \\ c_{e,2}(t) \\ c_{e,3}(t) \\ \vdots \\ c_{e,n}(t) \end{pmatrix} = \begin{pmatrix} -P & 0 & 0 & \dots & 0 \\ P & -P & 0 & \dots & 0 \\ 0 & P & -P & \ddots & \vdots \\ \vdots & \ddots & \ddots & \ddots & 0 \\ 0 & \dots & 0 & P & -P \end{pmatrix} \cdot \begin{pmatrix} c_{e,1}(t) \\ c_{e,2}(t) \\ c_{e,3}(t) \\ \vdots \\ c_{e,n}(t) \end{pmatrix} \quad [\text{mol} \cdot \text{m}^{-3} \cdot \text{s}^{-1}] \quad (7)$$

where P is the system constant defined as:

$$P = \frac{i}{z_e \cdot F} \cdot Tn_e^* \cdot \frac{A}{V} \quad [\text{s}^{-1}] \quad (8)$$

Now we have rewritten equation (1) into a form in which the fluxes are linearly dependent of the concentration. Equation (7) can easily be solved yielding the dimensionless concentration ($C_{e,n}(t) = c_{e,n}(t) / c_{e,n}(0)$) of both enantiomers in each compartment:

$$C_{e,n}(t) = \frac{1}{(n-1)!} \cdot P_{e,n}^{(n-1)} \cdot e^{-P_{e,n} \cdot t} \cdot t^{(n-1)} \quad [-] \quad (9)$$

In chirotechnology usually the enantiomeric excess is studied instead of the enantiomer concentrations itself:

$$e.e. = \frac{c_D - c_L}{c_D + c_L} \quad [-] \quad (10)$$

Combining Equations (9) and (10) yields an expression for the e.e. as a function of time in each compartment (Figure 2). For these e.e. profiles the intercept equals:

$$\lim_{t \rightarrow 0} e.e.(t) = \frac{\left[\frac{1}{1 + \alpha \cdot K_L \cdot q_s} \right]^n - \left[\frac{1}{1 + K_L \cdot q_s} \right]^n}{\left[\frac{1}{1 + \alpha \cdot K_L \cdot q_s} \right]^n + \left[\frac{1}{1 + K_L \cdot q_s} \right]^n} \quad [-] \quad (11)$$

The slope is given by:

$$\lim_{t \rightarrow 0} \frac{de.e.(t)}{dt} = \frac{A}{V} \cdot \frac{2 \cdot K_L \cdot q_s \cdot T n_e^i \cdot i \cdot (\alpha - 1)}{\left[\frac{1}{1 + \alpha \cdot K_L \cdot q_s} \right]^n + \left[\frac{1}{1 + K_L \cdot q_s} \right]^n} \cdot F \cdot \left[(1 + \alpha \cdot K_L \cdot q_s) \cdot (1 + K_L \cdot q_s) \right]^{n+1} \quad (12)$$

Note that at low α ($0.5 < \alpha < 2$) the slopes in all compartments differ less than 10%. Furthermore, at these low α values the intercepts are equidistant. Both intercept and slope depend on the affinity constant K_L , the selectivity α and

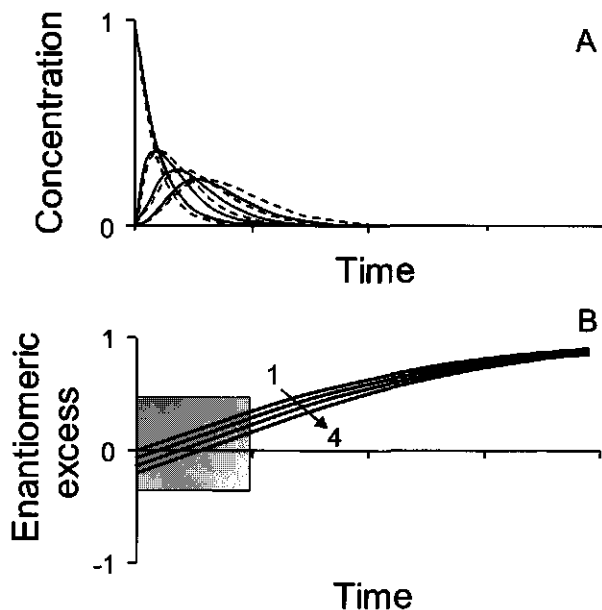


Figure 2: Theoretically calculated concentration profiles (A) and enantiomeric excess profiles (B). The selectivity ($\alpha_{D/L}$) used for the calculations is 1.15.

the transport number constant Tn_e^* . Therefore, one of the unknown parameters has to be estimated to determine the other two.

3.4 Experimental

Materials

D,L-Trp (>98%) was obtained from Bachem, D-Trp (>99%) and L-Trp (>99%) were obtained from Acros, α -cyclodextrin (>98%) was obtained from Fluka; analytical grade silver nitrate, perchloric acid (60%), polyethylene glycol ($M_w=1500$) and nitric acid (65%) were obtained from Merck. All chemicals were used as received. The nanofiltration membrane ASP50 was obtained from PTI advanced filtration (Oxnard, California), having an active layer of sulfonated polysulfone with a retention for NaCl of about 50%.

The experimental set-up is depicted in Figure 1 and was entirely made out of glass. The module consisted of 4 separation compartments and 2 electrode compartments. The volume of each compartment was $115 \cdot 10^{-6} \text{ m}^3$ and the membrane area between the compartments was $1.4 \cdot 10^{-3} \text{ m}^2$. This resulted in a membrane area to volume ratio of about $12 \text{ m}^2/\text{m}^3$. The compartments are relatively voluminous to allow measuring the different variables, such as pH, conductivity, concentration and temperature. A magnetic stirrer was used to stir the solution in the compartments (400 rpm). For the cathode a 1 x 1 cm platinum plate and for the anode a 1 x 1 cm stainless steel plate was used.

Factorial design

To prevent bacterial growth on the amino acid/ α -cyclodextrin solution, 5-20 v/v% methanol or 1 mM AgNO_3 was added. For both systems we determined the operational selectivity and the transport number constant as a function of pH. To study the influence of the methanol fraction and pH on the operational selectivity, a 2^2 factorial design [24] with 8 runs was performed. To check the linearity of the parameters, also 2 runs were performed in between. The levels studied for the factors are shown in Table 1. In the examination of the effects, the cross term was neglected, i.e. no interaction was assumed between the two

Table 1: Values of the experimental parameters used in the experimental design.

Factor	Level	
	-1	1
1. Methanol (v/v%)	5	20
2. PH	2.1	3.1

factors. Therefore, the following regression model was fitted through the data points:

$$y = \beta_0 + \beta_{\text{methanol}} \cdot x_{\text{methanol}} + \beta_{\text{pH}} \cdot x_{\text{pH}} \quad (13)$$

where y is the operational selectivity α or the transport number constant Tr_e^* , calculated with Equations (11) and (12), the β values are the regression parameters and x is defined on a coded scale from -1 to $+1$, i.e. the low and high levels of the factors, respectively. To evaluate the effects, the confidence interval of the regression parameters was also calculated [24]:

$$\hat{\beta}_j = \hat{\beta}_j \pm t_{\alpha/2, n-p} \cdot \sqrt{(s^2 \cdot V_j)} \quad (14)$$

where $t_{\alpha/2, n-p}$ is the student t value at a $100 \cdot (1-\alpha)$ confidence interval at n measurements and p parameters, V_j is the j -th element of the $(X'X)^{-1}$ matrix, X is an $(n \times p)$ matrix of the levels of the independent variables and s^2 is the estimate of the error variance. When the 95% confidence interval includes zero, the parameter is regarded as insignificant.

Analysis

Chiral HPLC was used for the sample analysis to determine the enantiomer concentration. The system consisted of a Spectra Physics SP8810 pump, a Thermo Separation® Products AS1000 auto sampler and a Separations UV detector. The column used for the separation was a 150 mm x 4 mm i.d. Daicel Crownpak CR(+) (5 μm). Mobile phase elution (1.2 mL/min) was performed isocratically using a filtered (0.45 μm) and degassed aqueous solution of perchloric acid (pH = 1.5). The column temperature during analysis was maintained at 25°C. The injected sample volume was 20 μL and the samples were injected without any pre-treatment. The wavelength setting of the UV detection was set at 254 nm. The calibration curve showed a linear relation up to a total concentration (D-Trp plus L-Trp) of 5 mM.

Enantiomer separation experiments

All separation compartments were filled with 125 mL of a 20 mM α -cyclodextrin solution containing the appropriate amount of methanol (5-20 v/v%) or AgNO_3 (1 mM) and HNO_3 . In compartment 1 also 1 mM D,L-Trp was added. The electrode compartments were filled with a solution containing the same amount of methanol/ AgNO_3 and HNO_3 as the separation compartments, however, the chiral selector was replaced by polyethylene glycol ($M_w = 1500$) to prevent an osmotic flow due to concentration differences.

The membranes were pre-wetted and positioned between the compartments with their top-layers facing the positive electrode. The pre-wetting procedure was found to be crucial to obtain selectivity values deviating from 1. The optimal

pre-wetting procedure was to wet the membranes with 35 v/v% methanol at pH=2.1 for 2 hours. Especially, the low pH appeared to be crucial for these membranes. At neutral or basic pH during pre-wetting no selectivity was observed, even when the pH was in the range of 2 to 3 during the experiment.

The experiment was started by switching on the current. Depending on the pH, the current was set to a value in accordance with an overall starting voltage difference of 200 V. During the experiment the current was kept constant by the dc power supply (Delta elektronika; E 0300-0.1). Typical current densities for the methanol system were 6 A/m² at pH =3.1 and 70 A/m² at pH = 2.1. For the AgNO₃ system the current densities ranged from 2-10 A/m². Samples were taken from all separation compartments and the concentration of both enantiomers was analyzed by HPLC. This resulted in concentration profiles as a function of time, which were converted into enantiomeric excess (e.e.) profiles using Equation (10). These profiles were fitted using a least squares method to obtain the slope (*a*) and intercept (*b*). The slope and intercept were converted to an operational selectivity and a transport number by means of Equations (11) and (12) and using a value of 20 M⁻¹ for the affinity constant of L-Trp (*K_i*) [25].

3.5 Results and discussion

Methanol system

A typical result of an experimentally measured enantiomeric excess (e.e.) profile is given in Figure 3. Indeed straight and equidistant e.e. curves are obtained. At the first period of time some scattering is observed. This is caused by the low absolute enantiomer concentrations, resulting in relatively large

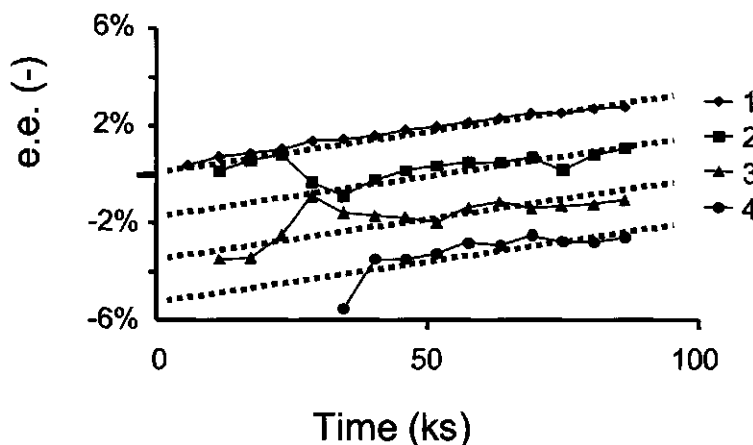


Figure 3: Typical experimental result of the enantiomeric excess profiles of 4 compartments. pH=3.1, methanol concentration = 5%, current density 6.5 A/m².

deviations in e.e. values. For the methanol system the operational selectivity and the transport number are determined as a function of pH and methanol concentration. For the calculation of the operational selectivity, we have used affinity constants between α -CD and L-Trp obtained from titration experiments [25], equal to 20 M^{-1} .

Importance of parameters

Table 2 shows the regression parameters and their 95% confidence interval obtained from the factorial design experiment (Equations (13) and (14), respectively). These values show that the methanol effect is less than 1% compared to the pH effect. Moreover, from the confidence interval it can be concluded that the effect of methanol is not significant, since zero is included. Therefore, the influence of methanol is neglected for the remainder of this paper. Table 2 also shows that the pH does have an influence on the operational selectivity. Therefore, all data points are taken as one single population to

Table 2: Effect of methanol and pH on the operational selectivity from results of factorial design.

Regression parameter	- 95%	Value	+ 95%
β_0	0.71	0.89	1.07
β_{Methanol}	$-5.6 \cdot 10^{-3}$	$-1.2 \cdot 10^{-3}$	$3.2 \cdot 10^{-3}$
β_{pH}	$8.1 \cdot 10^{-3}$	$7.4 \cdot 10^{-2}$	$1.4 \cdot 10^{-1}$

investigate this pH effect. The effect appears to be positive, indicating that the operational selectivity increases upon an increase in pH. The results of the experimental design for the transport number show no significant effects, neither for the methanol concentration nor for pH.

The operational selectivity

Figure 4 shows that although some experimental variation is observed, there is indeed an increase of the operational selectivity with increasing pH. The points at pH 2.4 and 2.7 indicate a non-linear relation. To our knowledge, no literature is available about the intrinsic selectivity as a function of pH for the cyclodextrin/Trp system. Only one selectivity value has been reported [26] for capillary zone electrophoresis. A selectivity of 1.3 has been found at pH 2.5 without the addition of methanol, which is higher than the values found in Figure 4.

For the methanol system the pH ranges from 2 to 3. The lower boundary is determined by the stability of the chiral selector [27]. Fortunately, Figure 4 shows that lower pH values are not important, since upon decreasing the pH the operational selectivity decreases. On the other hand, the electrical resistance of the system limits the upper boundary. At neutral pH the conductivity of the solution approaches zero. Therefore, the electrical resistance of the system becomes very high. Obviously, this problem will not occur for a racemic mixture which is charged at neutral pH. Another option to solve this conductivity problem is the addition of a background electrolyte. This will be shown in the next section, where a system containing AgNO_3 as a background electrolyte is described. In addition, this background electrolyte prevents bacterial growth, hence, the addition of methanol is not needed.

Transport as a function of pH

Figure 5 shows the transport numbers ($Tn(t=0) = Tn_e^+ \cdot c_e(t=0)$) as a function of pH for the methanol system. Despite the impression one might obtain from this graph, no statistically significant trend is present. The average value of the transport number is about 0.015. This value is very low for electro dialysis processes, as for the desalination of water transport numbers of 0.60-0.90 can be obtained. The low values in our experiments are caused by the relatively high H^+ concentration (1-10 mM) compared to the total Trp concentration (1mM). Moreover, at pH 3 only 10% of Trp is charged. Another reason for the low

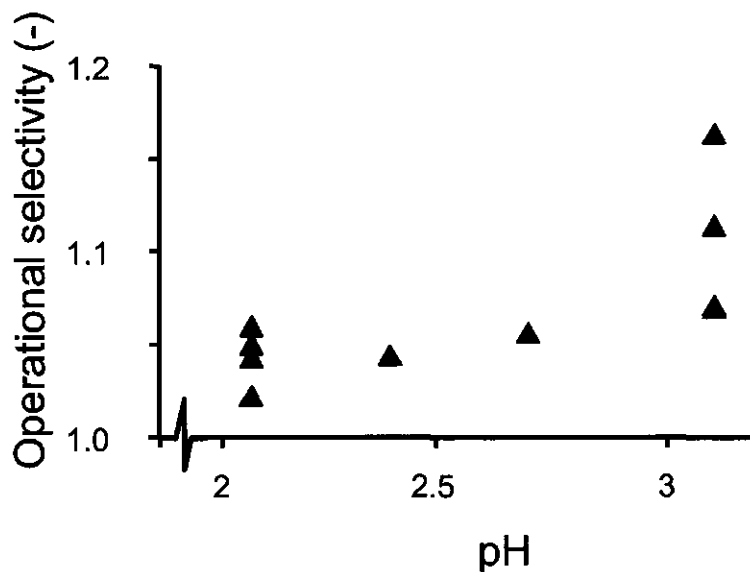


Figure 4: Operational selectivity for the methanol system as function of pH. Methanol concentration ranged from 5% to 20%.

transport number values is that the proton mobility is 60 times the mobility of Trp^+ ($363 \cdot 10^{-5}$ versus $5.6 \cdot 10^{-5} \text{ cm}^2 \cdot \text{s}^{-1} \cdot \text{V}^{-1}$, respectively) [26,28], which reduces the efficiency of Trp transport dramatically (Equation 5). Increasing the Trp concentration can in theory increase the low transport number values. This measure will influence the ratio of Trp^+ and H^+ in a positive direction. The increase thus obtained, however, will be limited by the solubility of the compound.

The theoretical transport numbers can be calculated as a function of pH using Equations (2) and (5), the electrophoretic mobilities and the pK value of Trp ($=2.38$ [29]). These theoretical values are about a factor of 10 lower compared to the experimental values. Enhanced transport can be the result of specific adsorption, diffusion effects, concentration polarization, or electro-osmotic flow. Equilibrium experiments with the membrane have not shown any specific ad/absorption of Trp. With the Nernst-Planck [30] equation the ratio of the electrophoretic flux (J_E) and the diffusion flux (J_D) can be calculated. For the membranes used, a J_E/J_D ratio of 125 is found, indicating a negligible contribution of diffusion effects. Concentration polarization effects are assumed to be minimal since low current densities ($2\text{-}70 \text{ A/m}^2$) are used in the experiments. Therefore, it is tempting to conclude that the enhanced transport number is due to a drift caused by an electro-osmotic flow. For an electro-osmotic flow charged porous structures are required. Sulfonated polysulfone nanofiltration membranes are known to have fixed charge densities of $100\text{-}1000 \text{ mol} \cdot \text{m}^{-3}$ depending on the bulk salt concentrations [31]. Since the ASP 50 membranes used here are composed of sulfonated polysulfone, the presence of these structures can be expected, thus explaining the occurrence of electro-osmotic flow.

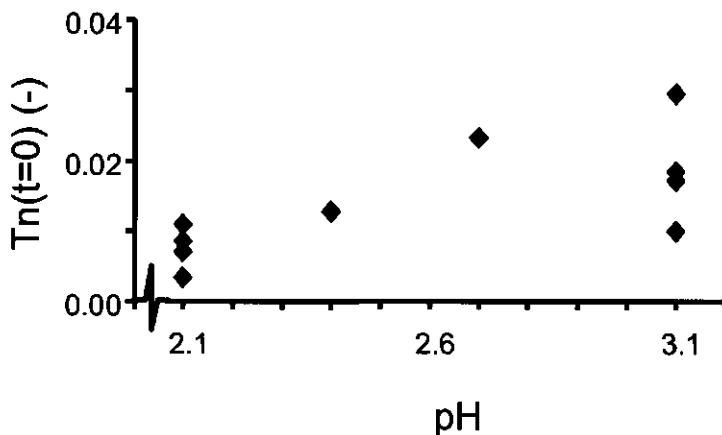


Figure 5: Transport number ($T_n(t=0)$) of Trp for the methanol system as function of pH. Methanol concentration ranged from 5% to 20%.

AgNO₃ system

The methanol system is limited in pH. At pH > 3 no Trp transport takes place, since the resistance of the system is too high and the current density will be zero in spite of a high voltage drop. In the AgNO₃ system, AgNO₃ is always present as a background electrolyte. This guarantees an electrically driven flux, even at neutral pH.

The results of the operational selectivity as a function of pH are given in Figure 6. This graph clearly shows a plateau value for operational selectivities at pH values higher than 3. This pH dependency very much resembles the fraction of zwitterions in solution (solid line in Figure 6). This graph indicates that the positively charged Trp reduces the operational selectivity. Since no literature is available on the intrinsic selectivity as a function of pH, no firm conclusions can be drawn yet about the separation mechanism.

The plateau value $\alpha = 1.08$ appears to be slightly lower than the maximum value found in the methanol system. This could indicate an influence of the Ag⁺ ions on the operational selectivity. From literature it is known that Ag⁺ is able to interact with double bonds [32], amino-acids [33] and carbohydrates [34], thus providing a means to transport the entire complex through the membrane. The effect of the pH on the transport number for the AgNO₃ system is shown in Figure 7. The transport number values for the AgNO₃ system are even lower than for the methanol system. This is not surprising, due to the addition of extra electrolyte. Unexpected, however, is the relatively high transport number at

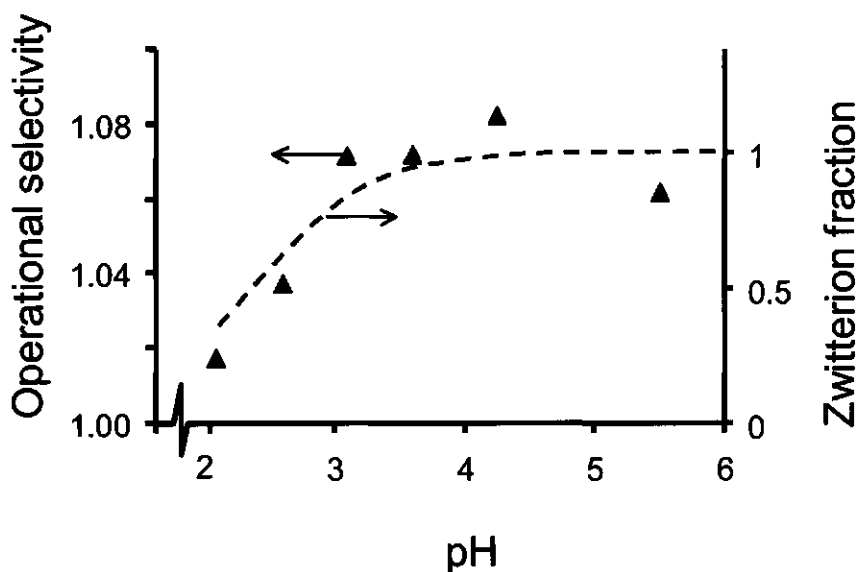


Figure 6: The operational selectivity for the AgNO₃ system as function of pH. On the secondary Y-axis is plotted the zwitterion fraction. [AgNO₃] = 1 mol/m³.

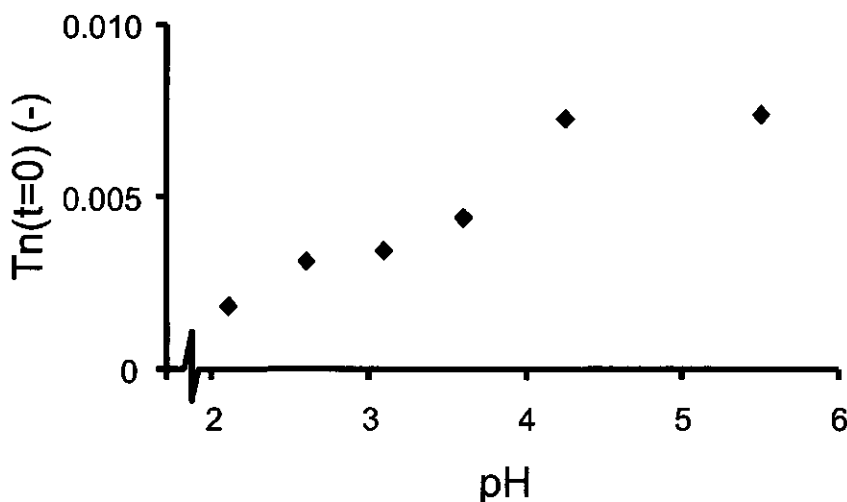


Figure 7: Transport number ($T_n(t=0)$) of Trp for the AgNO_3 system. $[\text{AgNO}_3] = 1 \text{ mol/m}^3$.

neutral pH. According to equation (2) the transport number of Trp should be about zero at neutral pH, since Trp is completely in the zwitterionic form. However, Figure 7 shows that at neutral pH the highest transport number is observed for the AgNO_3 system. Besides the above-mentioned interaction between Ag^+ and Trp, again the electro-osmotic drift could enhance the Trp flux.

3.6 Concluding remarks

In this paper it has been shown that electrical-potential driven membrane separation of enantiomers may provide a viable alternative for large-scale enantiomer separations. The combination of enantioselective complexation using α -cyclodextrins with size exclusion has been evaluated for two different systems. As the addition of a bacteriostatic agent is required, one system contains methanol and the other system contains AgNO_3 . It appears that the methanol-based system provides the most effective transport of amino acids, as parallel transport of Ag^+ ions is avoided. The major optimization parameter for the amino acid/cyclodextrin system is the pH. For this system the operational selectivity appears to be constant for pH values higher than 3, showing a strong resemblance with the fraction of amino acid present in the zwitterionic form.

To achieve a 99%+ separation this system needs a substantial number of equilibrium stages. This can easily be achieved by decreasing the volume to surface area ratio and implementing the system in an electrodialysis stack. Compared to a pressure-driven process, this has the advantage of easier scale-up as electrodialysis stacks can contain in the order of 1000 membrane compartments in series [14].

Nomenclature

α	Selectivity	[-]
β	Regression parameter	
μ	Electrophoretic mobility	$[\text{m}^2 \cdot \text{s}^{-1} \cdot \text{V}^{-1}]$
A	Membrane area between two compartments	$[\text{m}^2]$
c	Concentration	$[\text{mol} \cdot \text{m}^{-3}]$
F	Faraday constant	$[96486 \text{ C} \cdot \text{mol}^{-1}]$
i	Current density	$[\text{A} \cdot \text{m}^{-2}]$
J	Flux through the membrane	$[\text{mol} \cdot \text{m}^{-2} \cdot \text{s}^{-1}]$
K_e	Affinity constant	$[\text{m}^3 \cdot \text{mol}]$
q_s	Chiral selector concentration	$[\text{mol} \cdot \text{m}^{-3}]$
t	Time	[s]
Tn	Transport number	[-]
Tn^*	Transport number constant	$[\text{m}^3 \cdot \text{mol}^{-1}]$
V	Compartment volume	$[\text{m}^3]$
z	Ion valency	[-]

indices:

n	Compartment number
e	D or L enantiomer,
j	Ionic specie including the ionic enantiomer

References

- [1]. R. A. Sheldon, Racemate resolution via crystallization, in *Chirotechnology; Industrial synthesis of optically active compounds*, Marcel Dekker, Inc., New York, 1993, pp. 173-204.
- [2]. H. E. Schoemaker, W. H. J. Boesten, Q. B. Broxterman, E. C. Roos, B. Kaptein, W. J. J. van den Tweel, J. Kamphuis, E. M. Meijer, and F. P. J. T. Rutjes, Application of enzymes in industrial organic synthesis, *Chimia* 51 (1997) 308.
- [3]. B. Schulze and M. G. Wubbolts, Biocatalysis for industrial production of fine chemicals, *Curr. Opin. Biotech.* 10 (1999) 609.
- [4]. J. T. F. Keurentjes, L. J. W. M. Nabuurs, and E. A. Vegter, Liquid membrane technology for the separation of racemic mixtures, *J. Membrane Sci.* 113 (1996) 351.
- [5]. S. Fanali, Identification of chiral drug isomers by capillary electrophoresis, *J. Chromatogr. A* 735 (1996) 77.
- [6]. B. Gottfried, Chromatographic resolution of racemates, *Angew. Chem. Int. Edit.* 19 (1980) 13.
- [7]. W. H. Pirkle and T. C. Pochapsky, Chiral stationary phases for the direct LC separation of enantiomers, in Grushka, E., Giddings, J. C., and Brown, P. R. (Ed.), *Advances in Chromatography*, Marcel Dekker, New York, 1987, pp. 73-127.
- [8]. L. Miller, C. Orihuela, R. Fronek, D. Honda, and O. Dapremont, Chromatographic resolution of the enantiomers of pharmaceutical intermediate from the milligram to the kilogram scale, *J. Chromatogr. A* 849 (1999) 309.
- [9]. J. R. Chen, R. N. Zare, E. C. Peters, F. Svec, and J. J. Frechet, Semipreparative capillary electrochromatography, *Anal. Chem.* 73 (2001) 1987.
- [10]. A. M. Stalcup, R. M. C. Sutton, P. Painuly, J. V. Rodrigo, S. R. Gratz, and E. G. Yanes, Continuous free flow electrophoresis for preparative chiral separations of piperoxan using sulfated β -cyclodextrin, *The Analyst* 125 (2000) 1719.

- [11]. G. Barone, G. Castronuovo, V. D. Ruocco, V. Elia, and C. Giancola, Inclusion compounds in water: Thermodynamics of the interaction of cyclomaltohexaose with amino acids at 25°, *Carbohydr. Res.* 192 (1989) 331.
- [12]. M. Newcomb, J. L. Toner, R. C. Helgeson, and D. J. Cram, Host-guest complexation. 20. chiral recognition in transport as a molecular basis for a catalytic resolving machine, *J. Am. Chem. Soc.* 101 (1979) 4941.
- [13]. I. W. Wainer and J. Caldwell, The 1996 chirality debate, *Chirality* 9 (1997) 95.
- [14]. R. Rautenbach and R. Albrecht, *Membrane processes*, Bath Press Ltd., Bath, 1989.
- [15]. P. E. M. Overdeest and A. van der Padt, Optically pure compounds from ultrafiltration, *Chemtech* 29 (1999) 17.
- [16]. A. Higuchi, Y. Ishida, and T. Nakagawa, Surface modified polysulfone membranes: separation of mixed proteins and optical resolution of tryptophan, *Desalination* 90 (1993) 127.
- [17]. S. Poncet, J. Randon, and J. L. Rocca, Enantiomeric separation of tryptophan by ultrafiltration using the BSA solution system, *Separ. Sci. Technol.* 32 (1997) 2029.
- [18]. V. A. Davankov and A. V. Semechkin, Ligand-exchange chromatography, *J. Chromatogr.* 141 (1977) 313.
- [19]. P. E. M. Overdeest, A. van der Padt, J. T. F. Keurentjes, and K. van 't Riet, Langmuir isotherms for enantioselective complexation of (D-L)-phenylalanine by cholesteryl-L-glutamate in nonionic micelles, *Colloids Surfaces A* 163 (2000) 209.
- [20]. W. L. Hinze, T. E. Riehl, D. W. Armstrong, W. Demond, A. Alak, and T. Ward, Liquid chromatography separation of enantiomers using a chiral β -cyclodextrin-bonded stationary phase and conventional aqueous-organic mobile phases, *Anal. Chem.* 57 (1985) 237.
- [21]. Y. Liu, B. H. Han, A. D. Qi, and R. T. Chen, Molecular recognition study of a supramolecular system: -XI. chiral recognition of aliphatic amino

acids by natural and modified α -Cyclodextrins in acidic aqueous solution-, *Bioorg. Chem.* 25 (1997) 155.

- [22]. W. R. Bowen and A. W. Mohammad, Characterization and prediction of nanofiltration membrane performance-a general assessment, *T. I. Chem. Eng-Lond.* 76 (1998) 885.
- [23]. J. A. Manzanares and K. Kontturi, Transport numbers of ions in charged membrane systems, in Sorensen, T. S. (Ed.), *Surface chemistry and electrochemistry of membranes*, Marcel Dekker, New York, 1999, pp. 399-436.
- [24]. D. C. Montgomery, *Design and analysis of experiments*, John Wiley & Sons, New York, 1997.
- [25]. G. Castronuovo, V. Elia, D. Fessas, A. Giordano, and F. Velleca, Thermodynamics of the interaction of cyclodextrins with aromatic and α,ω -amino acids in aqueous solutions: a calorimetric study at 25°C, *Carbohydr. Res.* 272 (1995) 31.
- [26]. S. Fanali and P. Bocek, A practical procedure for the determination of association constants of the analyte-chiral selector equilibria by capillary zone electrophoresis, *Electrophoresis* 17 (1996) 1921.
- [27]. Y. B. Tewari, R. N. Goldberg, and M. Sato, Thermodynamics of the hydrolysis and cyclization reactions of α - β - and γ -cyclodextrin, *Carbohydr. Res.* 301 (1997) 11.
- [28]. R. Chang, *Physical chemistry for the chemical and biological sciences*, University Science Books, Sausalito, 2000.
- [29]. *CRC Handbook for Chemistry and Physics*, CRC Press, Boca Raton, 1978.
- [30]. R. P. Buck, Kinetics of bulk and interfacial ionic motion: Microscopic bases and limits for the Nernst-Planck equation applied to membrane systems, *J. Membrane Sci.* 17 (1984) 1.
- [31]. X. L. Wang, T. Tsuru, S. I. Nakao, and S. Kimura, The electrostatic and steric-hindrance model for the transport of charged solutes through nanofiltration membranes, *J. Membrane Sci.* 135 (1997) 19.

- [32]. D. J. Safarik and R. B. Eldridge, Olefin/paraffin separations by reactive absorption: A review, *Ind. Eng. Chem. Res.* 37 (1998) 2571.
- [33]. S. Y. Liao, D. C. Read, W. J. Pugh, J. R. Furr, and A. D. Russell, Interaction of silver nitrate with readily identifiable groups: relationship to the antibacterial actions of silver ions., *Lett. Appl. Microbiol.* 25 (1997) 279.
- [34]. H. D. Scobell, K. M. Brobst, and E. M. Steele, Automated liquid chromatographic system for analysis of carbohydrate mixtures, *Cereal Chem.* 54 (1977) 905.

4 Enantioselective binding of tryptophan to α -cyclodextrin: *A thermodynamic study*

Abstract

For the application of cyclodextrins in separation systems, it is important to understand the fundamental interactions occurring in these systems. In this study, the complexation thermodynamics of natural α -cyclodextrin with both enantiomers of tryptophan have been studied for pH 1.5–6 using isothermal titration calorimetry (ITC). Despite the low affinity for the α -cyclodextrin / tryptophan complex, isothermal titration calorimetry is found to be a versatile method to study complexation thermodynamics and chiral selectivity under different environmental conditions. A constant affinity value (K) has been found for both enantiomers for pH 2.5–6. The average K -value over this interval for D-tryptophan (D-Trp) is $17.0 \pm 0.5 \text{ M}^{-1}$ and for L-tryptophan (L-Trp) $15.2 \pm 0.5 \text{ M}^{-1}$, resulting in an intrinsic selectivity ($\alpha_{\text{D/L}}$) of 1.12 ± 0.04 . Below pH 2.5, however, both affinity constants drop due to the reduced affinity for positively charged tryptophan. The complexation enthalpy of D-Trp shows a similar pH effect, while for L-Trp the complexation enthalpy is constant over the entire pH range. For the constant region of the complexation enthalpy (pH 3–6), a more negative value has been obtained for D-Trp ($-8.46 \pm 0.48 \text{ kJ}\cdot\text{mol}^{-1}$) than for L-Trp ($-5.45 \pm 0.62 \text{ kJ}\cdot\text{mol}^{-1}$). At pH 1.5 the complexation enthalpy of D-Trp becomes equal to that of L-Trp. Regarding the entropy, this showed a similar effect, indicating "normal" enthalpy-entropy compensation. From the thermodynamic results it is concluded that D-Trp is able to undergo more favourable hydrogen bonding interactions with α -cyclodextrin than L-Trp when both enantiomers are present as zwitterion. However, the additional interaction of D-Trp disappears when tryptophan becomes positively charged. Consequently, the binding mechanism becomes similar, resulting in a drop in selectivity. From the absolute values of the entropy and the negative values of the enthalpy it is concluded that the complexation is an "enthalpy-driven" process. Since hydrophobic interactions are generally accepted to be "entropy driven" it can be concluded that hydrophobic interactions are not the major interactions for α -cyclodextrin/tryptophan binding.

This chapter has been submitted for publication as: E.M. van der Ent, A. van der Padt, J.T.F. Keurentjes, A. de Keizer, M.A. Cohen Stuart, Enantioselective binding of tryptophan to α -cyclodextrin: A thermodynamic study

4.1 Introduction

An important property of cyclodextrins is their capability to form inclusion complexes with a large variety of organic substances [1]. The guest molecule is surrounded or encapsulated by the cyclodextrin in the hydrophobic interior of the molecule, resulting in advantageous changes in its chemical and physical properties. In particular, properties such as stability, solubility and bioavailability can be improved [2]. Furthermore, the guest molecule often is coordinated in the cyclodextrin cavity allowing applications such as directing chemical reactions [2] (enzyme-like actions), or separation of substances as it is used in many chromatographic systems [3]. For these applications it is important to understand the interactions and the influence of process parameters on these interactions to find optimal process conditions.

Since cyclodextrins are composed of chiral D-glucose molecules [4], the complexation with a wide range of racemates is enantioselective. Armstrong [5] stated in 1998 that >95% of all gas chromatography (GC) enantiomer separations, >95% of all capillary electrophoresis (CE) enantiomeric separations and nearly 50% of all liquid chromatography (LC) separations reported are performed with the use of macrocyclic compounds as the chiral selector. This group of macrocyclic compounds consists, besides crown ethers and glycopeptide antibiotics, mainly of cyclodextrins and their derivatives [5], indicating a broad applicability of these compounds in various fields.

For chiral resolution, the smallest naturally occurring cyclodextrin, α -cyclodextrin (cyclohexaamylose), is the most interesting. The complexation with this cyclodextrin frequently results in a narrow fit between host and guest molecule, which is essential for chiral discrimination [1]. An example is the complexation with aromatic amino acids. α -Cyclodextrin can selectively complex these amino acids, while other cyclodextrins (β , γ , δ) do not. From this group of aromatic amino acids, tryptophan (Trp) is complexed most selectively [6]. Therefore, this Trp/ α -cyclodextrin complex is often used as a model system for separation problems. Also, the availability of both compounds in large quantities has contributed to thorough investigations of the complex by different groups [6-11].

Armstrong [6] was the first to separate underivatized D,L-Trp on an analytical scale with the use of an α -cyclodextrin bonded chiral stationary phase (CSP). Based on this work, a large number of groups have separated D,L-Trp using CE and α -cyclodextrin in the background electrolyte [8,9,12,13]. Generally, low-pH buffers are used for these CE separations, since this yields a in better resolution.

In our laboratory we have investigated the application of an electrodialysis process for the separation of D,L-Trp using α -cyclodextrin as a model system

for large-scale enantiomer separations [14]. For this system it has been found that the *operational* selectivity is a distinct function of pH. As in the case of CE separations it is not clear whether this effect is caused by process conditions or by *intrinsic* complexation thermodynamics.

Lipkowitz *et al.* [11] have studied the interactions between D,L-Trp and α -cyclodextrin using ^1H and ^{13}C NMR in combination with molecular dynamics. They have found that zwitterionic D-Trp can form two hydrogen bonds with α -cyclodextrin whereas zwitterionic L-Trp can form only one bond, resulting in a lower affinity for L-Trp. However, these results account only for the zwitterionic state of Trp, not for low pH values, which are of importance for CE separations and for our large-scale separation system. In this low pH region, the interaction might change resulting in a different complexation mechanism, providing an explanation of the empirical results. Therefore, in this paper the complexation thermodynamics between D,L-Trp and α -cyclodextrin is studied in a pH range of 1.5 to 6.

Isothermal titration calorimetry (ITC) is used for this purpose, since it is a sensitive technique to investigate the thermodynamics of complexation processes [15]. In turn, these thermodynamics can give insight into the intrinsic interactions involved in chiral discriminations [16]. Therefore, in this paper the complexation thermodynamics of Trp/ α -cyclodextrin is investigated as a function of pH using ITC.

4.2 Experimental

Materials.

D-Trp (Acros, >99%), L-Trp (Acros, >99%), sulphuric acid (Merck titrisol, 0.5 M), methanol (Lab scan, HPLC grade) and α -cyclodextrin (Fluka, >98%) were used as received.

Methods.

All solutions were made in a 5 % v/v mixture of methanol and degassed, doubly distilled water. This mixture was adjusted to the required pH using 0.5 M sulphuric acid. Stock solutions of 100 mL α -cyclodextrin ($64 \text{ mol}\cdot\text{m}^{-3}$) and 100 mL Trp ($5 \text{ mol}\cdot\text{m}^{-3}$) were freshly prepared before each experiment. Prior to filling, the syringe and the reaction cell were thoroughly rinsed. The reaction cell (1.35 mL) was filled with the Trp solution while the syringe was filled with the cyclodextrin solution.

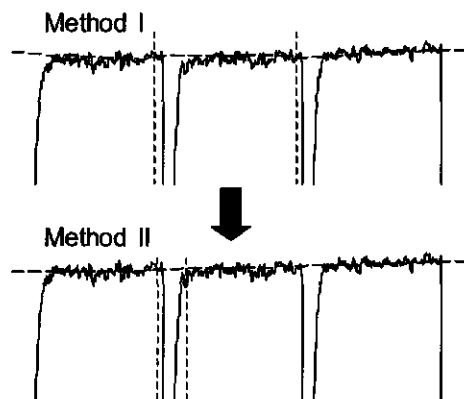


Figure 1: Effect of reprocessing the integration procedure. The top graph shows the standard integration, while the bottom graph shows the reprocessed result. In this graph, the integration stop mark is positioned directly after the peak and the integration baseline is adjusted to the corresponding average signal level in the noisy region

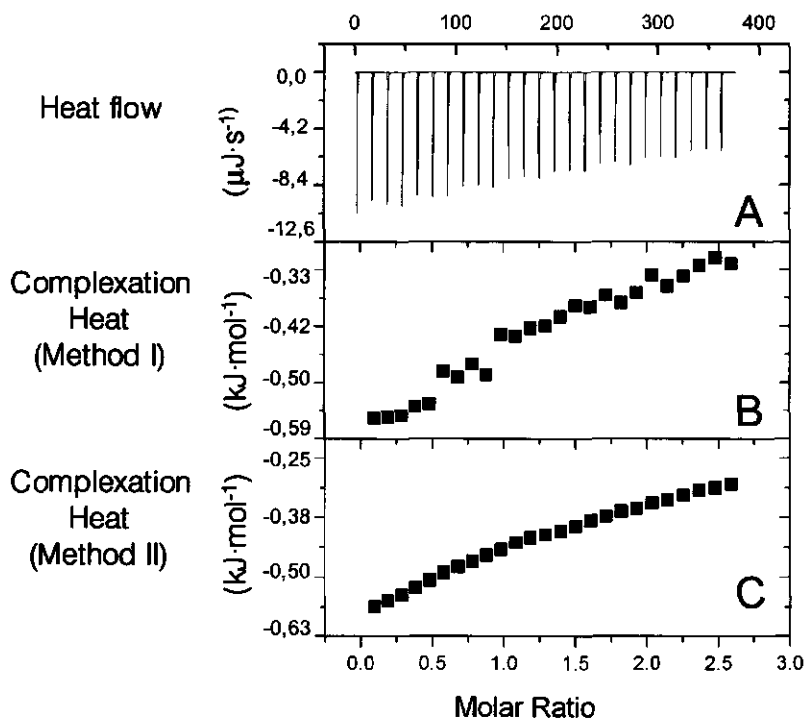


Figure 2: Typical results of a titration experiment with α -cyclodextrin and D-tryptophan, before (B) and after (C) processing the integration events. The top of one graph (A) shows the signal of the isothermal titration calorimeter. Due to the low complex stability, the normal S-shaped curve is flattened to a more gradually changing curve.

The calorimetric experiments were performed with an Omega titration micro calorimeter (MicroCal, Northampton, MA). The experimental temperature was set to 298 K and the external cooling bath temperature to 283 K. The reference cell was filled with doubly distilled water. The reference offset was set to 50%, which was sufficient for the range of our reaction heats. Each experiment was initially delayed by at least 120 seconds for baseline stabilization. The cyclodextrin solution was introduced into the reaction cell through 25 injections of about 10 μL . Each injection lasted 25 seconds and the lag time between injections was at least 300 sec. The stirring rate was 410 rpm.

Peak integration was performed using Microcal Origin 5.0 software (method I). The results were checked visually afterwards and corrected when necessary, by positioning the integration stop mark directly after the peak and by adjusting the integration baseline to the corresponding average signal level in the noisy region (method II) (Figure 1). Method II gives an improved binding curve as shown in Figure 2. This figure shows results as obtained by method I (Figure 2B) and by method II (Figure 2C) ; Figure 2A shows the heat flow [$\mu\text{cal}\cdot\text{s}^{-1}$] from the calorimeter cell. The integration procedure appeared to be crucial, since it resulted in a more accurate fit and consequently reduced the 95 % confidence interval of the fit parameters dramatically. For this particular data set shown in Figure 2, the affinity constant and confidence interval changes from $14.2 \pm 3.7 \text{ M}^{-1}$ to $14.5 \pm 0.5 \text{ M}^{-1}$.

From Figure 2 it can also be seen that the complexation heat as a function of the molar ratio (Figure 2C) does not have the "typical" S-shape. The reason for this is the relatively low affinity of α -cyclodextrin for Trp. This relative affinity is expressed in the parameter c , which is the product of the affinity (K) and the complexant concentration in the reaction cell (M_{tot}) [15]. For moderate binding c is between 1 and 1000. Such c -values result in S-shaped curves for the reaction heat as function of the molar ratio, as they are usually observed. From such curves, the affinity and heat of complexation are obtained independently from the experimental data. On the other hand, very weak binding (cf., $c=0.1$) yields a more gradual change of the complexation heat with the molar ratio, resulting in a less reliable fit for the affinity constant (K). The c -value in our experiments ranged from 0.08 to 0.12, which indeed corresponds to weak interactions. For data in this range, there is a large effect of noise on the integration procedure.

The experimental data points were fitted to the relation described by Wiseman *et al.* [15] with a non-linear least squares method. During this fit the stoichiometric constant (n) was kept equal to 1, because published studies have shown that the complex stoichiometry of α -cyclodextrin and Trp is 1:1 [11]. This resulted in two fit parameters, i.e. the affinity (K) and the reaction enthalpy (ΔH°).

From the fit parameters the entropy (ΔS^0) and free energy (ΔG^0) of binding are derived from the standard relations:

$$\Delta G^0 = -R \cdot T \cdot \ln K = \Delta H^0 - T \cdot \Delta S^0 \quad [\text{J} \cdot \text{mol}^{-1}] \quad (1)$$

where R is the gas constant [$8.314 \text{ J} \cdot \text{mol}^{-1} \cdot \text{K}^{-1}$] and T is the absolute temperature [K].

For both enantiomers the affinity and complexation enthalpy were measured and the intrinsic selectivity (α) was calculated as follows [16]:

$$\alpha_{D/L} = \exp\left(-\left(\frac{\Delta G_D^0}{R \cdot T} - \frac{\Delta G_L^0}{R \cdot T}\right)\right) = \frac{K_D}{K_L} \quad [-] \quad (2)$$

where D and L represent the D- and L-enantiomer, respectively.

4.3 Results and Discussion

Affinity/Selectivity.

The complexation heat has been measured for both D-Trp and L-Trp as a function of pH ($1.5 < \text{pH} < 6$). The fitted affinity constants and their 95% confidence intervals are shown in Figure 3. For each pH value an experiment is performed in duplicate except at pH 3.5 and 6. Although some scattering is observed, this figure shows that the affinity constant of D-Trp (K_D) is in all cases higher than the affinity constant of L-Trp (K_L). This result is in agreement with results found in previous studies [6,8,9,11].

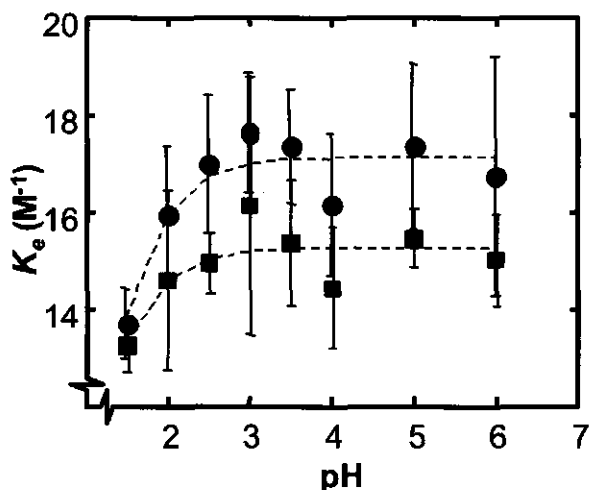


Figure 3: Complex stability constants of D-tryptophan (●) or L-tryptophan (■) with α -cyclodextrin as a function of pH. The error bars represent the 95% confidence interval of one single experiment. All experiments were performed in a 5% methanol solution at 298° K; syringe: $64 \text{ mol} \cdot \text{m}^{-3}$ α -cyclodextrin; reaction cell: $5 \text{ mol} \cdot \text{m}^{-3}$ tryptophan.

The average affinity values over the range pH 2.5-6 are $17.0 \pm 0.5 \text{ M}^{-1}$ for D-Trp and $15.2 \pm 0.5 \text{ M}^{-1}$ for L-Trp, respectively. According to Equation (2) this results in an average intrinsic selectivity for the α -cyclodextrin/Trp complex of 1.12 ± 0.04 over this range. The 95% confidence interval has been determined by means of a Monte Carlo procedure [17], since selectivity values often do not have a normal distribution. In their capillary electrophoresis experiments at pH 2.5 Fanali *et al.* [8] have found a K_I value of 15.4 M^{-1} and a K_D value of 20.2 M^{-1} . With ITC experiments Castronuovo *et al.* [10] have found a K_I value of $19 \pm 4 \text{ M}^{-1}$, where no K_D value has been reported. The agreement with our data is satisfactory, demonstrating the validity of our ITC method. It is interesting to note is that the confidence interval of our data is much narrower than that of the ITC data of Castronuovo *et al.*, demonstrating the value of a judiciously chosen integration procedure.

For low pH values (pH < 2.5) the affinity constants for both Trp enantiomers drop significantly. In this pH region a relatively large amount of Trp is present as a positively charged ion. This suggests a lower affinity constant for charged Trp than for zwitterionic Trp. A similar effect has also previously been reported in literature [18] for complexation of natural cyclodextrins with other charged compounds [19-21]. Around the pK_a of the acid group, where both neutral and charged forms are present, the affinity constant is an apparent value resulting from a weighted average of the two complexation constants (K_1 and K_2 in Figure 4). The only way to determine independently the affinity constant of the positively charged form (K_2) is to measure the affinity constant at a pH value more than 2 units below the lower pK_a value of the amino acid [18], i.e. at pH 0.4 ($\text{pK}_{\text{Trp}}=2.4$). At such a low pH, however, cyclodextrin is hydrolysed [22] and therefore this measurement cannot be done. On the other hand, the system we have studied

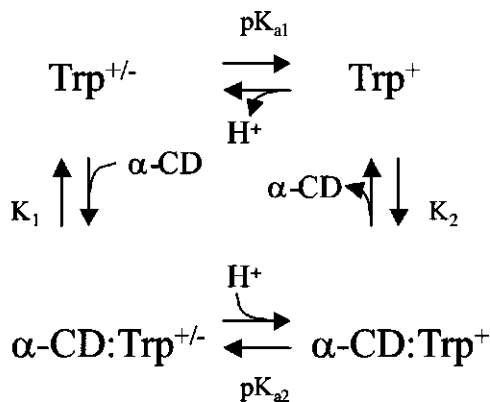


Figure 4: Schematic presentation of various possible equilibria for tryptophan(Trp)/ α -cyclodextrin(α -CD) around pH = pK_a .

behaves consistently with previous findings. The influence of the charge on the complexation will probably be better understood by considering the results obtained from the complexation enthalpy and entropy, which will be discussed later.

The selectivity, defined as the ratio of the affinity constants of both enantiomers according to Equation (2), is plotted as a function of pH in Figure 5. The solid line in this figure is the ratio of the dashed lines shown in Figure 3. Figure 5 shows a more or less constant selectivity for pH 2.5-6, while below these pH values the selectivity decreases. Decreasing selectivity in combination with decreasing affinity is frequently found for chiral interactions [6].

To make a comparison with the complexation behavior at high pH, the affinity and selectivity have been measured at pH 10. Despite the relatively high affinity ($18.2 \pm 0.9 \text{ M}^{-1}$ for both enantiomers) no selectivity could be observed at this pH. The origin of this behavior is still unclear.

Thermodynamics.

From the experimental results, the enthalpy (ΔH^0), free energy ($\Delta G^0 = -R \cdot T \ln K$) and entropy ($\Delta S^0 = \Delta G^0 / T - \Delta H^0 / T$) have been derived as a function of pH. Figure 6 shows the results obtained for the enthalpy in the pH range of 1.5 to 6. This graph shows a distinct pH effect for D-Trp only. For the pH region 3-6 the complexation enthalpy for D-Trp is constant and equals $-8.46 \pm 0.48 \text{ kJ} \cdot \text{mol}^{-1}$. This value becomes less negative for lower pH values and

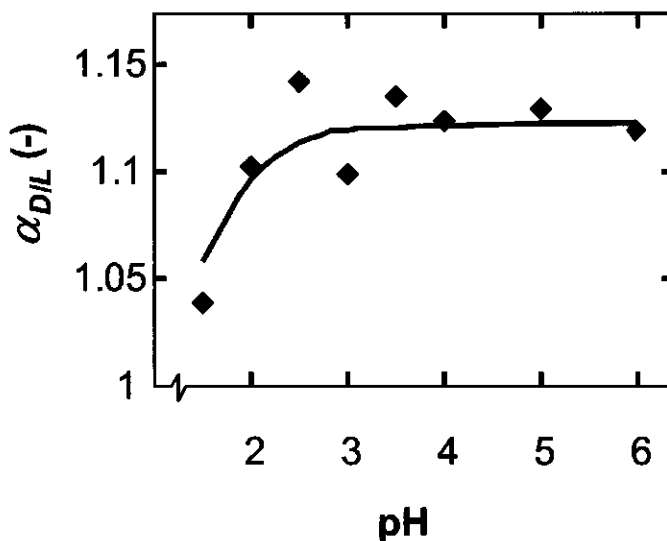


Figure 5: Intrinsic selectivity ($\alpha_{D/L} = K_D / K_L$) as a function of pH. Experimental conditions are as described in Figure 3. The solid line is the ratio of the dashed lines in Figure 3.

eventually coincides with the enthalpy value for L-Trp at pH 1.5. For L-Trp the complexation enthalpy remains more or less constant (average value $-5.45 \pm 0.62 \text{ kJ}\cdot\text{mol}^{-1}$) over the entire pH range. The occurrence of equal complexation enthalpy values at pH 1.5 indicates that under these conditions the binding mechanism for both enantiomers is similar, i.e. identical interactions are involved in this range.

Obviously, the pH effects cannot be explained by an influence of hydrophobic interactions only. Other interactions must be responsible for this effect. Lipkowitz *et al.* [11] have shown that not only the hydrophobic interactions, but also the carboxyl group of Trp is important for complexation as well as chiral discrimination. Using ^1H and ^{13}C NMR in combination with molecular dynamics, it has been shown that the carboxyl group of the zwitterion forms intermolecular hydrogen bonds with the secondary OH groups of α -cyclodextrin. For D-Trp the carboxyl group can form two such hydrogen bonds whereas L-Trp has only one possibility to form a hydrogen bond. Each hydrogen bond contributes to a negative enthalpy, explaining the more negative complexation enthalpy for D-Trp at pH 3–6 as is reported in Figure 6.

Going from neutral to low pH the carboxyl group changes from negatively charged to neutral, i.e. Trp changes from a zwitterion to a positively charged ion. This reduces the number of hydrogen bonding possibilities, since the carboxyl group changes from hydrogen bonding acceptor to a combination of a

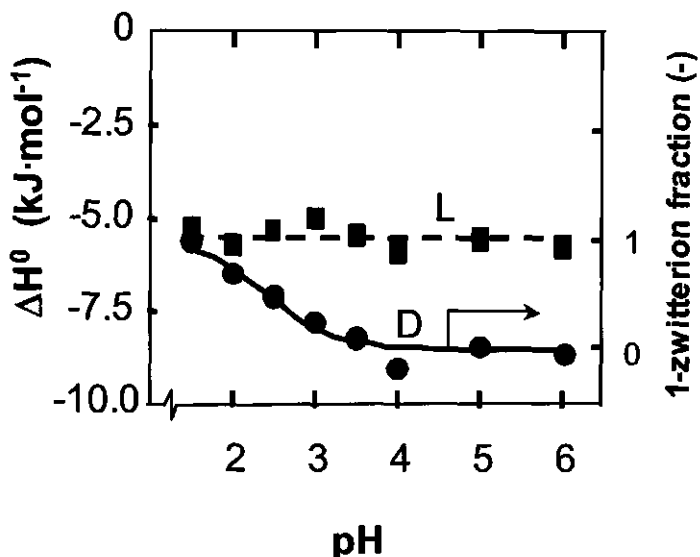


Figure 6: Complexation enthalpy (ΔH^0) of D-tryptophan (●) or L-tryptophan (■) with α -cyclodextrin as a function of pH. Experimental conditions are as described in Figure 3. The solid line through the D-tryptophan points corresponds with the zwitterion relation.

hydrogen-bonding donor and an acceptor. Therefore, the complexation enthalpy of D-Trp changes from more negative than L-Trp at pH 3-6, to equal to that of L-Trp at pH 1.5. At this low pH both enantiomers can probably form only one hydrogen bond with cyclodextrin.

The entropy values are plotted as a function of pH in Figure 7. The values of L-Trp appear to be constant whereas the values of D-Trp are again a function of the zwitterion fraction, similar to the enthalpy values. The values of the entropy, as shown in Figure 7, in combination with the negative enthalpy values indicate an "enthalpy-driven" complexation process. Since hydrophobic interactions are generally accepted to be "entropy driven" [23] our conclusion is that for α -cyclodextrin/Trp hydrophobic interactions are not the major interactions causing binding.

Often, in the case of weak complexes with natural cyclodextrins, a linear relation between ΔH° and ΔS° is observed [1]. When $T\Delta S^{\circ}$ is plotted versus ΔH° for our data, a straight line is again obtained (Figure 8). The slope of the line equals 0.98 ± 0.09 and the intercept is $-6.7 \pm 0.6 \text{ kJ}\cdot\text{mol}^{-1}$. The slope indicates the fraction of the enthalpy gain that is not cancelled out by the entropy loss associated with complex formation. The intercept, which has a positive value, represents the inherent complex stability (ΔG°) obtained at $\Delta H^{\circ} = 0$. This means that the complex is stable even in the absence of a negative enthalpy, because the remaining $T\Delta S^{\circ}$ term is positive [1]. The slope found for the Trp/ α -cyclodextrin system seems to be higher than that for other α -cyclodextrin systems, for which an average value of 0.88 [1] is found. Unfortunately, only the

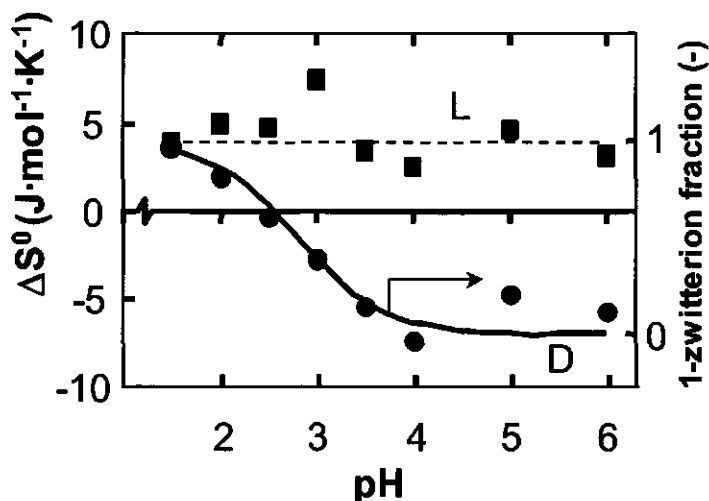


Figure 7: Complexation entropy (ΔS°) of D-tryptophan (●) or L-tryptophan (■) with α -cyclodextrin as a function of pH. Experimental conditions are as described in Figure 3. The solid line through the D-tryptophan points corresponds with the zwitterion relation.

r^2 value (=0.90) has been reported for this average value and not the 95% confidence interval. However, it is expected from this r^2 value that our value and the average value are statistically indistinguishable. The same reasoning holds for the average value of the intercept, which has been reported to be $8 \text{ kJ}\cdot\text{mol}^{-1}$ [1]. In conclusion, normal enthalpy-entropy compensation is observed for the Trp/ α -cyclodextrin system, which explains the behaviour of both complexes.

Based on the foregoing, it is tempting to suggest a mechanism explaining the phenomena observed. The linear relation between ΔH° and ΔS° suggest many complex states as a function of pH, which all have a similar Gibbs free energy for binding (ΔG°). However in the case of a relatively high number of advantageous interactions (low ΔH°) the "freedom of movement" of the guest molecule inside the cyclodextrin cavity is limited, resulting in a low $T\Delta S^\circ$ term. If the advantageous interaction is decreased, e.g. due to a change in charge density of the carboxylic group, resulting from a changing pH, the guest molecule is less tightly bound to the cyclodextrin. This looser binding results in more possible configurations of complexation. In between these two extreme configurations the number of states is almost unlimited. This can be the result of the many axes of symmetry of cyclodextrins, averaging any inequality of ΔG° . However, if the solvent condition passes a critical point (i.e. $\text{pH} < \text{pH}_{\text{critical}}$), the binding configuration dramatically changes compared to the state mentioned before, resulting in a high degree of freedom of the guest molecule and a drop of ΔG° . Additionally, the number of interactions becomes so small, that the configuration difference between both enantiomers disappears, resulting in a selectivity drop to a value of 1.

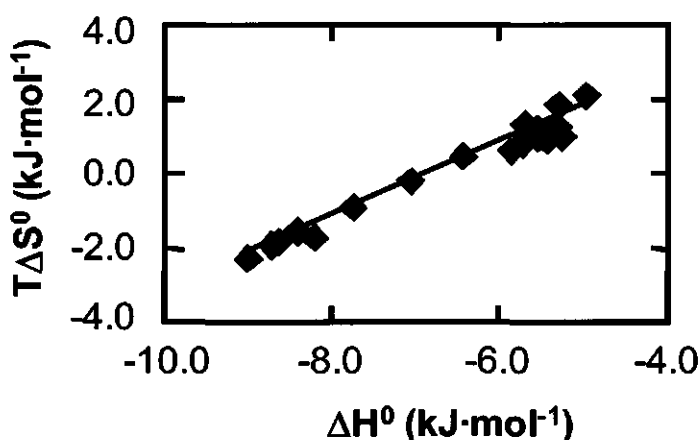


Figure 8: Relation between the complexation enthalpy (ΔH°) and complexation entropy (ΔS°) of both enantiomers. The slope of the curve equals 0.98 ± 0.09 and the intercept equals $6.7 \pm 0.6 \text{ kJ mol}^{-1}$.

4.4 Conclusions

The complexation thermodynamics of natural α -cyclodextrin and both enantiomers of Trp have been studied for pH 1.5 – 6 using isothermal titration calorimetry (ITC). The affinity constants of α -cyclodextrin/Trp can be divided into two regions. For pH 2.5 - 6 the affinity constants of both enantiomers are more or less constant and differ significantly from each other. A higher affinity is found for D-Trp than for L-Trp. On the other hand, for pH < 2.5 the affinity constants drop due to an increased influence of positively charged Trp and the affinity difference between D-Trp and L-Trp disappears. An important requirement for accurate results from ITC is the specific integration procedure of the ITC signal as is shown in the confidence intervals of our experiments compared to literature data.

From the complexation enthalpy (ΔH^0) data as a function of pH it is concluded that hydrogen bonding is important for complexation as well as for chiral discrimination. As a zwitterion, D-Trp can form extra hydrogen bonds compared to L-Trp resulting in a more negative complexation enthalpy. This additional interaction for D-Trp disappears when getting positively charged. This causes the complexation enthalpy of D-Trp to be scalable with the zwitterion fraction curve of Trp, while the complexation enthalpy of L-Trp is constant. The entropy as a function of pH showed a similar effect, representing normal enthalpy-entropy compensation. The absolute values of the entropy in combination with the negative enthalpy values indicate an "enthalpy-driven" complexation process. Since hydrophobic interactions are widely accepted to be "entropy driven" the conclusion is drawn that for α -cyclodextrin/Trp hydrophobic interactions are not the major interactions causing binding. In conclusion, despite the low affinity of α -cyclodextrin for Trp, isothermal titration calorimetry (ITC) is a suitable method to give insight in the intrinsic complexation thermodynamics as a function of pH, which is valuable information for a wide range of applications.

Acknowledgements

The authors wish to thank Anton Korteweg for technical assistance.

References

- [1] M. V. Rekharsky and Y. Inoue, Complexation thermodynamics of cyclodextrins, *Chem. Rev.* 98 (1998) 1875.
- [2] A. R. Hedges, *Industrial applications of cyclodextrins*, *Chem. Rev.* 98 (1998) 2035.
- [3] J. L. Hoffman, Chromatography of nucleic acids on cross-linked cyclodextrin gels having inclusion-forming capacity, *J. Macromol. Sci. Chem.* A7 (1973) 1147.
- [4] K. B. Lipkowitz, Applications of computational chemistry to the study of cyclodextrins, *Chem. Rev.* 98 (1998) 1829.
- [5] D. W. Armstrong, The evolution of chiral stationary phases for liquid chromatography, *Journal of the Chinese Chemical Society* 45 (1998) 581.
- [6] D. W. Armstrong, X. Yang, S. M. Han, and R. A. Menges, Direct liquid chromatographic separation of racemates with an α -cyclodextrin bonded phase, *Anal. Chem.* 59 (1987) 2594.
- [7] K. Ishihara, N. Suzuki, and K. Matsui, Optical resolution of amino acids by a polymer membrane having cyclodextrin moieties, *J. Chem. Soc. Jpn.* 3 (1987) 446.
- [8] S. Fanali and P. Bocek, A practical procedure for the determination of association constants of the analyte-chiral selector equilibria by capillary zone electrophoresis, *Electrophoresis* 17 (1996) 1921.
- [9] S. Fanali and P. Bocek, Enantiomer resolution by using capillary zone electrophoresis: Resolution of racemic tryptophan and determination of the enantiomer composition of commercial pharmaceutical epinephrine, *Electrophoresis* 11 (1990) 757.
- [10] G. Castronuovo, V. Elia, D. Fessas, A. Giordano, and F. Velleca, Thermodynamics of the interaction of cyclodextrins with aromatic and α,ω -amino acids in aqueous solutions: a calorimetric study at 25°C, *Carbohydr. Res.* 272 (1995) 31.
- [11] K. B. Lipkowitz, S. Raghothama, and J. Yang, Enantioselective binding of tryptophan by α -cyclodextrin, *J. Am. Chem. Soc.* 114 (1992) 1554.

- [12] K. D. Altria, P. Harkin, and M. G. Hindson, Quantitative determination of tryptophan enantiomers by capillary electrophoresis, *J. Chromatogr. B* 686 (1996) 103.
- [13] P. Dzygiel, P. Wieczorek, and J. A. Jonsson, Enantiomeric separation of amino acids by capillary electrophoresis with alpha-cyclodextrin, *J. Chromatogr. A* 793 (1998) 414.
- [14] E. M. van der Ent, T. P. H. Thielen, M. A. Cohen Stuart, A. van der Padt, J. T. F. Keurentjes. 2001. Electrodialysis system for large-scale enantiomer separation. *Ind.Eng.Chem.Res.* 40 (2001) 6021-6027.
- [15] T. Wiseman, S. Williston, J. F. Brandts, and L. N. Lin, Rapid measurement of binding constants and heats of binding using a new titration calorimeter, *Anal. Biochem.* 179 (1989) 131.
- [16] T. J. M. de Bruin, A. T. M. Marcelis, H. Zuilhof, and E. J. R. Sudhölter, Enantioselectivity measurements of copper(II) amino acid complexes using isothermal titration calorimetry, *Langmuir* 16 (2000) 8270.
- [17] P. E. M. Overdevest, Padt A. van der, J. T. F. Keurentjes, and K. van 't Riet, Langmuir isotherms for enantioselective complexation of (d/l)-phenylalanine by cholesteryl-l-glutamate in nonionic micelles, *Colloids and Surfaces A Physicochemical and Engineering Aspects* 163 (2000) 209.
- [18] E. Junquera and E. Aicart, Effect of pH on the encapsulation of the salicylic acid salicylate system by hydroxypropyl-beta-cycle dextrin at 25 degrees C. A fluorescence enhancement study in aqueous solutions, *J. Inclusion Phenom.* 29 (1997) 119.
- [19] E. Junquera and E. Aicart, Potentiometric study of the encapsulation of ketoprofen by hydroxypropyl-beta-cyclodextrin. Temperature, solvent, and salt effects, *J. Phys. Chem. B* 101 (1997) 7163.
- [20] H. Aki, T. Niiya, Y. Iwase, and M. Yamamoto, Two types of inclusion realized in the complexation between phenobarbital and 2-hydroxypropyl-beta-cyclodextrin in aqueous solution, *Thermochim. Acta* 308 (1998) 115.
- [21] E. Junquera, M. Martin-Pastor, and E. Aicart, Molecular encapsulation of flurbiprofen and/or ibuprofen by hydroxypropyl-beta-

cyclodextrin in aqueous solution. Potentiometric and molecular modeling studies, *J. Org. Chem.* 63 (1998) 4349.

[22] J. Szejtli, *Cyclodextrin technology*, Kluwer academic publishers, Dordrecht, 1988.

[23] K. A. Connors, The stability of cyclodextrin complexes in solution, *Chem. Rev.* 97 (1997) 1325.

5 Multistage electro dialysis for large-scale separation of racemic mixtures

Abstract

A new counter-current process has been developed for large-scale enantiomer separations, based on a combination of enantioselective complexation in solution, counter-current fractionation and electro dialysis. The counter-current principle is obtained by the electrophoretic transport of the free enantiomer through size-selective membranes, whereas the complexed enantiomer is retained by the membranes and is transported with the liquid flow in the opposite direction. This design has been validated in an electro dialysis stack containing 20 membrane compartments. A racemic mixture has been fed to one side of the closed system, simulating one half of a complete separation apparatus. Using this set-up the enantiomeric excess (e.e.) and the concentrations of both enantiomers have been determined as a function of the current density at a constant liquid flow velocity. As a model system the separation of D,L-tryptophan in combination with α -cyclodextrin as the chiral selector is used. Despite the low selectivity of this selector (1.12), an e.e. difference of 14% has been obtained. Based on these experimental data, model calculations have shown that using an electro dialysis stack of 250 membrane compartments a complete separation (e.e. >99%) can be accomplished for this system. The proposed multi-stage electro dialysis separation principle has the advantage of using elements from existing analytical separation methods. As this method is suitable for low selective (1.1-2) chiral selectors, it provides a viable alternative for the current large-scale enantiomer separation processes.

This chapter has been submitted for publication as: E.M. van der Ent, P. van Hee, J.T.F. Keurentjes, K. van 't Riet, A. van der Padt, Multistage electro dialysis for large-scale separation of racemic mixtures

5.1 Introduction

During the last decade, the interest in chirality and its consequences has induced a substantial research effort. For various scientific and economic reasons, the main contributor and driving force for this is the pharmaceutical industry. Many pharmaceuticals contain one or more asymmetric carbon atoms resulting in at least two stereoisomers. Often, one of the stereoisomers is more active for a given action (eutomer) while the other one (distomer) is inactive or even causes severe side effects [1]. As a result, the worldwide production and sales of single enantiomeric drugs show a continuous growth at this moment [2].

On analytical scale, almost any enantioseparation can be achieved with at least one of the about 200 commercially available chiral selectors in combination with well-established GC, LC, and CE separation techniques [3]. However, for large-scale production the number of methods is limited. To date, the two basic techniques are crystallization and kinetic resolution [4]. However, over the last decade new promising routes have been introduced. Most of them are based on multistage counter-current technology, since the selectivity of the applied chiral selectors usually is low (i.e. 1.1-2) [5-7].

Three separation systems have been described in the literature, which can potentially be operated on a large scale (multi-tons per year). Firstly, systems based on liquid/liquid extraction [8-10] and related to that extraction via liquid membranes [11] have been developed [12]. However, the lack of process stability and leakage of the chiral selector are still problems to be overcome for these processes. Secondly, micellar-enhanced ultrafiltration (MEUF) is a new counter-current separation process and has been introduced for chiral separations by Overvest et al. [13]. In this system a pressure difference is used to separate the bulk solution from the chiral selective micellar phase. However, the scale-up of this system is complicated, since every single stage is implemented as a single membrane module, including pumps, piping and valves. The third technique described in the literature that does not experience this drawback is the simulating moving bed (SMB) technique, which can be regarded as a counter-current and scaled-up result of existing HPLC methods. It has been shown that SMB systems can separate enantiomers in large quantities (1 kg/day) [14] or even multi-tons per year [15]. Therefore, the strength of this system is its use of already available chiral stationary phases (CSP) from analytical methods, which reduces the development time and costs.

Another widely applied analytical method is capillary electrophoresis (CE) [2], which potentially can be considered for the same scale-up and counter-current procedure as the SMB technique. However, no continuous large-scale

separation process based on the CE concept have been developed yet [2]. Previously, we have shown the potential of a membrane separation system using an electrical potential as the driving force [16]. In this system the bulk phase is separated from the chiral selector phase using an electrical potential and size selective membranes. On a large scale this separation principle will have to be applied counter-currently, resulting in a system with the same advantages as the SMB technique.

In this paper we present a counter-current and multi-stage electro dialysis process for large-scale enantiomer separations, based on analytical CE methods. This system has the advantage of easy scale-up, since multiple stages are incorporated in one single apparatus. An experimental procedure for the process characterization is suggested. The results are described by model calculations and the feasibility of the process is shown.

5.2 Process description

When a chiral selector is added to a racemic mixture (i.e. a compound with 50:50 proportion of enantiomers), the chiral selector will selectively bind one of the two enantiomers. The free enantiomer population will be enriched in one of the enantiomers while the complexed population will be enriched in the other one. The complexed and free enantiomers differ in size and hence a separation can be established by size discrimination, e.g. using synthetic membranes [17]. For this separation a driving force is needed, which can be a concentration difference (as it is used in liquid/liquid extraction), a pressure difference (as it is used for micellar enhanced ultrafiltration (MEUF)), or an electrical potential, as it is used for the system presented in this paper.

Since selectivity values (α) of commonly used chiral selectors in CE methods are low ($1.1 < \alpha < 2$), a racemic mixture is not completely separated using one single stage. Combining multiple stages in a counter-current flow configuration will result in any desired degree of separation. This counter-current flow is easily obtained using an electro dialysis stack containing synthetic membranes, which can separate the complexed enantiomers from the free enantiomers. Depending on the polarization of the electrodes, the electrophoretic flow of the free enantiomers flows counter-currently with respect to the liquid flow containing the chiral selector and thereby the complexed enantiomers (Figure 1). This chiral selector flow is pumped in a meander pattern through all membrane compartments in the module to allow a simple design of the spacers between the membranes. This module configuration has the advantage of giving a multi-stage counter-current flow in a single apparatus.

There are two contributions to the electrophoretic transport of the free enantiomers through the membranes. For charged species the transport will

mainly be the result of the electrochemical potential and the accompanying current density. The charge flux (J [mol·m⁻²·s⁻¹]) and current density (i [A·m⁻²]) are connected by Faraday's constant ($F = 96486$ C·mol⁻¹) and the current efficiency or the transport number (Tn [-]) [17]:

$$J e_j = \frac{i}{F} \cdot Tn_j \quad [\text{mol} \cdot \text{m}^{-2} \cdot \text{s}^{-1}] \quad (1)$$

In absence of a background electrolyte, Tn approaches unity, i.e. all current is used for the transport of the charged free enantiomers. In this case, Tn is practically independent on the concentration of the charged enantiomers. On the other hand, in the presence of high amounts of background electrolyte the transport number for the free enantiomers will drop, since the current is mainly used for the transport of the background electrolyte. High amounts of background electrolyte will cause a volume flux due to the electro-osmotic flow [18]. This volume flux contains the free enantiomer concentration resulting in a free enantiomer flux through the membrane. Of course, the efficiency of the latter mechanism is much lower than that of the first mechanism, but transport of free enantiomers occurs, even for uncharged species.

In the literature, multi-stage electrodiagnosis systems have been described for the separation of metal ion mixtures [19-24], using a difference in transport velocity through the membranes. In our system, however, a difference in bulk

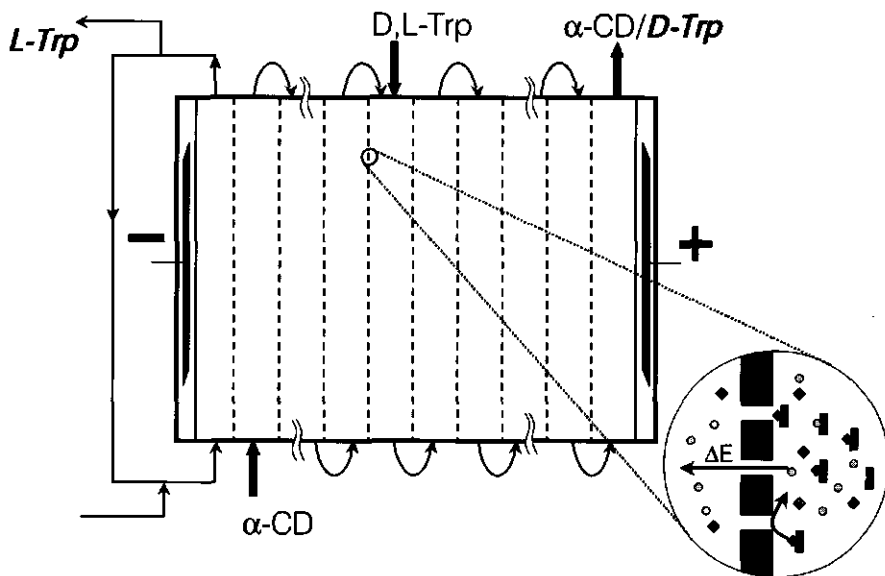


Figure 1: Representation of the continuous multi-stage electrodiagnosis process, including the separation principle (enlargement). The liquid flow including the complexed enantiomers flows from left to right in a meander pattern through the module, whereas the counter-current electrophoretic flux of the free enantiomers is from right to left.

concentration is responsible for selectivity. A similar concept has been described in literature [25] for the separation of calcium and cadmium using EDTA as selective complexing agent. However, only single stage experiments have been described.

5.3 Theory

To predict the behavior of the multi-stage electro dialysis system a model is derived, which allows the determination of the critical process parameters. Previously, multi-stage electro dialysis for the separation of two metal ions has been modeled in two different ways. Glueckauf and Kitt [20] have modeled the liquid flow through the membrane compartments (Figure 1) as a plug flow, resulting in a dynamic analytical solution for their system. On the other hand, Cruz et al. [19] assumed complete mixing in each membrane compartment. Residence time measurements in our system, i.e. measuring the response of an acetone pulse, have shown that the actual flow profile can be described by assuming 3 completely mixed stages for each membrane compartment. Therefore, we will use the number of 3 for our model calculations.

For each stage, a mass balance is set-up (Figure 2):

$$\frac{dc_{e,j}}{dt} = \frac{\Phi_v}{V} \cdot ((c_{e,j-1} - c_{e,j}) + (q_{e,j-1} - q_{e,j})) + \frac{1}{V} \cdot (Je_{e,j+1} - Je_{e,j}) - \frac{dS_{e,j}}{dt} - \frac{dq_{e,j}}{dt} \quad [\text{mol} \cdot \text{m}^3 \cdot \text{s}^{-1}] \quad (2)$$

where $c_{e,j}$ is the enantiomer concentration (D or L) in stage j [$\text{mol} \cdot \text{m}^{-3}$], Φ_v is the

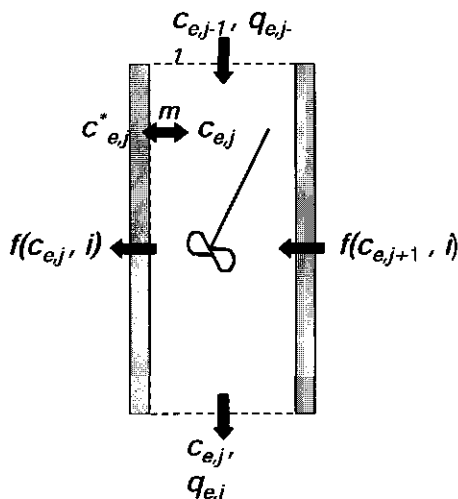


Figure 2: One single stage of the multi-stage system, including the entering fluxes and the leaving fluxes. For the model calculation in this paper it is assumed that each membrane compartment is divided in a series of 3 continuously stirred tanks.

liquid flow [$\text{m}^3 \cdot \text{s}^{-1}$], V is the stage volume [m^3], $q_{e,j}$ is the complexed enantiomer concentration [$\text{mol} \cdot \text{m}^{-3}$], $Je_{e,j}$ is the electrophoretic flux (Equation (1)), which can be described as a function of the concentration [16]:

$$Je_{e,j} = \frac{j \cdot A}{F} \cdot Tn = \frac{j \cdot A}{F} \cdot \frac{c_{e,j}}{1 - Tn + c_{e,j}} \approx \frac{j \cdot A}{F} \cdot Tn^* \cdot c_{e,j} \quad [\text{mol} \cdot \text{s}^{-1}] \quad (3)$$

Here A the membrane surface area [m^2], Tn is the transport number at an arbitrarily chosen enantiomer concentration of $1 \text{ mol} \cdot \text{m}^{-3}$ [-] and Tn^* is a concentration independent transport number constant [$\text{m}^3 \cdot \text{mol}^{-1}$]. The approximation on the right hand side of Equation (3) is only valid for low transport numbers ($Tn < 0.05$).

The term $\frac{dS_{e,j}}{dt}$ in equation (2) is the amount of enantiomers absorbed by the membrane matrix per unit of time [$\text{mol} \cdot \text{m}^{-3} \cdot \text{s}^{-1}$]. This term is incorporated since most (ion exchange) membranes can absorb quite high amounts of organic molecules [26,27]. This term is modeled using a linear driving force model [28]:

$$\frac{dS_{e,j}}{dt} = k_a \cdot \left(c_{e,j}^* - \frac{c_{e,j}}{m} \right) \quad [\text{mol} \cdot \text{m}^{-3} \cdot \text{s}^{-1}] \quad (4)$$

where k_a is the absorption rate constant [s^{-1}], $c_{e,j}^*$ is the membrane matrix concentration of the enantiomers in equilibrium with the liquid bulk concentration of the free enantiomers ($c_{e,j}^* = c_{e,j} \cdot m$) [$\text{mol} \cdot \text{m}^{-3}$] and m is the partition coefficient [-].

The term $\frac{dq_{e,j}}{dt}$ in Equation (2) is the change in the complexed enantiomer concentration ($q_{e,j}$) per unit of time; it can be described by adopting bi-component Langmuir adsorption isotherms [$\text{mol} \cdot \text{m}^{-3} \cdot \text{s}^{-1}$]. For the D-enantiomer the complexation term is described by:

$$\frac{dq_{D,j}}{dt} = \frac{dc_{D,j}}{dt} \cdot \frac{dq_{D,j}}{dc_{D,j}} = \frac{dc_{D,j}}{dt} \cdot \frac{q_s \cdot k_D \cdot (1 + c_{L,j} \cdot k_L)}{(1 + c_{D,j} \cdot k_D + c_{L,j} \cdot k_L)^2} \quad [\text{mol} \cdot \text{m}^{-3} \cdot \text{s}^{-1}] \quad (5)$$

where q_s is chiral selector concentration and k_D is the affinity constant for D-Trp. A similar equation can be obtained for the L-enantiomer.

The mass balance for the feed stage is slightly different, i.e. an extra term of $\Phi_{v,f} \cdot c_{f,e}$ is added in Equation (2), where $\Phi_{v,f}$ is the feed flow [$\text{m}^3 \cdot \text{s}^{-1}$] and $c_{f,e}$ is the feed flow enantiomer concentration [$\text{mol} \cdot \text{m}^{-3}$]. Consequently, the feed flow changes the liquid flow velocity of the stages after the feed stage. Numerical integration of Equation (2) results in the concentration profiles for all stages as a

function of time. Obviously, the stack outflow is most important, since this determines the product purity.

An important parameter for counter-current processes is the extraction factor (Λ_e), since this parameter determines the net direction of a species, i.e. whether it is taken along with the liquid flow ($\Lambda_e > 1$) or with the electrophoretic flow ($\Lambda_e < 1$). The extraction factor is described by the molar ratio of a species that leaves a separation stage in the two opposite directions. For the multi-stage electrodialysis system the extraction factor for each membrane compartment m can be described as:

$$\Lambda_{e,m} = \frac{\Phi_v \cdot c_{e,j=3,m} \cdot (1 + q_s \cdot k_e)}{\sum_{j=1}^3 J e_{e,j}} \quad [-] \quad (6)$$

In order to achieve any desired degree of separation, the extraction factor of the two enantiomers have to be at opposite sides of unity. This is achieved by controlling the ratio of the current density and the liquid flow velocity. The product purity is quantified by the enantiomeric excess values

$$(e.e. = \frac{c_{D-Trp} - c_{L-Trp}}{c_{D-Trp} + c_{L-Trp}}) \text{ of both product flows.}$$

5.4 Experimental

As a model system for large-scale enantiomer separations we used α -cyclodextrin to separate D,L-tryptophan (D,L-Trp). The CE method for this system is described in literature [29], which shows that α -cyclodextrin has a higher affinity for D-Trp than for L-Trp. Also, using Isothermal Titration Calorimetry (ITC) we have measured an affinity value for D-Trp (k_D) of 17.0 M^{-1} and for L-Trp (k_L) 15.2 M^{-1} resulting in an intrinsic selectivity ($\alpha_{D/L} = \frac{k_D}{k_L}$) of 1.12 [30].

Materials

D,L-tryptophan (>98%) was obtained from Bachem, α -cyclodextrin (>98%) was obtained from Fluka, analytical grade silver nitrate, perchloric acid (60%), and nitric acid (65%) were obtained from Merck. All chemicals were used as received. Nafion 117 cation exchange membranes were obtained from C.G. Processing, Inc. (Rockland, USA) and were equilibrated for 1 hour in doubly distilled water at 90°C . The bipolar membranes (Neosepta BP-1), a rectifier power supply (300 V, 1A) and an electrodialysis stack were obtained from Tholen Membrane Technology (Bussum, the Netherlands). The electrodialysis stack consisted of 20 membrane compartments (Figure 3B) with an effective

membrane area of 100 cm² per membrane compartment (10 x 10 cm), two electrode chambers containing iridium oxide-coated titanium electrodes and one product compartment (Figure 3A).

Analysis

Chiral HPLC was used for sample analysis to determine the enantiomer concentrations. The system consisted of a Spectra Physics SP8810 pump, a Thermo Separation® Products AS1000 auto sampler and a Separations UV detector. The column used for the separation was a 150 mm x 4 mm i.d. Daicel Crownpak CR(+) (5 µm). Mobile phase elution (1.2 mL/min) was performed isocratically using a filtered (0.45 µm) and degassed aqueous solution of perchloric acid (pH = 1.5). The column temperature during analysis was maintained at 28°C. The injected sample volume was 20 µL and the samples were injected without any pretreatment. The wavelength setting of the UV detection was fixed at 254 nm. The calibration curve showed a linear relation up to a total concentration (D-Trp plus L-Trp) of 5 mM.

Module experiments

Module experiments were performed to establish the degree of separation as a function of the current density at constant liquid flow. This allowed for the variation in the ratio of the two counter-current flows, i.e. the chiral selector flow

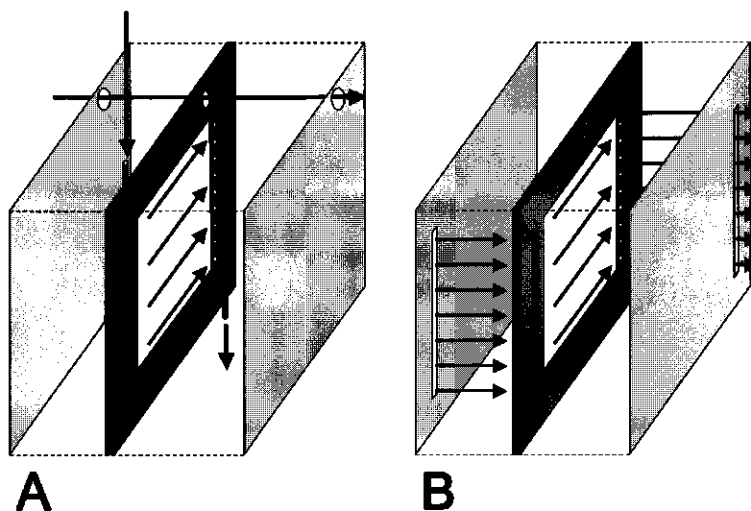


Figure 3: Details of the electrodiagnosis stack compartments, which are responsible for the meandering flow pattern through the module; (A) product compartment; (B) separation compartment. The outer dimensions are 0.2 x 15 x 15 cm while the inner dimensions are 0.2 x 10 x 10 cm.

and the electrophoretic flow.

To prevent a high consumption of chiral selector, the experiments were performed in a batch mode. A schematic drawing of the experimental set-up is presented in Figure 4. This figure shows that all liquid streams were recirculated into the stock vessel (1). The separation was monitored at the outflow of the electrodiagnosis stack. With this experimental configuration, one single half of the continuous system was studied. The only exception was that the feed concentration could change in this batch set-up, whereas the feed concentration in the continuous system will be constant. Nonetheless, this batch system should give the same insight as obtained from a continuous system.

The product compartment (2) in front of the negative electrode had a large flush to prevent accumulation of enantiomers, which are transported by the electrophoretic flow towards the negative electrode. This product flow (Φ_p) equaled 100 times the liquid flow through the stack (Φ_s). With these flow velocity values the enantiomer concentration in the product compartment was almost the same as the concentration in the stock vessel. The positive and negative electrode chambers (6) were filled with 10^{-2} M HNO_3 and 10^{-2} M NaOH , respectively. The liquid was circulated through a cooling device to prevent heating of the system. Although the set point was 5°C , the actual temperature

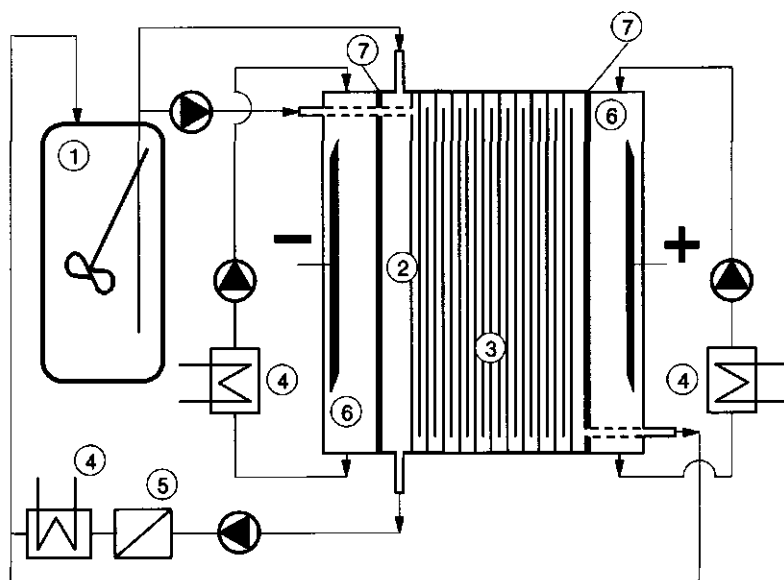


Figure 4: The batch multi-stage electrodiagnosis system used to investigate the separation principle. (1) stock vessel; (2) product compartment; (3) separation compartments; (4) cooler; (5) membrane to filter any AgOH deposits; (6) electrode chambers; (7) bipolar membranes. Enantiomer concentrations are determined by the stock vessel liquid and the stack outflow.

of the separation liquid was about 10° C due to a heat flux originating from the surroundings.

Since electro-osmotic flow is a major transport mechanism for charged and uncharged species in this electro dialysis system [16], bipolar membranes were applied to prevent loss of Trp to the electrode compartments. Theoretically, bipolar membranes hardly have any electro-osmotic flow and due to their charged structure all charged species will be repelled. Additionally, the hydroxyl producing side of the bipolar membrane faced the Trp solution. This could result in a local change of the Trp charge from positive to negative, resulting in an electrophoretic mobility into the solution instead of an electrophoretic mobility towards the membrane.

Since AgNO₃ was present in the liquid as an anti bacterial growth agent, AgOH deposits were formed due to the production of OH⁻ ions near the bipolar membrane in the product compartment. A dead end membrane filtration unit (5) (Bio-Nephross Allegro dialyzers by Cobe Nephross BV) filtered the product circulation flow to keep a clear solution.

Before each experiment the system was rinsed with 10⁻² M HNO₃ for at least 64 hours. During this period the Trp from preceding experiments was washed out of the membranes. The HNO₃ also transformed the membranes into the H⁺ form. Subsequently, the system was rinsed with demineralized water for at least another 24 hours. The flow rate through the system during both washing steps was about 1.5·10⁻⁷ m³·s⁻¹, resulting in a total washing of about 150 residence times. After this period, the system was flushed 4 times with a solution of 20 mol·m⁻³ α-cyclodextrin, 1 mol·m⁻³ AgNO₃ and 5 mol·m⁻³ D,L-Trp. Subsequently, the outflows were short-circuited into the stock vessel. Since a significant amount of Trp is absorbed by the membranes, about 2 g additional D,L-Trp was needed to obtain a final concentration of about 1 mol·m⁻³. Then, the system was equilibrated for another 24 hours. The experiment was started by decreasing the liquid flow from 1.5·10⁻⁷ m³·s⁻¹ to 1.7·10⁻⁸ m³·s⁻¹ and by switching on the power supply to a preset current density value. Samples were collected from the stack outflow and the stock vessel and were analyzed without any pretreatment using chiral HPLC.

5.5 Results and discussion

Stepwise current experiment

To demonstrate the separation principle of the multi-stage electro dialysis separation system, an experiment has been performed using a stepwise current density increase. The results are shown in Figure 5, where Figure 5A shows the concentrations of the stack outflow and the stock vessel and Figure 5B shows

the corresponding enantiomeric excess values (e.e.). The dotted line of the current density ($250 < t < 480$) indicates that the maximum voltage of the power supply has been reached during that period, resulting in a lower current density than the preset value. The current density just before switching off the voltage supply has been measured as $10 \text{ A}\cdot\text{m}^{-2}$. From the concentration levels (Figure 5A) it can be seen that the concentration difference between the stack outflow and the stock vessel increases with increasing current density. A higher current density causes an increase of the electrophoretic flux, resulting in an increased back transport of the enantiomers and thus a lower stack outflow concentration. For high current density values ($i = 15 \text{ A}\cdot\text{m}^{-2}$) the concentration in the stock vessel increases drastically, whereas up to intermediate current density values ($i < 10 \text{ A}\cdot\text{m}^{-2}$) the concentration remains more or less constant. This phenomenon is the result of the relatively high absorption capacity of the membranes, which acts as a buffer for the enantiomers. With model calculations a similar result is obtained, as will be shown below.

After switching off the power ($t > 480$) the concentrations should theoretically approach their initial concentrations. However, as can be seen in Figure 5A, this

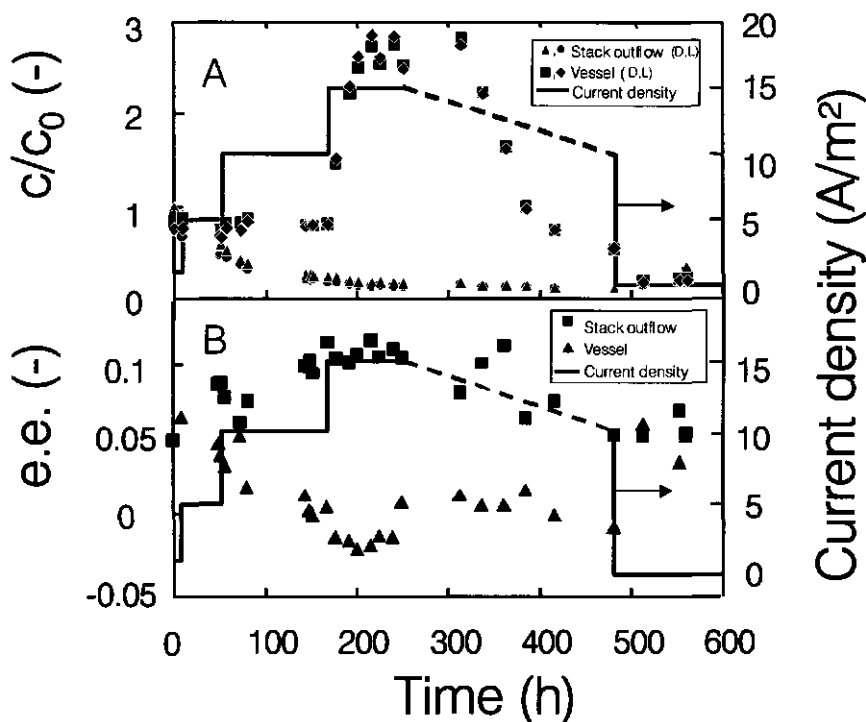


Figure 5: Influence of the current density on the stock vessel concentration, the stack outflow concentration (A) and the enantiomeric excess (B); $q_s = 20 \text{ mol}\cdot\text{m}^{-3}$; $[\text{AgNO}_3]_{t=0} = 1 \text{ mol}\cdot\text{m}^{-3}$;

appears not to be the case. One reason can be the loss of enantiomers during the foregoing period, e.g. by transport or diffusion through the bipolar membrane into the electrode chambers. Another reason can be that the time required for equilibrium is not yet reached, which is indicated by the fact that the stack outflow concentration still increases at the end of the experiment. However, it is interesting to note that the system can be operated during this 500 hours period without having any significant problems.

As is shown in Figure 5, not only a change is observed in the concentrations, but also in the enantiomeric excess values (e.e.), emphasizing the separation principle. The difference between the e.e. at the stack outflow and the e.e. at the stock vessel increases with increasing current density. Although the module used in these experiments only consists of 20 membrane compartments, an e.e. difference of about 14% can be obtained. For a single stage without liquid flow, the e.e. value is at most 4.3%, showing the relevance of the multi-stage counter-current principle. Since 14% is far from complete separation more compartments are needed to increase the separation.

A particular issue to note is that the e.e. values in Figure 5 differ from zero at $t=0$. This effect is caused by the absorption of Trp into the membranes. In the

Table 2: Parameters used for the model calculations

Parameter	Value	
k_D ¹	$17.0 \cdot 10^{-3}$	$[\text{m}^3 \cdot \text{mol}^{-1}]$
k_L ¹	$15.2 \cdot 10^{-3}$	$[\text{m}^3 \cdot \text{mol}^{-1}]$
q_s	20	$[\text{mol} \cdot \text{m}^{-3}]$
m ²	3	$[-]$
n	20	$[-]$
Tn ³	0.018	$[\text{m}^3 \cdot \text{mol}]$
S ⁴	50	$[-]$
k_a ⁴	1	$[\text{s}^{-1}]$
Φ_v	$1.67 \cdot 10^{-8}$	$[\text{m}^3 \cdot \text{s}^{-1}]$
A	0.01	$[\text{m}^2]$
V	$5 \cdot 10^{-6}$	$[\text{m}^3]$

- 1 Obtained from the Isothermal Titration Calorimetry that has been used for the determination of the affinity constants [30].
- 2 Obtained from a fit of the residence time distributions of acetone pulses to a tanks in series model.
- 3 Obtained from batch electro dialysis experiments [16].
- 4 Obtained by residence time distributions of Trp pulses in combination with residence time distribution of acetone pulses.

bulk liquid the free enantiomers concentration is enriched in one of the enantiomers, due to the enantioselective complexation of the chiral selector. Since only the free enantiomer is absorbed, the absorption will cause an enriched liquid phase of the other enantiomer. Microbial degradation of Trp is not observed during the experiment: Figure 5B shows that the e.e. values of both stack outflow and stock vessel return to their initial values.

Single current experiments

In order to examine the influence of the current density more accurate, experiments have been performed using a constant current density per experiment. The results are shown in Figure 6, where, the e.e. difference (A), the stack outflow concentration (B) and the stock vessel concentration (C) are plotted as a function of the current density. The lines in these graphs represent model calculations. It has to be noted that for the model calculation represented by the solid lines no fit parameters are used, but only independently measured parameters. The parameters and their respective values are shown in Table 2.

Figure 6A shows that the model describes the e.e. difference accurately. The absolute values of the e.e. difference in this figure is somewhat lower than the value obtained in Figure 5, i.e. 14% at $15 \text{ A}\cdot\text{m}^{-2}$. The experiments of Figure 6 have taken about 50 hours and the model calculations have shown that after this period of time the system has not yet reached steady state. This takes

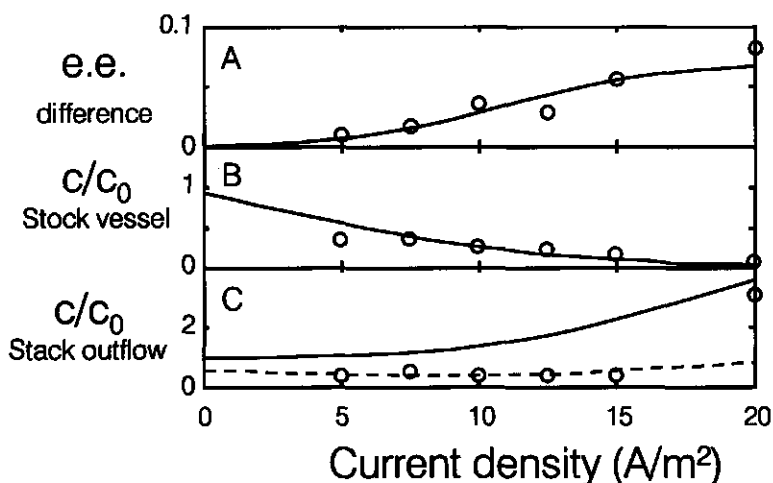


Figure 6: Current dependency of (A) enantiomeric excess difference between the stock vessel and the stack outflow; (B) stock vessel concentration and (C) stack outflow concentration, obtained by single current experiments. The lines are the results of independent model calculation. For the dashed lines a diffusion of enantiomers through the bipolar membranes is incorporated ($D=1\cdot 10^{-10} \text{ m}\cdot\text{s}^{-2}$).

about 25 times the experimental time of 50 hours. These long equilibrium times are again a result of the absorption of Trp in the membranes. Therefore, reducing Trp absorption by choosing other membrane materials may reduce the equilibrium time significantly. Model calculations have shown that in the absence of absorption, equilibrium is reached after about 25 hours (≈ 4.5 residence times). Although the absorption has a large influence on our dynamic experiments, it is not expected to have any influence on a continuous process, as this is operated at steady state.

Figure 6B shows that the model also accurately describes the concentration of the stack outflow. However, the concentration in the stock vessel (Figure 6C) is overestimated, except for the higher current density values. The experiments at lower current density values all show a lower stock vessel concentration than the starting concentration, while from the mass balance at least the same concentration is expected. Although we did not expect this effect, this indicates a loss of enantiomers through the bipolar membranes into the electrode chambers.

Using model calculations we have tried to verify this by including the diffusion of enantiomers through the bipolar membranes. The results of the model calculations are described by the dashed line in Figure 6. It appears, that a diffusion coefficient through the bipolar membrane of $1 \cdot 10^{-10} \text{ m}^2 \cdot \text{s}^{-1}$ is required to describe all experiments at $i \leq 15 \text{ A} \cdot \text{m}^{-2}$. Obviously, the loss of product due to diffusion only influences the stock vessel concentration and hardly the e.e. difference or the stack outflow concentration, which is probably due to the relatively short length of the experiments.

The diffusion through the bipolar membrane can be explained by the low current density values used in our experiments. It is known that below the limiting current density no water splitting occurs in bipolar membranes [31]. Consequently, no hydroxyl ions are formed, which should have prevented the diffusion of Trp through the bipolar membrane. From the foregoing is concluded that the model calculations describe the experimental data accurately. These allow further design calculations to show the viability of the system.

Design Calculations

To demonstrate the potential of the system for obtaining both enantiomers in high purity, model calculations have been performed for the counter-current system as shown in Figure 1. The parameters used for the model calculations are the same as the parameters given in Table 2. Additionally, an arbitrary feed flow is chosen of 1/100 times the chiral selector flow in combination with a feed flow concentration (c_f) of 2 or 20 $\text{mol} \cdot \text{m}^{-3}$ for each enantiomer.

First, the influence of the number of stages (m) and the chiral selector concentration (q_s) on the degree of separation is calculated. For this purpose, the optimal current density is calculated, i.e. the current density at which the absolute e.e. values of both product flows are the same. The steady state e.e. values are plotted in Figure 7, where the solid lines describe the relations for a feed flow concentration of $2 \text{ mol}\cdot\text{m}^{-3}$ and the dashed lines describe the relations for a feed flow concentration of $20 \text{ mol}\cdot\text{m}^{-3}$. The differences between these two sets of lines indicate an overload of the system for the highest feed flow concentration, resulting in a lower degree of separation. Overdevest et al. [32] have shown for a counter-current ultrafiltration system that the feed flow concentration has to drop to zero as the selectivity approaches unity, in order to prevent overload of the system. Of course, this negatively influences the productivity of the system. Therefore, the chiral selector properties in combination with the feed flow concentration should be one of the optimization criteria for this counter-current separation system.

Figure 7 shows that for both feed flow concentrations an increase in the number of stages as well as an increase of the chiral selector concentration results in a higher product purity, which is comparable to other counter-current processes [33]. It also shows that the experimental chiral selector concentration of $20 \text{ mol}\cdot\text{m}^{-3}$ is relatively low. Using this concentration a complete separation cannot be obtained without increasing the number of membrane compartments to unrealistically high values. For an efficient process the chiral selector

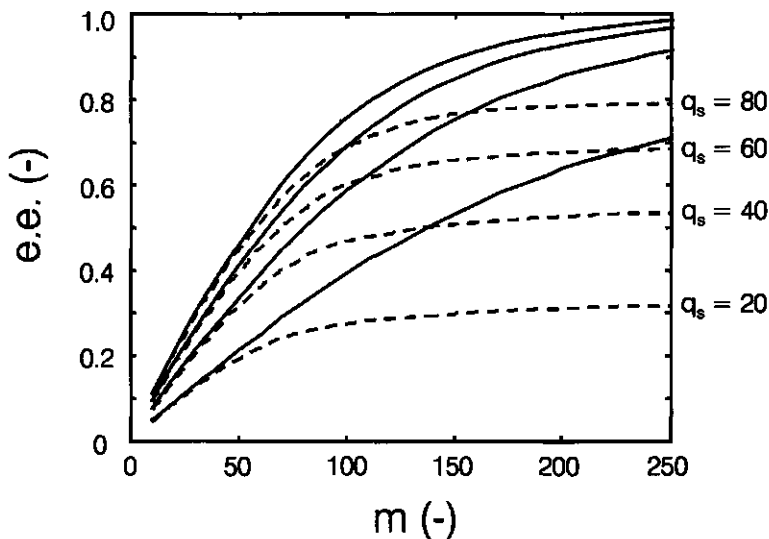


Figure 7: Estimated effect of the chiral selector concentration (q_s) and the number of membrane compartments (m) on the enantiomeric excess of both product flows obtained from the continuous multi-stage electro dialysis system.

concentration should be as high as possible. The maximum solubility of α -cyclodextrin is about $150 \text{ mol}\cdot\text{m}^{-3}$ [34], however, since the complex is often less soluble than the pure cyclodextrin, this concentration cannot be used in practice. An α -cyclodextrin concentration of $80 \text{ mol}\cdot\text{m}^{-3}$ has been reported in literature [29] for this Trp/ α -cyclodextrin model system, indicating this value to be a realistic value. If the system is not overloaded, a complete separation (99%+) can be obtained using this chiral selector concentration in an electro dialysis stack containing about 250 membrane compartments (Figure 7), despite the low selectivity of 1.12. In practice, this number of compartments is already used in electro dialysis stacks for the treatment of water desalination [17]. Therefore, it is supposed that this separation process can easily be implemented for large-scale enantiomer separation technology.

Besides the positive influence of an increased chiral selector selectivity on the feed flow concentration, also an influence is expected on the degree of separation. For this purpose, we calculated the e.e. values of the product flows as a function of the chiral selector selectivity (Figure 8). This figure shows that an increase of the selectivity from 1.12 to 1.3 reduces the number of membrane compartments from 250 to about 100, while maintaining a complete separation (e.e. >99%). The additional advantage is that this will also reduce the energy consumption for this system by a factor of about 2.5, indicating the relevance of this parameter. Although the selectivity of 1.3 is not observed for our system, other systems are available in which this value can be achieved easily, e.g. by

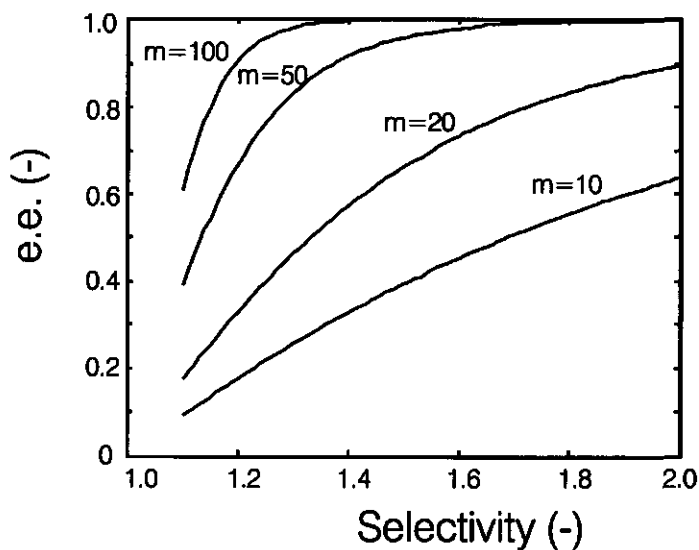


Figure 8: Estimated effect of the chiral selector selectivity and the number of membrane compartments on the enantiomeric excess; $c_f = 20 \text{ mol}\cdot\text{m}^{-3}$; $\phi_{v,i} = 1/100 \cdot \phi_r$

using modified cyclodextrins [35]. To illustrate the influence of the chiral selector selectivity on the extraction factor, and thereby on the degree of separation, the extraction factor values are plotted in Figure 9 for a selector selectivity of 1.12 and 2, respectively. This figure shows that the band width is increased with increasing selectivity, resulting in a better degree of separation per membrane compartment. Figure 9 also shows that the extraction factors are more or less constant throughout the module except at both ends of the module and at the feed stage, which has also been observed for other counter-current processes [32]. The reason for the deviation of the extraction factor at both ends of the module is the enantiomer concentration drop at these locations of the module, due to dilution with "fresh" extraction phases. Therefore, this deviation of the extraction factors can be prevented, if necessary, by introducing a reflux at both ends of the system [24].

In conclusion, the model calculations have shown that a complete separation can be obtained using the proposed multistage electro dialysis system. The design parameters for this multi-stage electro dialysis system are the same as those of other counter-current processes, indicating the general applicability of this process.

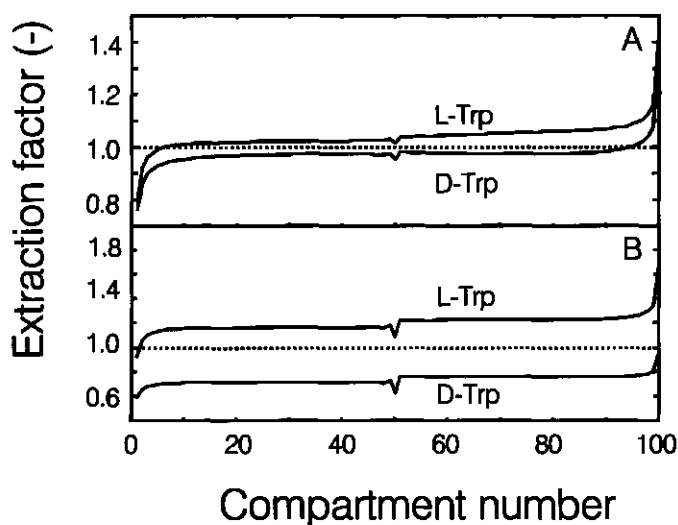


Figure 9: Estimated extraction factors as a function of the membrane compartment number for two different chiral selector selectivity values: (A) $\alpha=1.12$ and (B) $\alpha=2.0$; $q_s=80 \text{ mol}\cdot\text{m}^{-3}$; $m=100$; $c_f=20 \text{ mol}\cdot\text{m}^{-3}$; $\phi_{e,r}=1/100\cdot\phi_e$.

Nomenclature:

F	Faraday constant	[96486 C·mol ⁻¹]
A	Membrane surface area	[m ²]
Tn	Transport number at an arbitrarily chosen enantiomer concentration of 1 mol·m ⁻³	[-]
k_s	Absorption rate constant	[s ⁻¹]
$c_{e,j}^*$	Membrane concentration of the enantiomer	[mol·m ⁻³]
m	Membrane partition coefficient	[-]
q_s	Chiral selector concentration	[mol·m ⁻³]
k_e	Affinity constant	[m ³ ·mol ⁻¹]
$\Phi_{v,f}$	Feed flow	[m ³ ·s ⁻¹]
$c_{f,e}$	Feed flow concentration	[mol·m ⁻³]
Λ_e	Extraction factor	[-]
$\alpha_{D/L}$	Selectivity ($= \frac{k_D}{k_L}$)	[-]

Subscripts

- e One of the two enantiomers (D or L)
- f Feed flow
- s Saturated
- j Stage counter
- m Membrane compartment counter

References

1. FDA's policy statement for the development of new stereoisomeric drugs, *Chirality* 4 (1992) 338.
2. N. M. Maier, P. Franco, and W. Lindner, Separation of enantiomers: needs, challenges, perspectives, *J. Chromatogr. A* 906 (2001) 3.
3. C. Roussel, P. Piras, and I. Heitmann, An approach to discriminating 25 commercial chiral stationary phases from structural data sets extracted from a molecular database, *Biomed. Chromatogr.* 11 (1997) 311.
4. A. N. Collins, G. N. Sheldrake and J. Crosby, *Chirality in industry II; Developments in the commercial manufacture and applications of optically active compounds*, John Wiley & Sons, Chichester, 1997.
5. S. Fanali, Identification of chiral drug isomers by capillary electrophoresis, *J. Chromatogr. A* 735 (1996) 77.
6. B. Gottfried, Chromatographic resolution of racemates, *Angew. Chem. Int. Edit.* 19 (1980) 13.
7. W. H. Pirkle and T. C. Pochapsky, Chiral stationary phases for the direct LC separation of enantiomers, in Grushka, E., Giddings, J. C., and Brown, P. R. (Ed.), *Advances in Chromatography*, Marcel Dekker, New York, 1987, pp. 73-127.
8. H. B. Ding, P. W. Carr, and E. L. Cussler, Racemic leucine separation by hollow-fiber extraction, *AIChE J.* 38 (1992) 1493.
9. J. T. F. Keurentjes, L. J. W. M. Nabuurs, and E. A. Vegter, Liquid membrane technology for the separation of racemic mixtures, *J. Membrane Sci.* 113 (1996) 351.
10. T. Takeuchi, R. Horikawa, T. Tanimura, and Y. Kabasawa, Resolution of DL-Valine by countercurrent solvent extraction with continuous sample feeding, *Separ. Sci. Technol.* 25 (1990) 941.
11. W. H. Pirkle and W. E. Bowen, Preparative separation of enantiomers using hollow-fibre membrane technology, *Tetrahedron-Asymmetr.* 5 (1994) 773.

12. D. W. Armstrong and H. L. Jin, Enrichment of enantiomers and other isomers with aqueous liquid membranes containing cyclodextrin carriers, *Anal. Chem.* 59 (1987) 2237.
13. P. E. M. Overdeest and A. van der Padt, Optically pure compounds from ultrafiltration, *Chemtech* 29 (1999) 17.
14. D. C. S. Azevedo, L. S. Pais, and A. E. Rodrigues, Enantiomers separation by simulated moving bed chromatography - Non-instantaneous equilibrium at the solid-fluid interface, *J. Chromatogr. A* 865 (1999) 187.
15. B. Pynnonen, Simulated moving bed processing: escape from the high-cost box, *J. Chromatogr. A* 827 (1998) 143.
16. E. M. van der Ent, T. P. H. Thielen, M. A. Cohen Stuart, A. van der Padt, J. T. F. Keurentjes. 2001. Electrodialysis system for large-scale enantiomer separation. *Ind.Eng.Chem.Res.* (In Press)
17. R. Rautenbach and R. Albrecht, *Membrane processes*, Bath Press Ltd., Bath, 1989.
18. J. J. Schoeman and J. F. van Staden, Electro-osmotic pumping of sodium chloride solutions, *J. Membrane Sci.* 132 (1997) 1.
19. G. P. T. Cruz, S. Nii, F. K. Kawaizumi, and K. Takahashi, Simulation of Multistage Electrodialysis, *J. Chem. Eng. Jpn.* 32 (1999) 142.
20. E. Glueckauf and G. P. Kitt, A new electrolytic separation technique using semi-permeable membranes, *J. Appl. Chem.* 6 (1956) 511.
21. K. Kontturi, Countercurrent electrolysis in a cell where porous membranes have been connected in series with ion exchange membranes. Part 1 Method, *Separ. Sci. Technol.* 23 (1988) 227.
22. K. Kontturi and L. M. Westerberg, Countercurrent electrolysis in a cell where porous membranes have been connected in series with ion exchange membranes. Part 1 Experimental verification, *Separ. Sci. Technol.* 23 (1988) 235.
23. K. Kontturi, Trace ions in countercurrent electrolysis in a thin porous membrane, *Separ. Sci. Technol.* 21 (1986) 591.

24. K. Takahashi, H. Sakurai, S. Nii, and K. Sugiura, Multistage electro dialysis for separation of two metal ion species, *J. Chem. Eng. Jpn.* 28 (1995) 154.
25. M. Kubal, T. Machula, and N. Strnadova, Separation of calcium and cadmium by electro dialysis in the presence of ethylenediaminetetraacetic acid, *Separ. Sci. Technol.* 33 (1999) 1969.
26. B. MacMillan, A. R. Sharp, and R. L. Armstrong, An n.m.r. investigation of the dynamical characteristics of water absorbed in nafion, *Polymer* 40 (1999) 2471.
27. K. Singh and V. K. Shahi, Electrochemical studies on nafion membrane, *J. Membrane Sci.* 140 (1998) 51.
28. Z. Li and R. T. Yang, Concentration profile for linear driving force model for diffusion in a particle, *AIChE J.* 45 (1999) 196.
29. S. Fanali and P. Bocek, A practical procedure for the determination of association constants of the analyte-chiral selector equilibria by capillary zone electrophoresis, *Electrophoresis* 17 (1996) 1921.
30. E. M. van der Ent, A. van der Padt, J. T. F. Keurentjes, A. de Keizer, M. A. Cohen Stuart. 2001. Enantioselective binding of tryptophan to α -cyclodextrin: A thermodynamic study. (Submitted)
31. H. Strathmann, J. J. Krol, H. J. Rapp, and G. Eigenberger, Limiting current density and water dissociation in bipolar membranes, *J. Membrane Sci.* 125 (1997) 123.
32. P. E. M. Overdeest, Enantiomer separation by ultrafiltration of enantioselective micelles in multistage systems, Thesis (2000) Wageningen University and Research Centre.
33. J. T. F. Keurentjes, L. J. M. Linders, W. A. Beverloo, and K. van 't Riet, Membrane cascades for the separation of binary mixtures, *Chem. Eng. Sci.* 47 (1992) 1561.
34. J. Szejtli, Cyclodextrin technology, Kluwer academic publishers, Dordrecht, 1988.

35. M. Fillet, P. Hubert, and J. Crommen, Method development strategies for the enantioseparation of drugs by capillary electrophoresis using cyclodextrins as chiral additives, *Electrophoresis* 19 (1998) 2834.

6 Concluding remarks

6.1 Introduction

In this thesis, two enantiomer separation principles using membranes have been studied. The difference between these two is the location of the chiral environment, which is essential for chiral separation processes. The first method, which is described in Chapter 2, has its chiral environment located inside a membrane matrix, resulting in intrinsically selective membranes. As discussed in Chapter 2, the enantioselective permeation of enantiomers through these membranes can be the result of selective sorption or selective diffusion. The second method, which is described in Chapters 3-5, has its chiral recognition located in the liquid bulk solution and membranes are used to separate the free enantiomers from the complexed enantiomers. The proposed method uses an electrical potential as the driving force for a counter-current separation of the two enantiomers, resulting in a new large-scale enantiomer separation process called multi-stage electro dialysis (MS-ED).

6.2 Intrinsically selective membranes

The development of an intrinsically enantioselective membrane, as described in Chapter 2, has resulted in essential design criteria for these membranes. Often, an inverse proportionality between the permeability and the selectivity is observed for these membranes. Applying a fundamentally different separation mechanism for these membranes can potentially solve this dilemma. To achieve this, the mechanism for chiral discrimination has to be changed from diffusion selective to sorption selective. However, model calculations have shown that a sorption selective mechanism is only applicable under specific boundary conditions. One of the most essential boundary conditions determining the operational selectivity is the mobility of the selectively adsorbed enantiomer population. Low mobility values result in affinity membranes only, which do not provide any separation after being saturated. On the other hand, for mobile adsorbed enantiomers the operational permeation selectivity approaches the intrinsic selector selectivity.

The results of our diffusion experiments have shown that in practice the mobility of the selectively adsorbed population is often very low. Also other research groups have found this for BSA coated membranes [1] and molecular imprinted membranes [2], resulting in a lack of permeation selectivity for these membranes. However, Yoshikawa et al. [2] have been able to create an increased mobility using an electrical potential as an additional driving force. In

agreement with our model, this resulted in a permeation selective membrane, where the selectivity is a function of the applied electrical field. Also Thoelen et al. [3] have shown that using an electrical potential, a continuous enantioselective permeation of the preferentially adsorbed enantiomer of acetyl-tryptophan could be obtained for their poly(γ -methyl-L-glutamate) membrane. Without a potential difference, no permeation selectivity has been observed, whereas for high potential differences the permeation selectivity again approaches unity.

The question arises from these observations why the concentration difference over the membrane is not able to induce the mobility of the selectively adsorbed enantiomers, whereas an electrical potential can. This is explained by the large contribution of the electrical potential to the chemical potential. The driving force for transportation is the chemical potential gradient ($\frac{d\mu}{dz}$) over the membrane,

which can be described as [4]:

$$\frac{d\mu}{dz} = - \left[R \cdot T \cdot \frac{d \ln(x)}{dz} + F \cdot z_i \cdot \frac{d\phi}{dz} \right] \quad [\text{J} \cdot \text{mol}^{-1} \cdot \text{m}^{-1}] \quad (1)$$

Here μ is the chemical potential [$\text{J} \cdot \text{mol}^{-1}$], z is the distance [m], R is the gas constant [$8.314 \text{ J} \cdot \text{mol}^{-1} \cdot \text{K}^{-1}$], T the absolute temperature [K], x is the mol fraction [-], F is the Faraday constant [$\text{C} \cdot \text{mol}^{-1}$], z_i is the ion valency [-] and ϕ is the electrical potential [$\text{V} \cdot \text{m}^{-1}$]. The contribution of the electrical potential can easily be 10 times the contribution of the concentration difference, which can be demonstrated using the data for the molecular imprinted membrane of Yosikawa et al. [2]. For a concentration difference of $1 \text{ mol} \cdot \text{m}^{-3}$ they found an optimal electrical potential difference of 2.5 V, resulting in a contribution to the chemical potential of about $20 \text{ kJ} \cdot \text{mol}^{-1}$ for the concentration difference and about $250 \text{ kJ} \cdot \text{mol}^{-1}$ for the electrical potential difference. In this calculation the electrical field through the membrane is assumed to be homogeneous, which will probably not be the case, resulting in an even stronger electrical field. From these numbers it can be concluded that indeed the electrical driving force is at least a factor 10 higher than the concentration driving force.

Besides electric fields, other tools are available for influencing the physicochemical process of adsorption and desorption, e.g. magnetic fields (microwave), acoustic fields (ultrasound) and elevated temperatures [5]. Microwave radiation interacts with solutions via the mechanism of dipole rotation and ionic conduction. Kubrakova [5] states that microwave radiation causes a disruption or partial deformation of solvate shells, affecting the kinetic parameters of reactions. The complexation of metal ions with organic reagents in solution and sorbent phases in a microwave field has been studied well. The reaction of metal ions with nitrogen-, sulfur-, or oxygen-containing reagents is a

multistep process, which is accelerated to a variable degree under exposure to microwave radiation, as was demonstrated by Kubrakova et al. [5]. These results suggest that the experimental system of dodecylhydroxyproline:copper(II):phenylalanine, as it is described in Chapter 2, can be positively influenced by microwave radiation, resulting in a higher mobility of the selectively adsorbed population. The effect of microwave radiation on other systems has to be considered individually; it will depend on the physical properties of the system. Nevertheless, microwave irradiation is a promising technique for the enhancement of reaction limited diffusion processes.

The mechanical and physical effects of ultrasound have found many applications in chemical and biological industries. Applications include acceleration of chemical reactions, degradation of polymers and the enhancement of processes where diffusion takes place [6]. For example, the diffusivity of hydrocortisone through a dense cellulose membrane can be increased using ultrasound without irreversibly damaging the membrane. Furthermore, it has been shown that ultrasound only increases the diffusivity of the permeating molecule and not the sorption coefficient, indicating the potential of this technique to be used for permeation selective membranes for enantiomer separation.

Elevated temperatures might be another option to create an increased mobility of the selectively adsorbed population. A possible effect of higher temperatures is lower affinity values [7-9]. However, increasing the temperature not only reduces the affinity, but frequently also reduces the selectivity. Therefore, whether a higher temperature is effective will be dependent on the relative effect of the temperature on the affinity and on the selectivity.

In addition to that, in our theoretical approach for sorption selective membranes the relation between the mobility of the adsorbed enantiomers and the affinity of the chiral selector is not incorporated. Intuitively it is expected that high affinity values will cause low mobility values and vice versa. This is indicated by the work of Bauer [10], who synthesized a polymer membrane containing modified cyclodextrin moieties. These sorption selective membranes show a permeation selectivity of about 1.5 for butanalcyanhydrin in a pervaporation process at 15°C. It is known that cyclodextrins have a low affinity for their guest molecules (see also Chapter 4), which may result in a high mobility of the selectively adsorbed enantiomers. Therefore, it would be of relevance to know the relation between affinity and mobility for further insight in the design criteria of enantioselective selective membranes.

6.3 Multi-stage electro dialysis

In Chapters 3-5 an enantioselective separation method is studied which is a combination of an enantioselective complexation process and a non-selective membrane process. For the separation process described in this thesis an electrical potential is used to transport the free enantiomers through size-selective membranes. The retained complexes are transported along with the liquid flow in a direction opposite to the electrophoretic flow, resulting in a counter current separation. Implementing this principle in a modified electro dialysis stack results in a multi-stage electro dialysis (MS-ED). This proposed new separation process can be considered as a scaled-up version of capillary electrophoresis.

In Chapter 3 an experimental set-up is developed to evaluate the separation principle and to determine the critical process parameters. As a model system D,L-tryptophan is used with α -cyclodextrin as the chiral selector. It has been shown that for this experimental set-up the enantiomeric excess (e.e.) profiles as a function of time are linear, resulting in an easy and straightforward analysis of the process conditions on the operational selectivity and the transport efficiency. Mathematical model equations have been derived for the batch system. It has been found that the slope of the profiles is dependent on the operational selectivity, whereas the intercept depends on both the operational selectivity and the transport efficiency.

Using the model equations it has also been shown that the linear relations are only obtained under specific boundary conditions, i.e. a linear concentration dependency of the chiral selector complexation and a linear concentration dependency of the electrophoretic transport. This is only obtained for low transport efficiency values (<0.05). Since the model system is operated at a low pH (pH 2-3), the transport efficiency values are less than the boundary value of 0.05. Of course, this value is unfavourable for the energy consumption of the process, since a significant part of the current is not used for enantiomer transport.

As is described in Chapter 3, the transport mechanism of the free enantiomers is mainly due to electro osmotic flow. As is described in the previous section, one of the consequences of this transport mechanism is that the electrophoretic flux is linearly proportional to the free enantiomer bulk concentration. Also, concentration polarization due to this transport mechanism is negligible, since no depletion of the enantiomer occurs (Figure 1A). The only compound that is accumulated in front of the membrane is the chiral selector and the complex. Fortunately, since the ratio of the chiral selector concentration and the complex concentration remains the same, this has no effect on the

operational selectivity. This can be seen from the definition of the affinity constant (k_a):

$$k_a = c_e \cdot \frac{c_{CS}}{c_{CS:e}} \quad [\text{mol} \cdot \text{m}^{-3}] \quad (2)$$

where c_e is the free enantiomer concentration [$\text{mol} \cdot \text{m}^{-3}$], c_{CS} is the chiral selector concentration [$\text{mol} \cdot \text{m}^{-3}$] and $c_{CS:e}$ is the complex concentration [$\text{mol} \cdot \text{m}^{-3}$]. However, in the case of depletion of free enantiomers due to high current efficiency values, the ratio of the chiral selector and the complex will be changed. This influences the operational selectivity in a negative way, since the preferentially complexed enantiomer is desorbed. Therefore, in order to have the highest benefit of the intrinsic selector selectivity, concentration polarization should be prevented in this MS-ED system.

Parameters influencing the power consumption of MS-ED

By definition, energy is required for the separation of substances in order to maintain a driving force for transport of matter. It is shown that the MS-ED system is able to separate a mixture of enantiomers, however, an important factor to know for the viability of the process is the amount of energy required to separate a certain amount of enantiomers. Also important to know is which process parameters have a major influence on this energy consumption.

Using ohmic analysis, i.e. assuming proportionality between current and voltage, the power consumption in a given stack of constant resistance R at current I is $I^2 \cdot R$. The resistance of the stack equals the summation of all

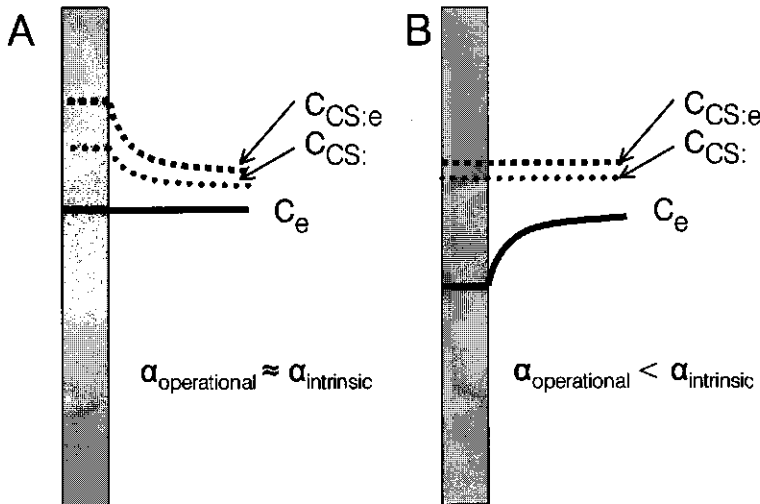


Figure 1: Effect of transport mechanism on concentration polarization; A electro-osmosis; B electrophoretic transport.

individual membrane resistances and resistances of solution. The membrane resistance of the electrodialysis membrane Nafion 117 has experimentally been measured as a function of pH. The following fit relation has been found that describes the membrane resistance (R_m) in the pH range 1.5-4.5:

$$R_m = \frac{2.2 \cdot 10^{-4}}{[H^+]} \quad [\Omega \cdot m^2] \quad (3)$$

The ohmic resistance of the homogeneous solution in the compartments (R_s) can be described by [11]:

$$R_s = \frac{l}{\sum_i \Lambda_{m,i} \cdot c_i} \quad [\Omega \cdot m^2] \quad (4)$$

where l is the distance between the membranes [m], $\Lambda_{m,i}$ is the equivalent conductance [$\Omega^{-1} \cdot \text{mol}^{-1} \cdot \text{m}^2$] of species i and c_i is the concentration [$\text{mol} \cdot \text{m}^{-3}$]. As a rough estimation, the power consumption can be calculated using equations (3) and (4) in combination with the optimal current density, which is obtained using model calculations. Figure 6 shows the calculated power consumption as

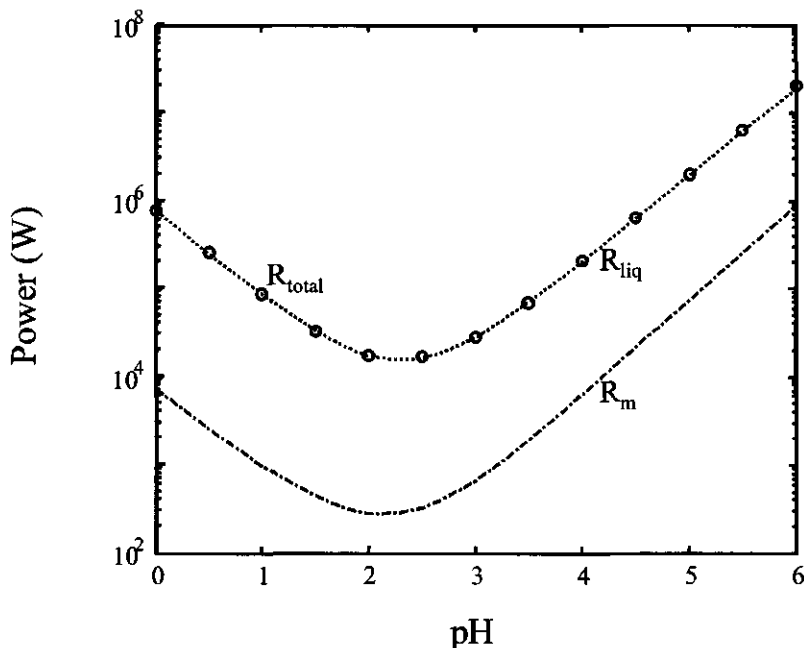


Figure 6: Estimated power consumption for the MS-ED stack for a large-scale model system. The open circles indicate the total resistance of the module (R_{tot}), which is the summation of the membrane resistance (R_m) and the liquid resistance (R_{liq}). For the calculations the following module constants are used: distance between the membranes is $2 \cdot 10^{-3}$ m; liquid flow velocity is $1.67 \cdot 10^{-6}$ m³·s⁻¹; feed flow velocity is $6.7 \cdot 10^{-8}$ m³·s⁻¹; the feed flow racemate concentration is 300 mol·m⁻³, resulting in a production capacity of 350 grams per day; the chiral selector concentration is 80 mol·m⁻³.

a function of pH. The power consumption (R_{tot}) is divided in a power consumption due to the membrane resistances (R_m) and in a power consumption due to the resistance of solution (R_{liq}). The calculations are performed for an electrodialysis stack containing 50 membrane compartments with a cross sectional area of 1 m². Using a chiral selector selectivity of 2.0, the demand of a 99%+ separation for both enantiomers is satisfied. For the pH-dependency of the current efficiency constant (Tn') the following equation is used:

$$Tn' = \frac{1}{6.7 \cdot 10^3 \cdot 10^{-pH} + 27.5} \quad [m^3 \cdot mol^{-1}] \quad (5)$$

which is a fit function describing the transport efficiency data of the methanol system as is described in Chapter 3.

From this figure it can be seen that for this model system a minimum in the power consumption is expected around the pK_a of the amino acid, i.e. 2.4 for tryptophan. For pH values below the pK_a value the current efficiency approaches zero, since protons will transport the major part of the current. Therefore, an increased current density is needed for the same flux of enantiomers and, consequently, the power consumption is increased. On the other hand, for pH values above the pK_a value the liquid resistance increases due to the absence of ionic species, resulting in an increased power consumption.

Figure 6 shows that even the minimum power consumption for this system at optimal pH is about 15 kW. The production capacity of this system is about 350 gram per day, which results in a specific power consumption of about 1 kWh per gram of product. For many products this specific power consumption number will probably be too high. The extraction of citric acid from a fermentation broth using electrodialysis can be operated using a specific power consumption of 1 kWh per kg product [12], indicating the desired range for operation. Therefore, at least a tenfold reduction of the present specific energy consumption is necessary to make the MS-ED process applicable for a broad range of separation problems.

Figure 6 also shows that the membrane resistance is more or less negligible compared to the liquid resistance. Therefore, only reducing the liquid resistance can lower the power consumption significantly. However, the dilemma arises how to reduce the liquid resistance without influencing the transport efficiency. From equation (4) it can be seen that reducing the distance between two membranes is one option. However, for these calculations a value of only 2·10⁻³ m is used, further reduction of the thickness will increase the pressure drop over the membrane stack due to an increased liquid flow resistance. Another possibility for the reduction of the liquid resistance is the introduction of conducting spacers between the membranes. Korngold et al. [13] have shown

that with an anion-exchange spacer the electrical resistance of an electrodialysis stack for the desalination of water could significantly be reduced.

Not only a reduction of the liquid resistance, but also an increase of the transport efficiency will result in a reduced power consumption. Since the transport number constant at the optimal pH is only 0.02, this might be a good alternative. Increasing the transport efficiency can only be obtained by changing the enantiomer, i.e. using enantiomers that have a higher pK_a value or that are charged around neutral pH. For economical reasons, the optimal current efficiency is 1, i.e. all current is transported by the enantiomers. However, for current efficiency values larger than about 0.1 the process design becomes less straightforward. An analysis of the extraction factor can explain this effect.

The extraction factor ($\Lambda_{e,m}$) is defined as the ratio of the two counter-current enantiomer fluxes leaving a membrane compartment (Equation 6 of Chapter 5):

$$\Lambda_{e,m} = \frac{\Phi_v \cdot (1 + q_s \cdot k_e) \cdot c_{e,j=3,m}}{\sum_{j=1}^3 J e_{e,j}} \quad [-] \quad (6)$$

From this equation it can be seen that as a result of the liquid flow the flux is linearly dependent on the concentration. Also, the electrophoretic flux depends linearly on the concentration for low current efficiency values (Equation 3 of Chapter 5):

$$J e_{e,j} = \frac{i \cdot A}{F} \cdot T n = \frac{i \cdot A}{F} \cdot \frac{c_{e,j}}{\frac{1 - T n}{T n} + c_{e,j}} \approx \frac{i \cdot A}{F} \cdot T n \cdot c_{e,j} \quad [\text{mol} \cdot \text{s}^{-1}] \quad (7)$$

Consequently, the extraction factor is independent of the concentration and is only dependent on adjustable parameters, i.e. the current density, the liquid flow and the membrane area. Therefore, the extraction factors of the different membrane compartments throughout the stack are more or less constant and can easily be positioned oppositely around unity for the two enantiomers. However, if the current efficiency equals 1, according to Equation (7) the electrophoretic flow becomes *in*dependent of the concentration. Thus, the extraction factor becomes a linear function of the enantiomer concentrations. Since the enantiomer concentrations vary throughout the electrodialysis stack, the extraction factors vary and cannot easily be positioned oppositely around unity by changing the current density or liquid flow. The only solution for this problem would be a varying current density per membrane compartment. This can theoretically be obtained by varying the cross sectional area of the membrane compartments. However, in practice this is not easily implemented in an electrodialysis stack.

Future perspectives

The application of MS-ED for binary separation problems is not restricted to the large-scale separation of enantiomers. The strength of the MS-ED process is its ability to cope with low selective separation problems, the use of a 'green solvent', and the translation of an analytical separation to a large-scale production process. On the other hand, the need for low current efficiency values for a straightforward process design and consequently the relatively large energy consumption will reduce its application to more 'sophisticated' products for which the economical margins are high, e.g. pharmaceutical products or nutraceuticals. This picture may change if the issue of low current efficiency values can be solved.

This delicate balance between a low current efficiency for an easy process design and a high current efficiency for economical reasons is the ultimate optimization criterion for this MS-ED process. The window of operation is strongly dependent on the chiral selector properties, such as selectivity, solubility, and affinity, as has been shown in Chapter 5. Therefore, for future work this has to be one of the major research topics.

A different process configuration might be an answer for a reduction of the operational costs. In the previous sections it is shown that the power consumption can be reduced by a decrease in the membrane distance, i.e. the compartment thickness. In the limiting case the membrane distance is zero and no liquid is present between the membranes. However, to achieve a liquid flow, including the chiral selector, membranes have to be used that are permeable

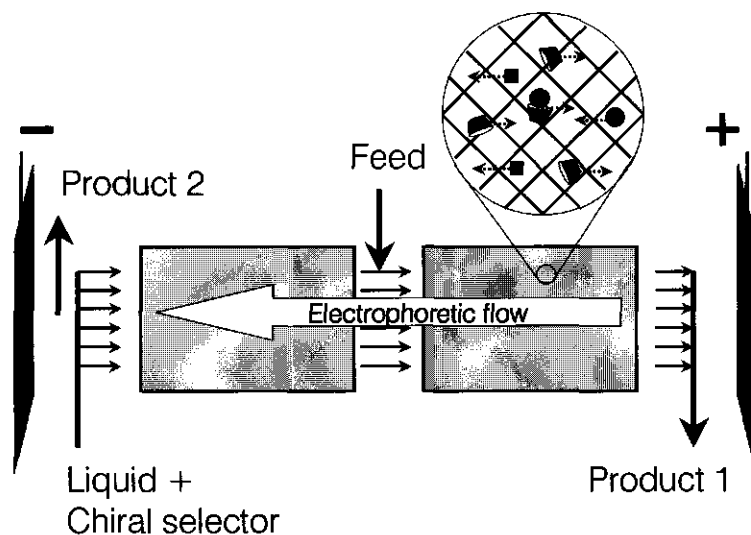


Figure 3: Schematic representation of a continuous elution gel electrophoresis process

not only for the enantiomers, but also for the chiral selector. Actually, instead of permeable membranes, a permeable polyelectrolyte gel can be used, resulting in a continuous elution gel electrophoresis (Figure 7). Now the separation is no longer based on a size difference, but on a velocity difference in an electrical field. In this process the gel matrix is only necessary to prevent back mixing of the liquid flow and to allow for high current efficiency values. On micropreparative (1-10 μg) scale, these systems have already been used for the purification of proteins [14], but are to our knowledge not yet applied for large-scale separations.

This also opens an additional application area: protein fractionation and related to that oligopeptide fractionation. The differences between two proteins or oligopeptides, in e.g. net charge, hydrophobicity or molecular weight, can be very small [15]. This will in most cases result in a low selective separation process, thus complying with one of the advantages of MS-ED. Obviously, the membranes used for this separation process have to be different from the membranes used in this thesis. Ultrafiltration or nanofiltration membranes should be more suitable, depending on the charge density and the molar mass of the protein.

Conclusions

In this chapter several critical issues and improvements for the two processes described in this thesis have been discussed. For the intrinsically selective membranes the major issue is obtaining an increased mobility of adsorbed enantiomers, for which several options have been suggested. For the MS-ED system, the major issue is the transport mechanism, which has a large influence on the power consumption. A dilemma exists between the current efficiency, influencing the power consumption and the separation efficiency. This topic is extensively discussed.

In this thesis two membrane-based separations have been described, however, from the discussion in this chapter it will be obvious that significant improvements are still required and many other alternatives can be thought of. In our view, this will eventually lead to a new range of process concepts based on low selectivity systems, thus broadening the scope of separation technology.

Nomenclature

c_{CS}	= Chiral selector concentration	$[\text{mol}\cdot\text{m}^{-3}]$
$c_{CS:e}$	= Complex concentration	$[\text{mol}\cdot\text{m}^{-3}]$
c_e	= Free enantiomer concentration	$[\text{mol}\cdot\text{m}^{-3}]$
F	= Faraday constant	$[\text{C}\cdot\text{mol}^{-1}]$
k_e	= Affinity constant	$[\text{mol}\cdot\text{m}^{-3}]$

l	= Compartment thickness	[m]
R	= Gas constant	[8.314 J·mol ⁻¹ ·K ⁻¹]
R_m	= Membrane resistance	[Ω·m ²]
R_s	= Ohmic resistance of a homogeneous solution	[Ω·m ²]
T	= Absolute temperature	[K]
Tn'	= Transport number constant	[m ³ ·mol ⁻¹]
x	= Mol fraction	[-]
z	= Distance	[m]
z_i	= Ion valency	[-]
μ	= Chemical potential	[J·mol ⁻¹]
Φ	= Electrical potential	[V·m ⁻¹]
$A_{e,m}$	= Extraction factor	[-]
$A_{m,i}$	= Equivalent conductance	[Ω ⁻¹ ·mol ⁻¹ ·m ⁻²]

Indices:

e	= D or L enantiomer
i	= Species i
m	= Membrane
s	= Solution

References

- [1]. A. Higuchi, M. Hara, T. Horiuchi, and T. Nakagawa, Optical resolution of amino acids by ultrafiltration membranes containing serum albumin, *J. Membrane Sci.* 93 (1994) 157.
- [2]. M. Yoshikawa, T. Fujisawa, and J. Izumi, Molecularly imprinted polymeric membranes having EFF derivatives as a chiral recognition site, *Macromol. Chem. Phys.* 200 (1999) 1458.
- [3]. C. Thoelen, M. De Bruyn, E. Theunissen, Y. Kondo, I. F. J. Vankelecom, P. Grobet, M. Yoshikawa, and P. A. Jacobs, Membranes based on poly([gamma]-methyl--glutamate): synthesis, characterization and use in chiral separations, *J. Membrane Sci.* 186 (2001) 153.
- [4]. R. Taylor and R. Krishna, *Multicomponent mass transfer*, Wiley, New York, 1993.
- [5]. I. V. Kubrakova, Effect of microwave radiation on physicochemical processes in solutions and heterogeneous systems: Applications in analytical chemistry, *J. Anal. Chem.* 55 (2000) 1113.

- [6]. T. N. Julian and G. M. Zentner, Ultrasonically mediated solute permeation through polymer barriers, *J. Pharm. Pharmacol.* 38 (1986) 871.
- [7]. E. Grushka, R. Leshem, and C. Gilon, Retention behaviour of amino acid enantiomers in reversed-phase liquid chromatography, *J. Chromatogr.* 255 (1983) 41.
- [8]. J. M. Lin, T. Nakagama, K. Uchiyama, and T. Hobo, Temperature effect on chiral recognition of some amino acids with molecularly imprinted polymer filled capillary electrochromatography, *Biomed. Chromatogr.* 11 (1997) 298.
- [9]. P. D. Ross and M. V. Rekharsky, Thermodynamics of hydrogen bond and hydrophobic interactions in cyclodextrin complexes, *Biophys. J.* 71 (1996) 2144.
- [10]. B. Bauer, Preparation of homochiral cyanohydrins using an enzyme-membrane reactor, Thesis (1996) University of Twente.
- [11]. R. Chang, Physical chemistry for the chemical and biological sciences, University Science Books, Sausalito, 2000.
- [12]. S. Novalic, J. Okwor, and K. D. Kulbe, The characteristics of citric acid separation using electrodialysis with bipolar membranes, *Desalination* 105 (1996) 277.
- [13]. E. Korngold, L. Aronov, and O. Kedem, Novel ion-exchange spacer for improving electrodialysis I. Reacted spacer, *J. Membrane Sci.* 138 (1998) 165.
- [14]. M. Baumann and M. Lauraeus, Purification of membrane proteins using a micropreparative gel electrophoresis apparatus: purification of subunits of the integral membrane protein bacillus subtilis aa3-type quinol oxidase for low level amino acid sequence analysis, *Anal. Biochem.* 214 (1993) 142.
- [15]. I. Recio, M. Ramos, and Fandino R. Lopez, Capillary electrophoresis for the analysis of food proteins of animal origin, *Electrophoresis* 22 (2001) 1489.

Summary

Many compounds used in the agrochemical, food and pharmaceutical industry contain one or more chiral centers. The enantiomers of these compounds often have different effects on their targets. To prevent side effects or environmental burden, these compounds should rather be applied in their optically pure form. Different routes are available to obtain optically pure enantiomers. One is chemical synthesis using a chiral substrate or using a chiral (bio)catalyst. Another route is a straightforward chemical synthesis of a racemate followed by a resolution step.

Crystallization and enzymatic resolution are the two classical methods for the separation of a racemic mixture. However, crystallization usually requires many process steps, thus making the process complicated and inducing considerable losses of product. For enzymatic resolution an appropriate route has to be developed for each individual compound, leading to considerable costs and increased development time. Therefore, during the last decade much emphasis is on the development of alternative technologies to separate enantiomers in a continuous fashion.

Considerable effort has been spent on the development of enantioseparations based on membrane processes. Technically, membrane separation processes are designed for large-scale applications as they combine continuous operation, easy adaptation to different production-relevant process configurations, convenient scaling up and, in most cases, ambient-temperature processing. Membrane processes for enantiomer separation may be categorized into two types: direct separation using an "intrinsically" enantioselective membrane (e.g. a membrane made of a chiral polymer), or separation in which a non-selective membrane assists an enantioselective process. Both separation mechanisms are described in this thesis.

Design criteria have been evaluated for intrinsically enantioselective membranes, based on reviewed literature data, model calculations and experimental data. Literature data on dense permeation-selective membranes for enantiomer separation show that these membranes can be divided into two different classes: diffusion-selective membranes and sorption-selective membranes. Reviewing the literature on diffusion-selective membranes revealed that these membranes have one disadvantage: the inverse proportionality between permeability and selectivity. A dual sorption model showed for a sorption-selective mechanism that the permeation selectivity approaches the intrinsic selectivity of the selector if the selectively adsorbed population is "mobile" and the non-selective permeation is minimized. Therefore, we conclude that sorption selective membranes are able to surpass the inverse

proportionality relation between the permeation and selectivity, thus resulting in membranes that can be used for viable large-scale membrane processes for enantiomer separations.

Besides intrinsically selective membranes, a separation process is designed in which a non-selective membrane assists an enantioselective process. In this membrane system chiral selectors are used, which are retained by size-selective membranes. Applying an electrical potential, selective transport of the free enantiomer will occur, thus providing separation. First of all an experimental set-up is designed to evaluate the separation parameters. In a series of four separation compartments, α -cyclodextrin has been used as a chiral selector to separate D,L-tryptophan. For this batch system a mathematical model for the enantiomer concentrations as a function of time has been set up from which the accompanying enantiomeric excess profiles have been derived. Using this system, the influence of the pH and the methanol fraction (used as a bacteriostatic agent) on the operational selectivity and the transport efficiency has been examined. Based on a transport model, a 2² factorial design for the experimental set-up is used to investigate the effects of various process parameters. The results have shown that the addition of methanol (5 – 20% v/v) is of minor influence, whereas the pH (2 – 6) has a major effect, both on the operational selectivity and on the transport number. Experiments with AgNO₃ instead of methanol have shown that the operational selectivity has a plateau value of 1.08 at a pH ranging from 3 to 6. For lower pH values the selectivity drops for both systems.

In order to compare the pH dependency of the operational selectivity with the pH dependency of the intrinsic selectivity, measurements have been performed using isothermal titration calorimetry. Using ITC the thermodynamic complexation parameters (complexation affinity, complexation enthalpy and complexation entropy) for both enantiomers are determined as a function of pH. Despite the low affinity for the α -cyclodextrin/tryptophan complex, isothermal titration calorimetry appears to be a versatile method to study complexation thermodynamics and the chiral selector discrimination mechanism. Constant affinity values (K) have been found for both enantiomers for pH 2.5 – 6, resulting in an intrinsic selectivity ($\alpha_{D/L}$) of 1.12±0.04. Below pH 2.5, however, both affinity constants drop due to the reduced affinity for positively charged tryptophan. From the thermodynamic results it is concluded that D-Trp is able to undergo more favourable hydrogen bonding interactions with α -cyclodextrin than L-Trp when both enantiomers are present as zwitterion. However, the additional interaction of D-Trp disappears when tryptophan becomes positively charged. Consequently, the binding mechanism becomes similar, resulting in a selectivity

drop to unity. The effect observed in the operational selectivity is explained by the pH dependency of the intrinsic selectivity.

In the last part of this thesis a model is developed and validated for a continuous multi-stage electro dialysis system. This model is evaluated using a 20-compartment electro dialysis stack containing the counter-current and multi-stage principle. During validation a racemic mixture has been fed at one side of the module, which has been placed in a closed system, thereby simulating one half of a complete separation apparatus. Using this set-up the enantiomeric excess (e.e.) and the concentrations of both enantiomers have been determined as a function of the current density at a constant liquid flow velocity. Despite the low selectivity of this selector (1.12), an e.e. difference of 14% has been obtained. Based on these experimental data, model calculations have shown that using an electro dialysis stack of 250 membrane compartments a complete separation (99%+) can be accomplished for this model system. In conclusion, the proposed multi-stage electro dialysis separation principle has the advantage of making use of existing analytical separation methods and is suitable for low selectivity (1.1-2) separations. Therefore, it provides a viable addition to the current range of large-scale enantiomer separation processes.

Samenvatting

Veel stoffen die worden toegepast in de agrochemische, voedingsmiddelen- en farmaceutische industrie bevatten één of meerdere chirale koolstofatomen. Vaak is de gewenste biologische activiteit slechts gelegen in één van de twee enantiomeren. Om ongewenste bijwerkingen en milieubelasting te voorkomen worden deze stoffen steeds vaker toegepast in hun optisch pure vorm. Voor het verkrijgen van de optisch pure vorm van een enantiomeer zijn verschillende routes mogelijk. Eén daarvan is door chemische synthese waarbij gebruik gemaakt wordt van een chirale grondstof of een chirale (bio)katalysator. Een andere route is door het uitvoeren van een relatief eenvoudige racemaatsynthese gevolgd door een scheidingsstap.

Kristallisatie en enzymatische resolutie zijn de twee klassieke methoden die gebruikt worden voor de scheiding van een racemisch mengsel. Diastereomere kristallisatie brengt echter vaak vele processtappen met zich mee, waardoor deze processen gecompliceerd zijn en waarmee aanzienlijke hoeveelheden product verloren kunnen gaan. Voor enzymatische resolutie moet voor ieder nieuw product een nieuwe methode worden ontwikkeld, hetgeen vaak tot aanzienlijke kosten en ontwikkelingstijd leidt. Om deze reden is in de afgelopen jaren steeds meer onderzoek gedaan naar alternatieve scheidingstechnologieën, waarbij veel inspanningen zijn gepleegd in de ontwikkeling van enantiomeerscheidingstechnieken gebaseerd op membraantechnologie. Technisch gezien zijn membraanprocessen uitstekend geschikt voor toepassingen op grote schaal, omdat ze een aantal aantrekkelijke eigenschappen kunnen combineren: continu bedrijven van de scheiding, eenvoudige aanpassingsmogelijkheden voor de gewenste productiecapaciteit en in de meeste gevallen uit te voeren bij kamertemperatuur. Membraanprocessen voor enantiomeerscheidingen kunnen worden ingedeeld in twee categorieën: directe scheiding door middel van een intrinsiek selectief membraan, of een indirecte scheiding waarbij een niet-selectief membraan een hulpfactor is bij een enantioselectieve herkenningsreactie. Beide scheidingsmethoden zijn onderwerp van studie geweest voor het onderzoek zoals beschreven in dit proefschrift.

De ontwerpcriteria voor enantioselectieve membranen zijn onderzocht door middel van een literatuurstudie, modelberekeningen en experimentele data. Literatuurgegevens laten zien dat enantioselectieve membranen kunnen worden ingedeeld in twee groepen: diffusieselectieve membranen en sorptieselectieve membranen. Diffusieselectieve membranen hebben in het algemeen als nadeel dat er een omgekeerd evenredigheid bestaat tussen de permeabiliteit en de selectiviteit. Sorptieselectieve membranen daarentegen zouden deze relatie niet

moeten hebben, hetgeen met een dual-sorptie model is gestaafd. Daarnaast laten deze modelberekeningen zien dat de operationele selectiviteit van deze membranen alleen gelijk wordt aan de intrinsieke selectiviteit wanneer de selectief geadsorbeerde enantiomeren niet "vast" zitten, maar beweeglijk zijn over de selectieve plaatsen in het membraan en wanneer de α -selectieve diffusie minimaal is. Uit bovenstaande resultaten kan worden geconcludeerd dat deze sorptieselectieve membranen de omgekeerd evenredige relatie tussen de permeabiliteit en de selectiviteit kunnen overstijgen. Dit heeft tot gevolg heeft dat deze membranen in principe gebruikt kunnen worden voor nieuwe en levensvatbare grootschalige scheidingsprocessen, onder meer op het gebied van enantiomeerscheidingen.

Tevens is in dit proefschrift een scheidingsproces beschreven dat bestaat uit een selectieve herkenningreactie in een vloeistof in combinatie met een α -selectief membraanproces. In dit gestapelde systeem zijn chiraalselectoren gebruikt die worden tegengehouden door membranen die op molecuulgrootte kunnen scheiden. Door gebruik te maken van een elektrische potentiaal vindt selectief transport van het ongecomplexeerde enantiomeer plaats, waardoor scheiding van de twee enantiomeren ontstaat. Allereerst is een systeem beschreven dat gebruikt kan worden voor de ontwikkeling van dit scheidingsprincipe. Het systeem bestaat uit 4 scheidingscompartimenten en is gebruikt voor de bestudering van de scheiding van de modelstof D,L-tryptofaan met behulp van de chiraalselector α -cyclodextrine. Voor dit batchsysteem zijn de modelvergelijkingen opgesteld voor de enantiomeerconcentraties in de tijd en de daaruit volgende waarden voor de enantiomere overmaat. In deze opstelling en de daarbij behorende modelvergelijkingen is de invloed van pH en methanolfractie (remmer bacteriegroei) bepaald op de operationele selectiviteit en de mate van enantiomeertransport door het membraan. Hiervoor is een 2^2 factorieel experimentontwerp gebruikt. De resultaten tonen aan dat de toevoeging van methanol (5 – 20% v/v) nauwelijks invloed heeft op de operationele selectiviteit en het transportgetal. De pH (2 – 6) heeft echter wel degelijk invloed op zowel de operationele selectiviteit als het transportgetal. Wanneer AgNO_3 wordt gebruikt in plaats van methanol is voor de operationele selectiviteit een constante waarde gevonden van 1,08 over het pH-gebied van 3 tot 6. Voor lagere pH waarden valt de selectiviteit voor beide systemen terug naar 1.

Om de pH-afhankelijkheid van de operationele selectiviteit te vergelijken met de intrinsieke selectorselectiviteit zijn metingen gedaan met behulp van isotherme titratie calorimetrie (ITC). Hiermee zijn de thermodynamische complexatie parameters (affiniteitconstante, enthalpie en entropie) bepaald voor beide enantiomeren als functie van de pH. Ondanks de lage affiniteit van de

chiraalselector is gebleken dat ITC een geschikte methode is om de thermodynamica van complexering te bestuderen. Een constante affiniteit is gevonden voor beide enantiomeren voor het pH gebied 2,5 tot 6. De gemiddelde selectiviteit over dit interval voor D-tryptofaan is $1,12 \pm 0,04$. Beneden pH 2,5 nemen beide affiniteitconstanten af door de invloed van een lage affiniteit van de chiraalselector voor het positief geladen tryptofaanmolecuul. Uit de waarden van de thermodynamische grootheden is geconcludeerd dat D-tryptofaan in staat is om meer gunstige waterstofbrug interacties aan te gaan met α -cyclodextrine dan L-tryptofaan in het geval dat beide enantiomeren als zwitterion aanwezig zijn. De extra interactie voor D-tryptofaan verdwijnt echter als deze positief geladen is. Dit heeft tot gevolg dat het bindingsmechanisme van deze geladen vormen gelijk worden en dat de selectiviteit verdwijnt. Hieruit kan worden geconcludeerd dat het pH-effect dat gevonden wordt bij de operationele selectiviteit volledig verklaard kan worden door het effect van de pH op de intrinsieke selectiviteit.

In het laatste gedeelte van dit proefschrift is een model ontwikkeld en gevalideerd dat het continu meertrapselectrodialyseproces beschrijft. Hiervoor zijn experimenten uitgevoerd in een tegenstroom electro-dialyse module met 20 compartimenten. Tijdens de validatie-experimenten is een racemaat toegevoerd aan één zijde van de module. Op deze manier is de helft van het complete scheidingsapparaat nagebootst. In dit systeem zijn de enantiomeer concentraties in beide uitgaande stromen gemeten als functie van de stroomdichtheid bij een constant vloeistofdebiet. Ondanks de lage selectiviteit is een enantiomere overmaat verschil van 14% bereikt. Gebaseerd op deze resultaten is met het ontwikkelde model berekend dat voor dit modelsysteem een complete scheiding (99%+) verkregen kan worden door gebruik te maken van een electro-dialyse module bestaande uit 250 membraancompartimenten. Omdat het voorgestelde meertrapselectrodialyse scheidingsprincipe een schaalbaar proces is dat gebruik kan maken van bestaande selectoren ontwikkeld voor analytische scheidingsmethoden, is het geschikt is voor laagselectieve scheidingen (1,1 – 2), waarmee dit proces een potentieel alternatief vormt voor de bestaande grootschalige enantiomeerscheidingstechnologieën.

Curriculum vitae

Eduard Marinus van der Ent werd geboren op 25 december 1970 te Papendrecht. In 1987 behaalde hij zijn MAVO diploma aan De Blokkerd te Alblasterdam, waarna hij in 1989 zijn HAVO diploma behaalde aan De Lage Waard te Papendrecht. In datzelfde jaar begon hij met een studie Nederlandse Landbouw aan de Agrarische Hogeschool te Delft.

Na het behalen van zijn propedeuse en na een jaar doctoraal onderwijs gevolgd te hebben stapte hij over naar de studie Bioprocestechnologie aan de toenmalige Landbouwniversiteit te Wageningen. In maart 1996 studeerde hij af met afstudeervakken in Fysische- en Kolloïdchemie en Proceskunde. Zijn stageperiode voerde hij uit bij Akzo Nobel Central Research te Arnhem in de groep van dr. J.T.F. Keurentjes.

Van juni 1996 tot juni 2001 was hij werkzaam aan de sectie Proceskunde van Wageningen Universiteit waar het onderzoek, zoals beschreven in dit proefschrift, werd uitgevoerd.

Vanaf augustus 2001 is hij werkzaam als procestechnoloog in de groep Process Development van DMV-International te Veghel/Fraser (U.S.A.)